CHALMERS
UNIVERSITY OF TECHNOLOGY

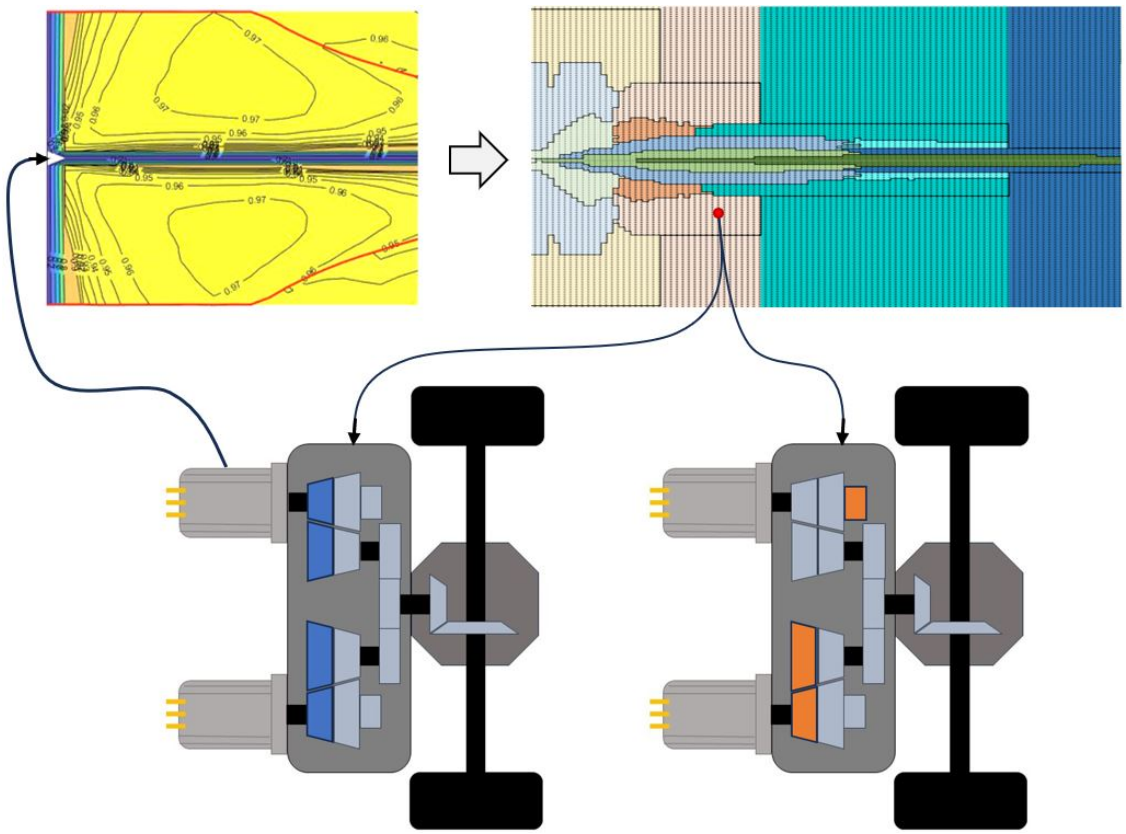

Gear Selection for Dual Electrified Axles with Multiple Electric Machines

Development of a Map-Based Gear Selection Methodology

Master's thesis in M.Sc Mobility Engineering

Emil Alexsson
Shamith Satish

DEPARTMENT OF ELECTRICAL ENGINEERING
CHALMERS UNIVERSITY OF TECHNOLOGY
Gothenburg, Sweden 2024
www.chalmers.se

Master's thesis 2024

Gear Selection for Dual Electrified Axles with Multiple Electric Machines

Development of a Map-Based Gear Selection Methodology

EMIL ALEXSSON
SHAMITH SATISH

CHALMERS
UNIVERSITY OF TECHNOLOGY

Department of Electrical Engineering
Chalmers University of Technology
Gothenburg, Sweden 2024

Gear Selection for Dual Electrified Axles with Multiple Electric Machines
Development of a Map-Based Gear Selection Methodology
EMIL ALEXSSON
SHAMITH SATISH

Supervisor: Andreas Magnusson, Volvo GTT
Supervisor: Jonas Fredriksson, Department of Electrical Engineering, Chalmers University of Technology
Supervisor: Samuel Jakobsson, Volvo GTT
Examiner: Jonas Fredriksson, Department of Electrical Engineering, Chalmers University of Technology

Master's Thesis 2024
Department of Electrical Engineering
Chalmers University of Technology
SE-412 96 Gothenburg
Telephone +46 31 772 1000

Cover: Visualization of signals, from electric machine efficiency map to selected gears.

Typeset in LaTeX
Printed by Chalmers Reproservice
Gothenburg, Sweden 2024

Gear Selection for Dual Electrified Axles with Multiple Electric Machines
Development of Gear Selection Methodology for Electrified Axles
EMIL ALEXSSON
SHAMITH SATISH
Department of Electrical Engineering
Chalmers University of Technology

Abstract

The electrification of heavy-duty trucks has been at the forefront of efforts to achieve sustainability in transportation by replacing conventional internal combustion engine propulsion systems. With advancements in electric propulsion technology, the concept of electrified axles has emerged as a way to build more efficient propulsion systems. This propulsion system configuration is the focus of this thesis, which specifically examines dual electrified axles with multiple electric machines. The aim of this thesis is to design a methodology for gear selection and to formulate a control strategy for the gear selection process.

The project utilizes Volvo's simulation environment in MATLAB and Simulink to construct the gear selection system. Each eclectic axle consists of two electric machines and two two-speed gearboxes. The foundation of the gear selection control strategy is based on the efficiency maps of the electric machines and the gearboxes. Using these maps and the combinations of gear ratios (*states*) from the two-speed transmission for each motor, a wheel torque versus vehicle speed map was generated to facilitate map-based gear selection, referred to as the *state selection map*. To implement this map-based gear selection, a control methodology was developed in Simulink, ensuring an optimized number of gearshifts and the efficiency of each electrified axle.

The benefit of engaging different usage of the two axles is also evaluated using two different control strategies: independent and parallel. The parallel control strategy lacks the capability to independently assign different states to the two axles, which is used for comparison with the independent control strategy that can send distinct signals to each axle. Each strategy is tested under different operating conditions including city driving, EU highway driving, and US highway driving. The results show that the efficiency of the electrified axle for the independent and parallel control strategies is similar. The independent strategy enables up to 1.79% higher efficiency in every driving condition, except for when the truck is fully loaded to 64000 kg and is operating in city traffic. In that case, it was found that the parallel control strategy achieved 1.09% higher efficiency.

Keywords: Gear Selection, Dual Electrified Axles, Heavy Duty Vehicle, Truck Propulsion System

Acknowledgements

We would like to express our deepest gratitude to everyone who has supported us throughout the course of this M.Sc thesis project. First and foremost, we extend our heartfelt thanks to our supervisors at Volvo, Jakob Samuelsson and Andreas Magnusson. Your expertise and support have been invaluable in navigating the complexities of our research. We are profoundly grateful for your input during the project. Additionally, we would like to thank Xavier Huin at Volvo, whose assistance with the simulation aspects of the project has been greatly appreciated.

Finally, we express our sincere appreciation to our supervisor and examiner, Jonas Fredriksson, for your regular supervision and insightful feedback. Your dedication and commitment to our academic growth have been instrumental in shaping the direction and outcome of this thesis.

Thank you all for your unwavering support and guidance.

Emil Alexsson & Shamith Satish, Gothenburg, June 2024

List of Acronyms

Below is the list of acronyms that have been used throughout this thesis listed in alphabetical order:

BEV	Battery Electric Vehicle
EM	Electric Machine
EMF	Electromotive Force
ESS	Energy Storage System
EU	European Union
FD	Final Drive
GB	Gearbox
HDV	Heavy Duty Vehicle
MDS	Motor Drive System
RPM	Revolution Per Minute
US	United States

Nomenclature

Below is the nomenclature of indices, sets, parameters, and variables that have been used throughout this thesis.

Parameters

P_{out}	Output power
P_{in}	Input power
P_{loss}	Loss power
P_{Mech}	Mechanical power
P_{EMLoss}	EM power loss
$P_{InvLoss}$	Inverter power loss
ω_{EM}	Speed of EM
η_{tot}	Total Efficiency
η_{ESS}	Efficiency of ESS
η_{MDS}	Efficiency of MDS
η_{GB}	Efficiency of GB
η_{FD}	Efficiency of FD
η_{EM}	Efficiency of EM
T_{EM}	EM Torque
G_{eff}	Efficiency of gear
G_{Coeff}	Co-efficient of gear
T_{out}	Output torque
T_{in}	Input torque
$V_{vehicle}$	Vehicle speed
r_{wheel}	Wheel radius
T_{wheel}	Wheel Torque

Variables

i	Gear ratio
i_1	Gear ratio of gear 1
i_2	Gear ratio of gear 2
i_3	Gear ratio of gear 3
i_4	Gear ratio of gear 4
i_{FD}	Gear ratio of final drive
ϵ_{sat}	Satellite filter amplitude
$G_{LP}(s)$	Transfer function for this derivative low-pass filter
$k_d(s)$	Gain of low pass filter
T_d	Time Constant of low pass filter

Contents

List of Figures

List of Tables

1
Introduction

Since the advent of commercial vehicles on the road, there has been a continuous evolution of technology. In recent years, this trajectory of technological advancement has taken a significant turn towards electrification to achieve sustainable transport goals. This shift has given the possibilities for building more efficient propulsion systems. One such innovative approach is the concept of electric axles. This thesis project is centered around the concept of the dual electric axle with dual motors on each axle for heavy-duty vehicles. The thesis aim is to explore the gear shifting sequence possibilities with multi speed transmission for better overall vehicle efficiency.

1.1 Background

Internal combustion engine propulsion systems have traditionally been powering the heavy-duty vehicle (HDV) sector. Considering the environmental impact, the demand for sustainable alternatives has risen and has led to the electrification of the propulsion system. Electrification opens up new powertrain designs, like the introduction of electric axles. Furthermore, the purpose of using multiple-speed transmissions has risen to accommodate heavy-duty vehicles' torque requirements efficiently. This approach is aimed to meet the performance demands of heavy loads but also to enhance energy efficiency by optimizing gear ratios for varying driving conditions.

1.1.1 Electrification

The heavy-duty vehicle (HDV) sector, which includes trucks and busses, has historically been powered by internal combustion engines (ICEs), which emit CO_2 from the combustion of fossil fuels. In 2022, the HDV sector emitted 2282 million metric tonnes of tailpipe CO_2 globally [1]. As the total emitted tailpipe emissions from road transport was 5870 million metric tonnes in 2022, the HDV sector stood for 38.9% of the total CO_2 emissions [2]. Since CO_2 is a greenhouse gas emission that affects climate change towards a warmer climate, the demand for more sustainable propulsion systems than the conventional ICE has increased both from consumers and due to legislation [3]. Therefore, HDV manufacturers have begun *electrifying* trucks by developing electric propulsion systems with zero tailpipe emissions to replace products in their existing segments [4].

1.1.2 Electrified Axles

The common parts in a battery electric vehicle (BEV) propulsion system typically consist of the battery pack(s), inverter(s), electric machine(s), and power electronics such as control modules for auxiliary components and chargers, etc [5]. As the components are connected through cables with only a few mechanical connections, they can be packaged in various *configurations*. When manufacturers began electrifying trucks, a *central drive system* configuration was often opted for because of similarities with a conventional ICE configuration, see Figure 1.1, [6].

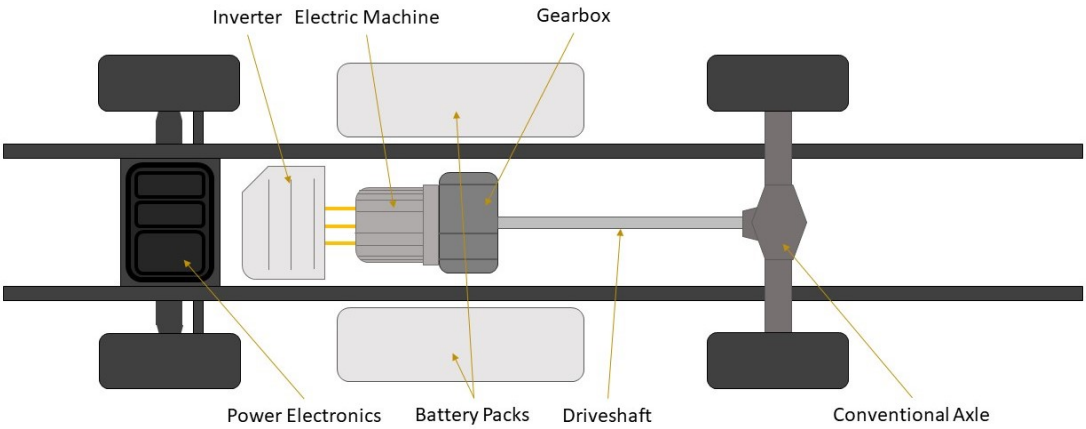

Figure 1.1: Illustration of a truck with a central drive system configuration, [5].

As seen in Figure 1.1, the electric machine(s) drives a conventional axle through a gearbox and a driveshaft while the battery packs are mounted on the side of the chassis. The power electronics, inverter, and electric machine, are packaged in the location of the ICE and transmission in a conventional ICE truck layout. The batteries are packaged on the sides of the frame where fuel tanks and storage compartments would typically be mounted. Therefore, the driveshaft and drive axle can be carried over from a conventional ICE truck while the batteries replace the fuel tanks, which simplifies the development. As research on electrification has proceeded, another configuration has been developed with fewer similarities to a conventional ICE configuration, see Figure 1.2 for illustration.

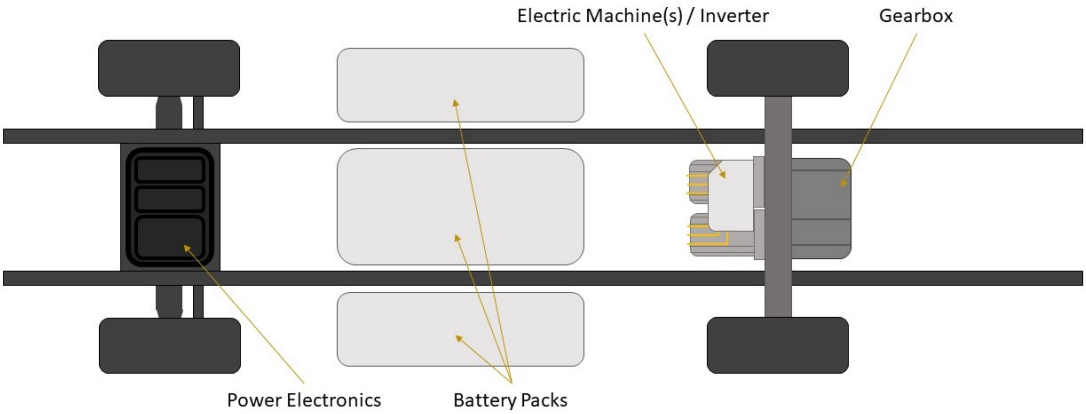

Figure 1.2: Illustration of a truck with an electrified axle configuration. [5]

This configuration is called an *electrified axle* where the inverter(s), electric machine(s), gearbox, differential, and axle are integrated into one unit. There are a number of benefits of this configuration over the central drive system, since there is no driveshaft, battery packs can be packaged in the middle of the truck as well as the sides if needed. This configuration is also more compact with fewer moving parts, which simplifies the propulsion system and potentially makes it cheaper than a central drive system [7].

1.1.3 Dual Driven Axles

This thesis work will be centered on heavy-duty truck applications where two electrical axles are utilized. This axle configuration is commonly called a *dual* or *tandem* axle, and the nomenclature for these heavy-duty truck types is typically the number of wheels in total and the number of driven wheels separated by an "X", e.g., 6X4, 8X4 and 10X4. The relevant applications for this propulsion system layout are all applications where four driven wheels are desired for better traction than a two wheel driven propulsion system. One large market for dual axles is the United States [11], where the maximum axle weight limit is 9000kg compared to EU's 11500kg limit. Due to this legislation, dual axles are preferred to allow for higher loads, [12] [13].

In a central drive unit propulsion system, both axles in a dual axle configuration are sent power from the same engine/electric machine and gearbox. However, with electrified axles, each axle is powered by its own electric machine(s) which enables them to operate at different gear ratios. This means that for one axle, the electric machine(s) might operate at a certain operating point while the electric machine(s) in the other axle are operating at a completely different operating point. Since the operation points of electric machines greatly affect their energy efficiencies, it is interesting from a research point of view to evaluate if this ability could be taken advantage of with a control system.

1.1.4 Electric Heavy-duty Vehicle Gearbox

The ideal torque-speed and power characteristics of a typical electrical machine used for automotive use are illustrated in Figure 1.3. From standstill to the field weakening region, the maximum torque is constant. When the speed of the electric machine reaches the field weakening region, the maximum torque reduces, and the maximum power remains constant. This is due to the fact that the electric machine starts producing a counteracting electric magnetic field because of the motor speed, called back-EMF [10].

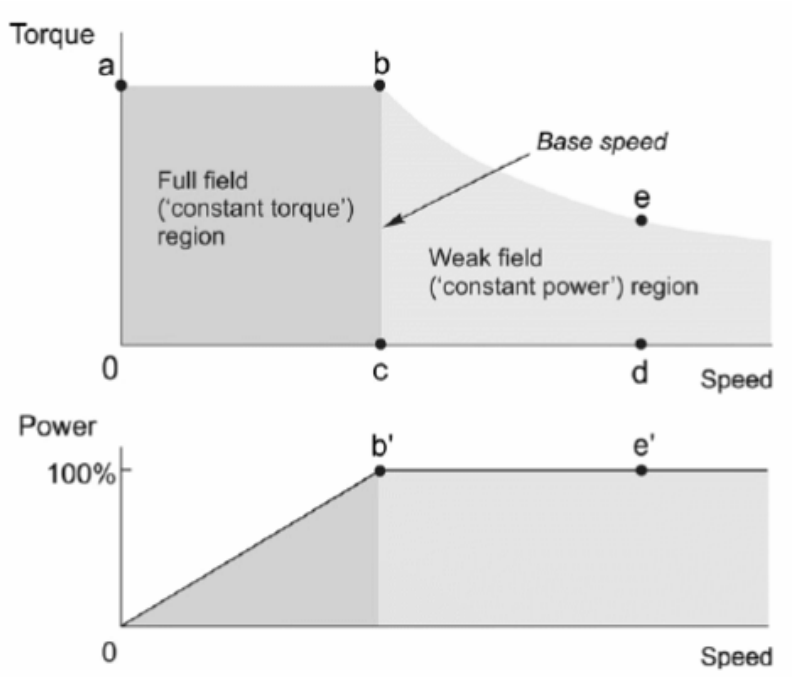

Figure 1.3: Illustration of torque, speed and power characteristics of an automotive electric machine. [10]

For lighter vehicles, such as cars or motorcycles, one single-gear reduction between the electric machine and the driven wheels is typically used. The electric machine's constant torque from standstill and relatively high maximum rotational speed can often be matched to a gear ratio that results in satisfactory acceleration and top speed. However, for heavy-duty vehicles hauling heavy loads from standstill to highway speeds, the torque requirement to the wheels is significantly larger. If a single gear reduction is to be used in this application, the electric machine would either need to be very large or rotate very fast. Therefore, it is relevant for heavy vehicle manufacturers to utilize a gearbox with multiple gear ratios to ensure high torque at low speeds while being able to coast at high speeds and lower torque, [8].

1.2 Propulsion System Layout

The dual electrified axle layout that will be studied in this thesis work is shown in Figure 1.4. It utilizes two identical electrified axles with two identical electric machines each: *EM1*, *EM2*, *EM3*, and *EM4*. The two electric machines on each axle are connected to their own *gearset*, consisting of two gears and a neutral position. The output shafts of the gearsets are connected to a shared output shaft, which in turn drives the final drive, ultimately propelling the wheels.

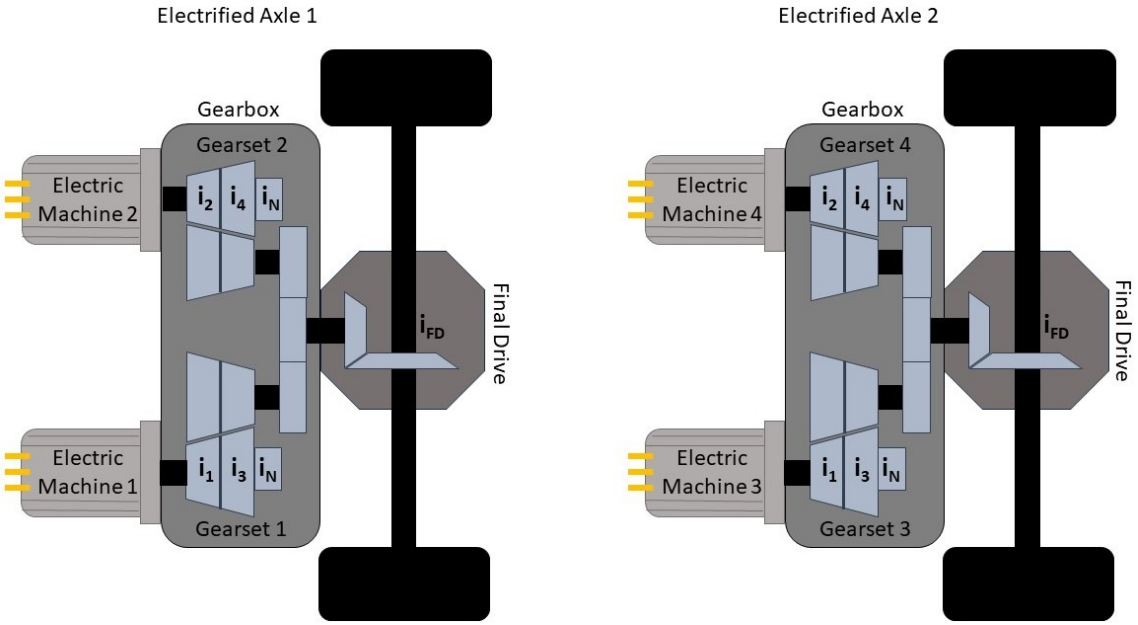

Figure 1.4: Layout of the dual electric axle propulsion system.

The gearsets driven by the odd motors, EM1 and EM3, have the gears i_1, i_3, and the neutral position, i_N. The even motors, EM2 and EM4, drive a gearset with the gears i_2 and i_4 as well as a neutral position, i_N. The gear ratios follow the enumeration, meaning that i_1 has the lowest gear ratio, i.e., highest torque and lowest speed, and i_4 has the highest gear ratio, i.e., lowest torque and highest speed. This means that each axle has a total of 9 theoretical gear combinations, of which 8 are physically possible. The combination of axle state using gear ratios i_4 and i_1 is neglected due to the substantial difference between these gear ratios. As a result, if this combination is used, the electric machine engaged to i_1 would be operating near its maximum speed limit, while the other electric machine would be operating at very low speeds. To simplify referencing, each gear combination within one axle is defined as an *axle state*, as shown in Table 1.1.

Table 1.1: Table of the axle states, where the impossible combination of i_1 and i_4 is marked with X.

Axle State	**0**	**1**	**2**	**3**	**4**	**7**	**8**	**9**	**X**
EM2/4 Gear	N	N	2	N	4	2	2	4	4
EM1/3 Gear	N	1	N	3	N	1	3	3	1

Since there are two axles with 8 possible axle states each, there is a total of 64 theoretical axle state combinations when both axles are considered. These axle state combinations are simply referred to as *states* in this report. Of the 64 theoretical states, 21 are given as relevant states to evaluate for the scope of this project. See Table 1.2.

Table 1.2: Table of the states to evaluate.

State	**0**	**1**	**2**	**3**	**4**	**7**	**8**	**9**	**11**	**22**	**33**	**44**	**71**	**72**	**82**	**83**	**93**	**94**	**77**	**88**	**99**
A1 State	0	1	2	3	4	7	8	9	1	2	3	4	7	7	8	8	9	9	7	8	9
A2 State	0	0	0	0	0	0	0	0	1	2	3	4	1	2	2	3	3	4	7	8	9

1.2.1 Independent Control Strategy

As seen in Table 1.2, some states do not share axle states between the axles, utilizing the capability to control each axle independently. For example, state 71 engages state 7 on axle 1 and state 1 on axle 2, resulting in gears 1 and 2 being engaged on axle 1, while only gear 1 is engaged on axle 2, see Figure 1.5. In the project, a control system capable of sending independent demands to the axles is referred to as the *independent control strategy*. The independent control strategy can utilize all 21 states shown in Table 1.2.

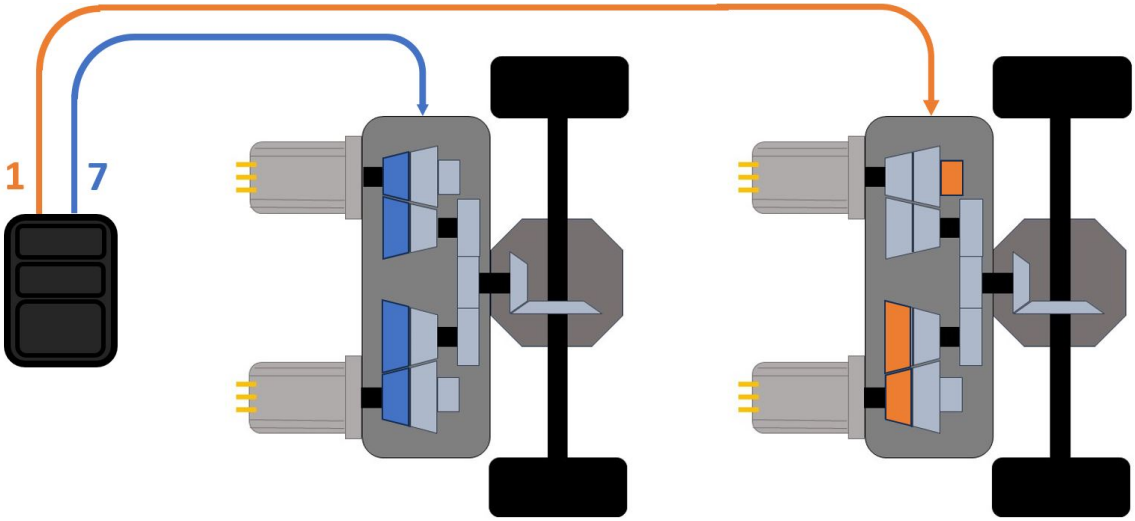

Figure 1.5: Illustration of the independent control strategy engaging state 71.

1.2.2 Parallel Control Strategy

To evaluate the benefits of the independent control strategy, a simplified control strategy is defined for comparison. The control system, referred to as the *parallel control strategy*, can only send identical signals to both axles. Consequently, the parallel control strategy utilizes only states 0, 11, 22, 33, 44, 77, 88, and 99, see Figure 1.6 for an example where state 77 is demanded from the control system.

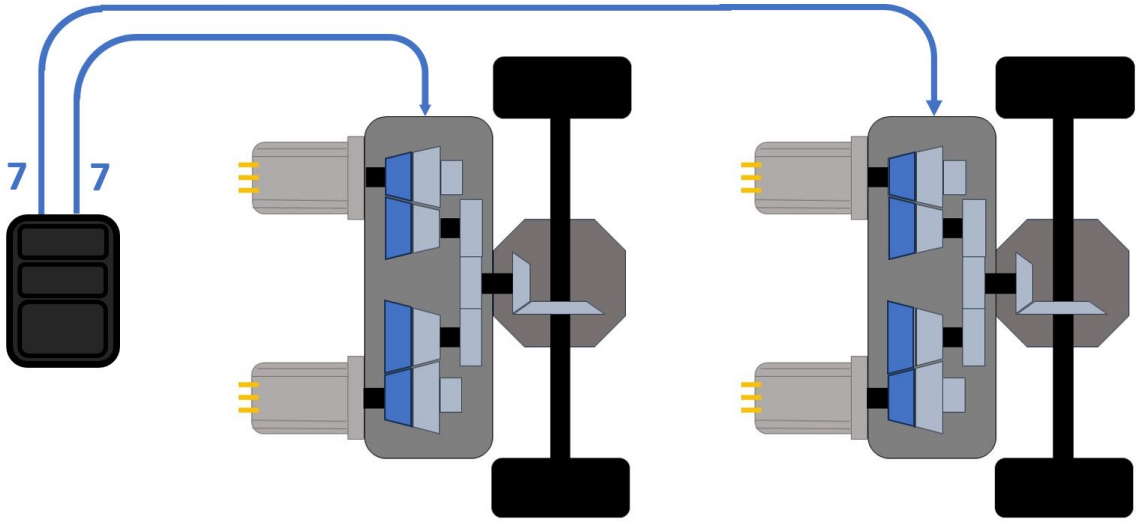

Figure 1.6: Illustration of the parallel control strategy engaging state 77.

1.3 Simulation Environment

The thesis work is carried out using MATLAB/Simulink as the modeling and simulation tool. MATLAB Simulink is commonly used in the automotive industry due to its model-based systems engineering (MBSE) capabilities. MBSE is a development method where hardware is represented by digital models, enabling developers to test systems and adjust parameters virtually. This approach is particularly advantageous for systems with numerous components, such as a heavy-duty truck. At the outset of the thesis work, a MATLAB/Simulink model of a heavy-duty truck equipped with all hardware for the propulsion system layout presented in Section 1.2 had been developed at Volvo Trucks. The model comprises the complete propulsion system and is enabled to run a variety of drive cycles. The input and output parameters of the state selection control system are illustrated in Figure 1.7. [17]

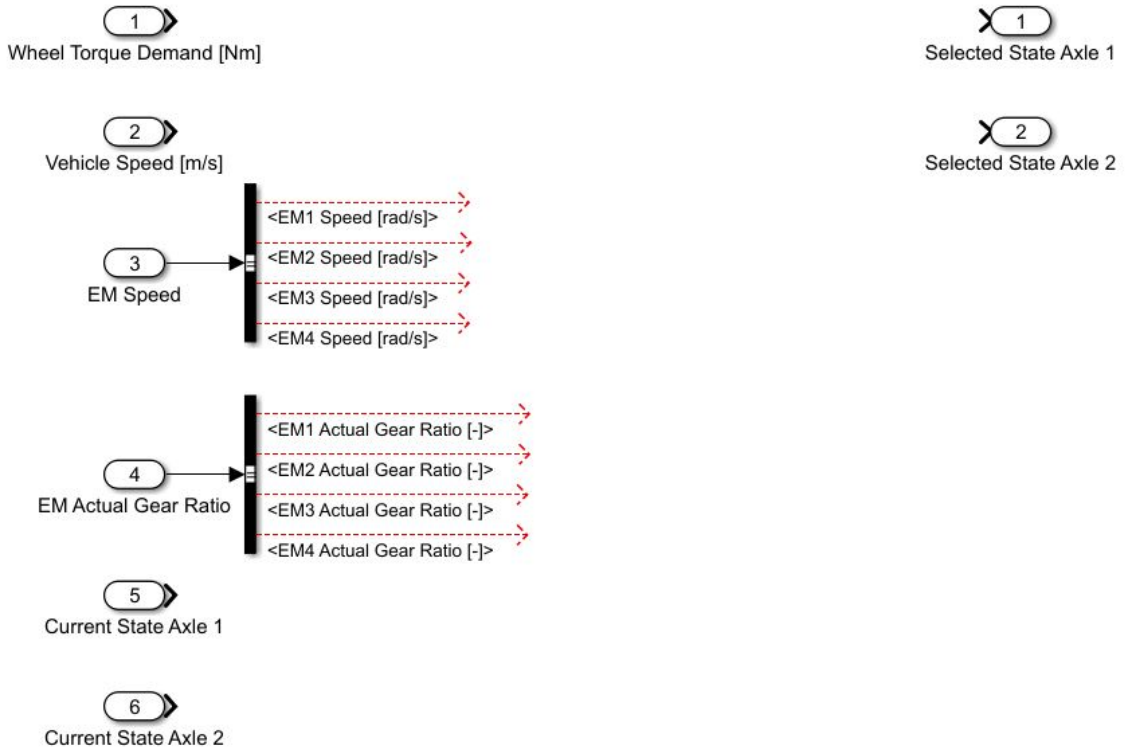

Figure 1.7: Illustration of input and output parameters of the state selection control system.

1.4 Aim

This thesis aims to investigate optimal control strategies for dual electrified axles regarding energy efficiency. Each electrified axle has a gearbox with multiple gear ratios as well as two electric machines. A control strategy for the gear selection of these axles will be developed and evaluated against energy efficiency and torque delivery. The strategy should select a gear for each axle which operates the electric machines in an optimal way given a wide range of operating conditions while enabling the axles to be individually controlled. Additionally, an alternate control system will be developed in which both axles are controlled by the same kind of single, where both axles have the same kind of gear selection and work as one unit. This control approach will be developed to evaluate the benefits of individually controlled gear selection.

1.5 Limitations

To streamline the work and make the thesis more concise, a set of limitations has been established. The gearbox layout, including fixed gear ratios, is predefined as described earlier. Specifications for the electric machines, gearboxes, and all other propulsion system components are also predetermined. Each electric machine has its own inverter and can operate independently. The two electric axles are identical

in terms of motor specifications and gear ratios. Torque distribution is computed using an existing model, which divides the wheel torque demand equally between the electric machines. Lastly, the thesis project will evaluate the performance of the gear selection strategy using three truck masses and three drive cycles.

1.5.1 Electrified Axle Layout

The layout of the dual electrified axle propulsion system is predefined as explained in Section 1.2. The number of gears for each electric machine is pre-determined, and there is no flexibility in changing the number of gears or the gear ratios. The section also defines the states that this thesis is limited to evaluating.

1.5.2 Propulsion System Components

The propulsion system's hardware is predefined, as it is already modeled in the simulation environment. The system consists of models for the battery, battery management system, inverters, electric machines, gearboxes, final drives, and wheels.

1.5.3 Torque Distribution

An existing model for distributing torque to the active electric machines is utilized. In this model, the wheel torque demand is divided equally among the active electric machines. The torque for each machine is then calculated based on the selected gear ratios and the proportioned wheel torque. Consequently, each activated electric machine produces the same amount of power.

1.5.4 Truck Mass

Three different truck masses are considered to evaluate the performance of the gear selection strategy. A truck mass of 18000 kg is considered for a light truck tractor without a trailer, while two different truck masses are considered for a truck with a trailer configuration; 35300 kg and 64000 kg.

1.5.5 Driving Cycles

Ideally, the gear selection strategy should be evaluated against all possible driving scenarios to guarantee its optimal functionality across various conditions. However, conducting simulations for each conceivable scenario is a time-intensive process, and given the project's time constraints, it becomes impractical to explore every possible driving situation. Consequently, the evaluation is streamlined to focus on three drive cycles.

The *City Drive Cycle* is a 4.5 km drive cycle designed to simulate city driving conditions characterized by low speeds and stops at stop signs or traffic lights.

The *EU Highway Drive Cycle* spans 120 km, simulating a scenario where a truck transitions from urban roads to the highway. The highway varies in inclination by

±5% and speed, with a maximum speed of 85 km/h which is the maximum speed limit allowed for heavy-duty trucks in the EU [15].

The *US Highway Drive Cycle* simulates 140 km where initial is urban driving followed by highway conditions similar to the EU Highway Drive Cycle, but with cruise speeds up to 70 mph, or 113 km/h, which is a common maximum speed limit allowed for heavy-duty trucks in most US states [16].

1.6 Outline of thesis

The subsequent chapters of this report detail the comprehensive workflow of the thesis:

- Chapter 2 - Methodology: This chapter outlines the methodology employed in the thesis work, including the considerations adopted for developing the control strategy. It details the development of the Simulink model used to implement these control strategies.

- Chapter 3 - Results: This chapter presents the results derived from the methodologies and Simulink model developed in the previous chapter. It discusses various test cases used to evaluate the model.

- Chapter 4 - Discussion: This chapter discusses the methodologies used and the results obtained. It analyzes the findings, highlighting the insights they provide.

- Chapter 5 - Conclusion: The final chapter consolidates all the information presented in the previous chapters and summarizes the thesis. It aims to synthesize the key findings and underscore their relevance to the field.

2

Methods

This chapter outlines the methodology used to investigate gear selection strategies for dual electrified axles. It covers the evaluation of propulsion system components to include in the efficiency map used for this project, as well as the iterative process to generate the state selection map. Finally, the methods for implementing the state selection map in Simulink are explained in detail.

2.1 Efficiency Map

As mentioned earlier, the aim of this thesis is to investigate gear selection strategies for dual electrified axles with respect to energy efficiency. Each component in the electric drive system has a power loss, which is due to factors such as electrical resistance or mechanical friction, for example. The efficiency of each component is determined by the output and input power according to:

$$\eta = \frac{P_{out}}{P_{in}} = \frac{P_{in} - P_{loss}}{P_{in}} \tag{2.1}$$

where η is the efficiency, P_{out} is the output power, P_{in} is the input power, and P_{loss} is the power loss of the system. The propulsion system of each electrified axle consists of a train of components as illustrated in Figure 2.1. The energy is supplied by the Electric Storage System (ESS), which consists of a model of a battery that outputs voltage and current to the Motor Drive System (MDS). The MDS consists of the inverter and the electric machine which outputs torque and output shaft speed to the mechanical propulsion system. The mechanical propulsion system consists of a gearbox, final drive, and wheel model where the mechanical losses are due to friction.

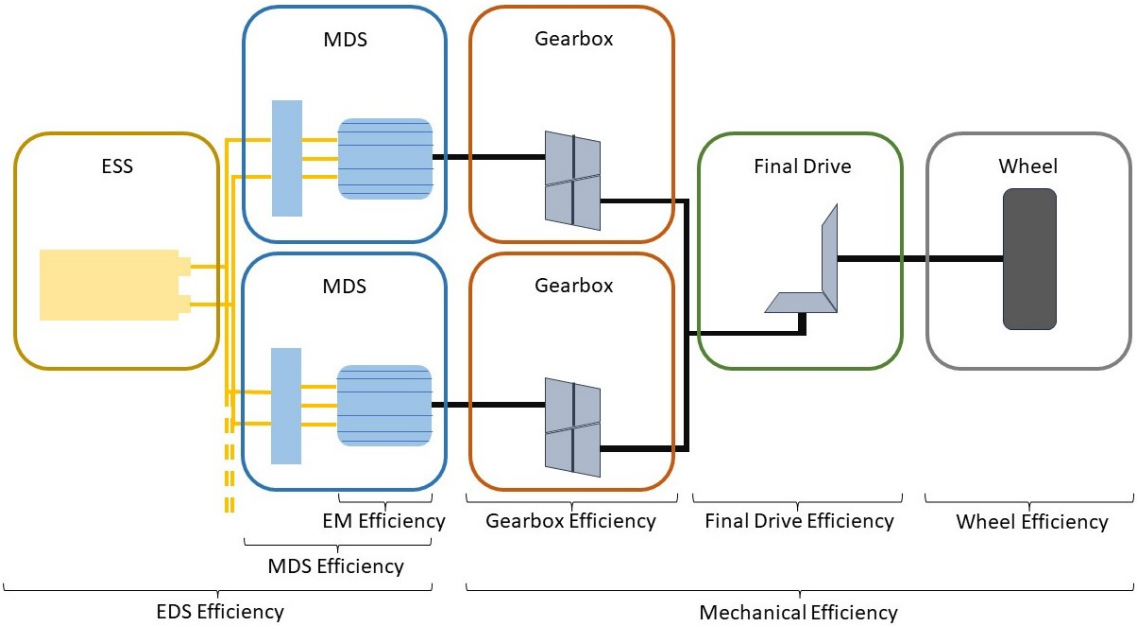

Figure 2.1: Illustration of one electrified axle's components in the Simulink model.

Since the components in the propulsion system are connected in series, the total efficiency can be divided into intermediate steps according to:

$$\eta_{tot} = \eta_{ESS} * \eta_{MDS} * \eta_{GB} * \eta_{FD} * \eta_{wheel} \tag{2.2}$$

where η_{tot} is the total efficiency, η_{ESS} is the efficiency of the ESS, η_{MDS} is the efficiency of the MDS, η_{GB} is the gearbox efficiency, η_{FD} is the final drive efficiency and η_{wheel} is the efficiency of the wheel model. To optimize the gear selection, only the components whose efficiency is affected by the rotational speed and torque of the electric machines are of interest. Starting from the right side in Figure 2.1, the wheel speed and torque demand follow the drive cycle and will remain unaffected by the gear selection, resulting in a wheel efficiency independent of what gears are engaged. The same principle applies to the final drive, which connects directly to the wheels and remains unaffected by gear selection in terms of torque output or rotational speed. However, the gearbox efficiency is largely dependent on the gear selection since the gears change the input shaft speed and torque throughput, which in turn affects the losses due to friction. Since the gear selection affects the rotational speed and torque output of the electric machine, the efficiencies of the electric machines are also largely dependent on the gear selection. The same is true for the inverter, which changes its output voltage and current depending on the speed and torque of the electric machine. The ESS however, will output a steady voltage and vary the current depending on the power demand of the inverters. The ESS efficiency is therefore linked to the drive cycle's power demand rather than the operation points of the electric machines, and can therefore be neglected for the gear selection.

Ideally, the gear selection would be optimized with respect to the efficiency of the inverter, electric machine, and gearbox. However, due to that the inverter is intertwined with the MDS, the MDS efficiency map is difficult to obtain. An attempt

to obtain the MDS efficiency is shown in Appendix A.1.1, which was deemed unreliable due to that the model is dependent on various environmental factors, such as ambient temperature, that can alter the result.

Thus, the gear selection is to be optimized with respect to the electric machine efficiency and gearbox efficiency. In this chapter, a method for extracting *efficiency maps* for these components is presented. An efficiency map can be seen as a matrix wherein each element represents the efficiency at a specific operating point, defined by the rows and columns representing the torque and rotational speed. By using the minimum and maximum torque and speed as the endpoints, the efficiency map covers all operating points:

$$\boldsymbol{\eta} = \begin{vmatrix} \eta_{T_1,\omega_1} & \eta_{T_1,\omega_2} & \cdot & \cdot & \eta_{T_1,\omega_n} \\ \eta_{T_2,\omega_1} & \cdot & & & \\ \cdot & & \cdot & & \\ \cdot & & & \cdot & \\ \eta_{T_n,\omega_1} & & & & \eta_{T_n,\omega_n} \end{vmatrix} \tag{2.3}$$

2.1.1 Electric Machine

The losses from the electric machines are highly dependent on the gear selection since it affects the rotational speed and torque output. An efficiency map used to compute the losses exist in the electric machine Simulink model, see Figure 2.2. This is a 42x21 matrix with rotational speed on the X-axis and torque on the Y-axis. The field weakening region is not defined in this matrix, but two vectors for maximum positive and negative torque are also available. As seen in Figure 2.2, the maximum positive and negative torque is 500 Nm, and the maximum rotational speed is 10,000 rpm. To standardize future data processing, the efficiency map is re-scaled to a square 50x50 matrix.

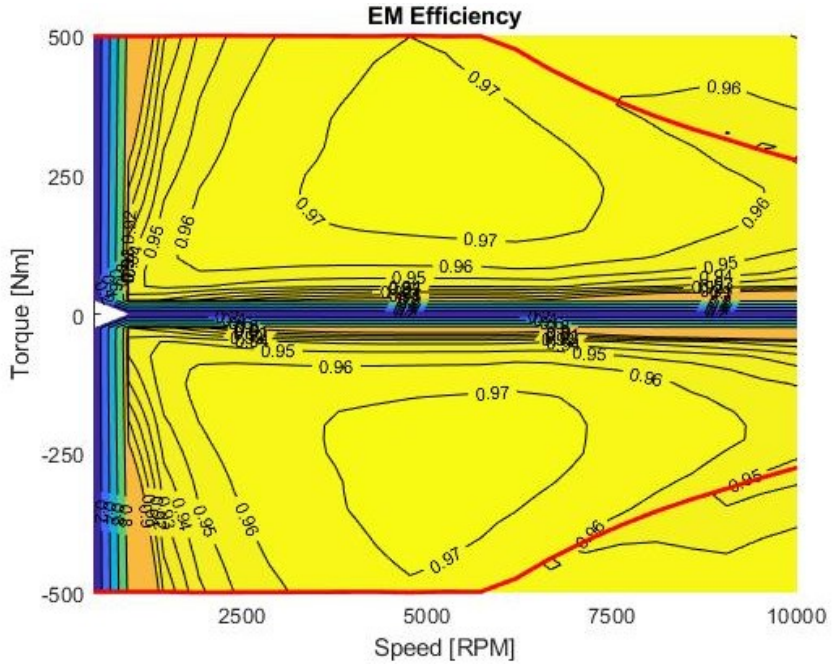

Figure 2.2: 42x21 efficiency matrix from Simulink model of electric machine

2.1.2 Mechanical Efficiency

The gearbox losses highly depend on the gear selection since the gear ratio determines the speed and torque on the input shaft bearings and gears. In the existing Simulink model of the transmission system provided by Volvo, the gearbox losses are calculated by the input shaft speed and torque using two constants, G_{eff} and G_{coeff}, which are defined for each gear. The output shaft torque T_{out} is calculated using the input shaft torque T_{in}, the gear ratio i for the selected gear, and the input shaft speed w_{in} according to:

$$T_{out} = T_{in} * i * G_{eff} - \frac{(\omega_{in} * \frac{30}{\pi})^{1.7} * G_{coeff}}{\omega_{in}}. \tag{2.4}$$

To convert the torque loss to efficiency, the gearbox efficiency η_{GB} is defined according to:

$$\eta_{GB} = \frac{P_{out}}{P_{in}} = \frac{T_{out} * \omega_{out}}{T_{in} * \omega_{in}} = \frac{T_{out}}{T_{in} * i} \tag{2.5}$$

and by combining (2.4) and (2.5), the gearbox efficiency is calculated according to:

$$\eta_{GB} = \frac{T_{in} * G_{eff} * i}{T_{in} * i} - \frac{(\omega_{in} * \frac{30}{\pi})^{1.7} * G_{coeff}}{\omega_{in} * T_{in} * i} = G_{eff} - \frac{(\omega_{in} * \frac{30}{\pi})^{1.7} * G_{coeff}}{\omega_{in} * T_{in} * i} \tag{2.6}$$

Using (2.6), the motor efficiency map can be processed to include the gearbox efficiency for each selected gear. This is done by first defining a $50x50$ speed matrix and a 50x50 torque matrix, $\boldsymbol{\omega}_{in}$ and $\boldsymbol{T}_{in}$, where each column represents the rotational speed of the electric machine from zero to maximum speed and each row

represents the torque from maximum negative to maximum positive torque. Then, an element-wise operation is done to produce the gearbox efficiency matrix $\boldsymbol{\eta}_{GB}$ according to:

$$\boldsymbol{\omega}_{in} = \begin{vmatrix} \omega_1 & \omega_2 & . & . & \omega_{50} \\ \omega_1 & . & & & \\ . & & . & & \\ . & & & . & \\ \omega_1 & & & & \omega_{50} \end{vmatrix} \quad \boldsymbol{T}_{in} = \begin{vmatrix} T_1 & T_1 & . & . & T_1 \\ T_2 & . & & & \\ . & & . & & \\ . & & & . & \\ T_{50} & & & & T_{50} \end{vmatrix}$$

$$\boldsymbol{G}_{eff} = \begin{vmatrix} G_{eff} & G_{eff} & . & . & G_{eff} \\ G_{eff} & . & & & \\ . & & . & & \\ . & & & . & \\ G_{eff} & & & & G_{eff} \end{vmatrix}$$

$$\boldsymbol{\eta}_{GB}(i) = \boldsymbol{G}_{eff} - \frac{(\boldsymbol{\omega}_{in} \cdot \frac{30}{\pi})^{1.7} \cdot G_{coeff}}{\boldsymbol{T}_{in} \cdot \omega_{in} \cdot i} = \tag{2.7}$$

$$\begin{vmatrix} \eta_{GB_{1,1}} & \eta_{GB_{1,2}} & . & . & \eta_{GB_{1,50}} \\ \eta_{GB_{2,1}} & . & & & \\ . & & . & & \\ . & & & . & \\ \eta_{GB_{50,1}} & & & & \eta_{GB_{50,50}} \end{vmatrix}$$

The resulting matrices $\boldsymbol{\eta}_{GB}(i)$ represents the gearbox efficiency for a specific gear at each operation point of the electric machine in the same 50x50 matrix format as the efficiency map.

2.1.3 Total Efficiency Map

The efficiency map representing the combined efficiency of the electric machines and the gearbox, $\boldsymbol{\eta}_{tot}$, is calculated by element-wise multiplication:

$$\boldsymbol{\eta}_{tot} = \boldsymbol{\eta}_{EM} \cdot \boldsymbol{\eta}_{GB}(i) = \begin{vmatrix} \eta_{EMGB_{1,1}} & \eta_{EMGB_{1,2}} & . & . & \eta_{EMGB_{1,50}} \\ \eta_{EMGB_{2,1}} & . & & & \\ . & & . & & \\ . & & & . & \\ \eta_{EMGB_{50,1}} & & & & \eta_{EMGB_{50,50}} \end{vmatrix} \tag{2.8}$$

2.2 State Selection Map

The previously defined total efficiency maps, $\boldsymbol{\eta}_{tot}(i)$, are used as the foundation for the gear selection strategy. Neglecting operating points with lower efficiency than a certain efficiency value, or *efficiency threshold*, constructs *efficiency islands*. Based

on these efficiency islands and the gear ratios, *gear operation islands* can then be constructed, specifying at which wheel torques and vehicle speeds each gear can operate. Since each state is a combination of one or multiple gears, the gear operation islands are then utilized to construct the *state operation islands* for each state. When all state operation islands are defined for a certain efficiency threshold, these are overlaid on each other to form the *state selection map*, where each element represents an operating point containing the possible states at the efficiency threshold.

Once the state operation islands are defined for a given efficiency threshold, they are overlaid to create the so-called state selection map. In this map, each element is a vector representing an operating point and contains the possible states that meet the specified efficiency threshold.

By incrementally raising the efficiency threshold from 0-100% while constructing a new state selection map at each increment, the most efficient states at each operating point are determined by overwriting the previous state selection map at every operating point containing one or more possible states.

2.2.1 Efficiency Islands

For the gear shifting strategy to be efficient, the efficiency map of the electric drive system (including mechanical losses) is divided into *efficiency islands*, where an efficiency island is a region of an efficiency map where all operating points are above a specified *efficiency threshold*.

A logic matrix is generated by comparing the threshold with the complete efficiency map, using the less-than operator. The efficiency island matrix $\boldsymbol{\eta}_{isl}$ is constructed by first making a copy of the efficiency map $\boldsymbol{\eta}_{tot}$ and then using the logic matrix to exclude all values less than the threshold efficiency by replacing these values with NaN values:

$$\boldsymbol{\eta}_{isl} = \begin{vmatrix} NaN & NaN & NaN & . & NaN \\ NaN & \eta_{tot_{2,1}} & . & & \\ \eta_{tot_{2,1}} & . & \eta_{tot_{2,1}} & & \\ . & & & . & \\ NaN & & & & NaN \end{vmatrix} \tag{2.9}$$

With this method, any efficiency threshold can be used to construct an efficiency island. See Figure 2.3 for a plot of multiple efficiency islands derived using the described method.

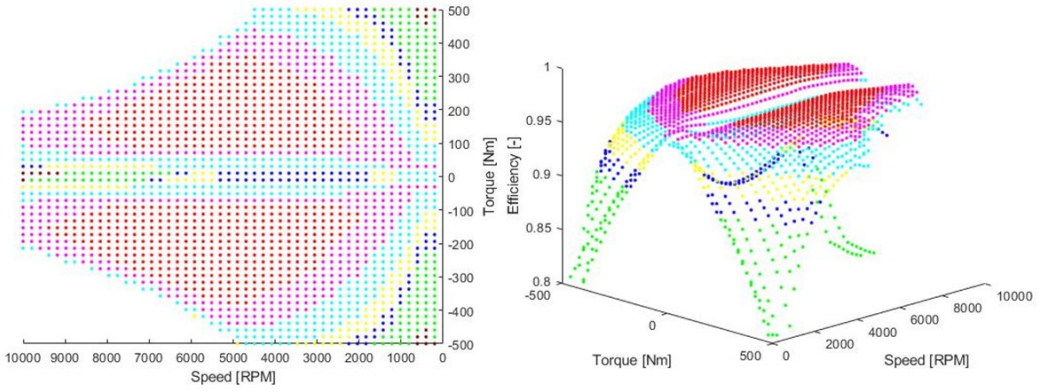

Figure 2.3: Plot of efficiency map with multiple efficiency islands differentiated by color.

2.2.2 Gear Operation Island

The efficiency islands define the motor speeds and torque an electric machine can operate at while ensuring that the propulsion system operates above a certain efficiency threshold. For a given gear, the motor's rotational speed and torque can be translated to vehicle speed and wheel torque according to:

$$v_{vehicle} = \frac{w_{EM}}{i_{gear} * i_{FD}} * r_{wheel} \tag{2.10}$$

$$T_{wheel} = T_{EM} * i_{gear} * i_{FD} \tag{2.11}$$

where w_{EM} and T_{EM} is the rotational speed and torque of the electric machine, i_{gear} and i_{FD} is the gear ratio for the selected gear and for the final drive, and r_{wheel} is the wheel radius. The operating points of a specific efficiency island can thus be scaled to vehicle speeds and wheel torque if the gear ratios and wheel dimensions are known. See Figure 2.4 for a plot of the vehicle speed and wheel torque operation points for EM1 engaged to gear 1 operating on the 97% efficiency island. This represents a *gear operation island*, $\mathbf{A}_{GOI}$, for gear 1 at 97% efficiency.

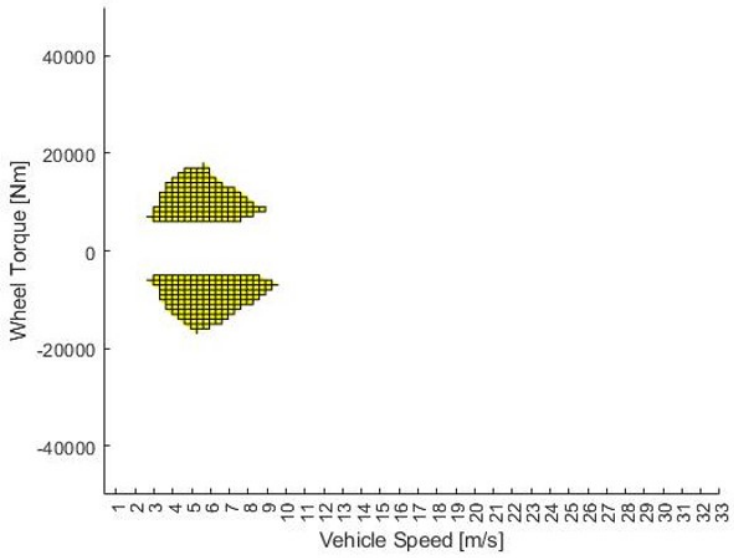

Figure 2.4: Gear operation island, $\mathbf{A}_{GOI}$, for EM1 engaged to gear 1 and 97% efficiency.

The core of the gear operation islands is two matrices, $\boldsymbol{\omega}$ and $\boldsymbol{T}$, which represent motor speeds and motor torque for all operating points of a selected gear. $\boldsymbol{w}$ and $\boldsymbol{T}$ are in turn constructed by two vectors, $\boldsymbol{v}$ and $\boldsymbol{T}_W$ supported by a vector of ones, $\boldsymbol{V}_1$:

$$\boldsymbol{v} = [0 \dots v_{max}] \tag{2.12}$$

$$\boldsymbol{T}_W = [-T_{W,max} \dots T_{W,max}] \tag{2.13}$$

$$\boldsymbol{V}_1 = [1 \dots 1] \tag{2.14}$$

where $\boldsymbol{v}$ is a vector incrementing from 0 to the maximum vehicle speed, v_{max}, which defines the X-axis of the map for the gear operation island. In this case, v_{max} is set to 34 m/s, which is equal to 122.4 km/h or 76.1 mph, which is higher than the maximum legal speed in the EU as well as in the US for heavy-duty trucks, [15] and [16]. The number of increments defines the resolution of the map of the gear operation island and can be varied, but in this project, 100 increments are used. $\boldsymbol{T}_W$ is a vector containing the wheel torque from the electric machine, incrementing from the maximum negative wheel torque to the maximum positive wheel torque. This vector defines the Y-axis of the map for the gear operation island, containing 100 increments to produce a square 100x100 matrix. V_1 is a vector of ones with 100 indices, which is used to produce the matrices $\boldsymbol{\omega}$ and $\boldsymbol{T}$ according to:

$$\boldsymbol{\omega} = \boldsymbol{v} \cdot \boldsymbol{V}_1^{\intercal} \cdot \frac{30 * i_{FD} * i_{gear}}{\pi * r} = \tag{2.15}$$

$$\begin{vmatrix} 0 & . & . & \omega_{v_{max}} \\ . & . & & \\ . & & . & \\ 0 & & & \omega_{v_{max}} \end{vmatrix}$$

$$\boldsymbol{T} = \boldsymbol{T}_W^{\intercal} \cdot \boldsymbol{V}_1 \cdot \frac{1}{i_{FD} * i_{gear}} = \tag{2.16}$$

$$\begin{vmatrix} -T_{EM,T_{W,max}} & . & . & -T_{EM,T_{W,max}} \\ . & . & & \\ . & & . & \\ T_{EM,T_{W,max}} & & & T_{EM,T_{W,max}} \end{vmatrix}$$

The elements in $\boldsymbol{\omega}$ and $\boldsymbol{T}$ represent the theoretical rotational speed and torque of the electric machine when it is engaged to the gear with gear ratio i_{gear} at all vehicle speeds and wheel torques. To evaluate which of these operation points are within the specified efficiency island, the efficiency at each operating point is evaluated by using the built-in MATLAB function `griddata`, the efficiency map, and two additional vectors defining the axes of the efficiency map, V_w and V_T:

$$\mathrm{V}_w = [0 \dots w_{max}] \tag{2.17}$$

$$\mathrm{V}_T = [-T_{max} \dots T_{max}] \tag{2.18}$$

where V_w and V_T represent the rotational speeds and torques of the electric machine. The MATLAB function `griddata` outputs an interpolated matrix where each element represents the efficiency at each operation point, and if the operation point is outside of the efficiency island, it outputs NaN. This constructs the *gear operation island*, $\mathbf{A}_{GOI}$, for this particular gear, according to:

$$\mathbf{A}_{GOI} = \sim isnan(griddata(\mathrm{V}_w, \mathrm{V}_T, \mathbf{A}_{\eta_{isl}}, \mathbf{A}_w, \mathbf{A}_{T_W}) = \tag{2.19}$$

$$\begin{vmatrix} a_{1,1} & a_{1,2} & . & . & a_{1,n} \\ a_{2,1} & . & & & \\ . & & . & & \\ . & & & . & \\ a_{n,1} & & & & a_{n,n} \end{vmatrix}.$$

Each element, $a_{r,c}$, represents a vehicle speed and wheel torque and is a 1 or 0 depending on if the operating point of the electric machine is on the efficiency island or not.

2.2.3 State Operation Island

The truck configuration utilizes two identical electrified axles with two electric machines each which in turn can be engaged to two gears or neutral. For states that only activate one out of four electric machines, the gear operation island $\mathbf{A}_{GOI}$ is sufficient to define all operation points of the truck. However, for states that activate multiple electric machines, the $\mathbf{A}_{GOI}$ of each activated electric machine must be combined into one efficiency island, which represents the accumulated wheel torque contribution. This leads to the introduction of the *state operation island*, $\mathbf{A}_{SOI}$,

which represents every state's operating points.

Each axle features two electric machines with distinct gear ratios, causing them to rotate at different speeds when both are engaged. To find the common operating points of the motors where they operate above an efficiency threshold, the minimum and maximum motor speeds must be taken into account. The *trailing* electric machine with the lower gear ratio will be rotating faster than the *leading* electric machine with the higher gear ratio. See Figure 2.5 for an example where EM1 is engaged to gear 1 while EM2 is engaged to gear 2, representing state 7 (see Table 1.1 for the definition of the states). To ensure that the trailing motor is not *overspeeding*, i.e., rotating faster than the efficiency island allows for, the upper limiting speed, v_{UL}, is defined as the vehicle speed where the trailing electric machine is operating at the highest rotational speed on the efficiency island. Similarly, the lower limiting speed, v_{LL}, is defined as the vehicle speed where the leading electric machine is operating at the lowest rotational speed on the efficiency island. v_{UL} and v_{LL} are found using the previously defined gear operation island matrices for the active gears, A_{GOI}, by finding the first and last column where all active motors have common operating points.

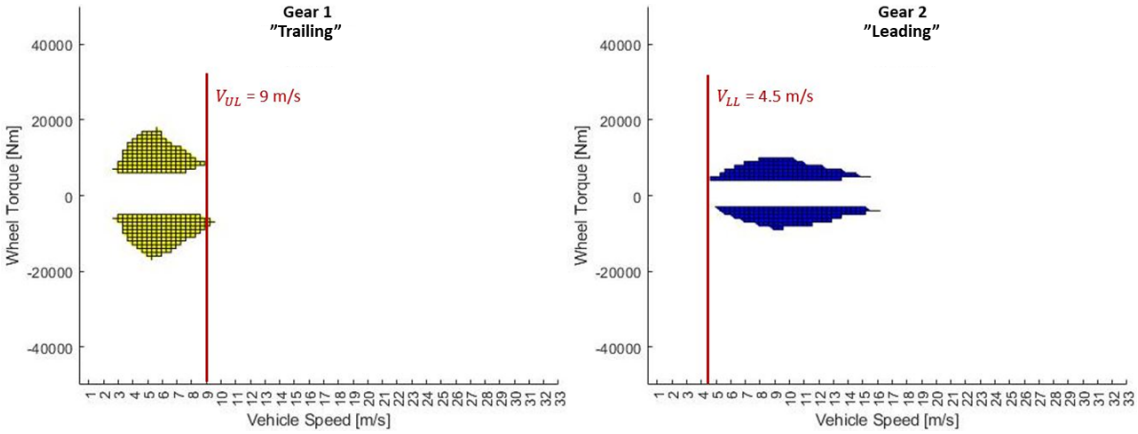

Figure 2.5: Illustration of gear operation islands, $\mathbf{A}_{GOI}$, for EM1 and EM2 in state 7, where v_{UL} and v_{LL} is marked.

For each vehicle speed between v_{LL} and v_{UL}, the minimum and maximum torque, T_{LL} and T_{UL}, for each electric machine defines the state's minimum and maximum wheel torque, see Figure 2.6 where the torque is marked at 7 m/s.

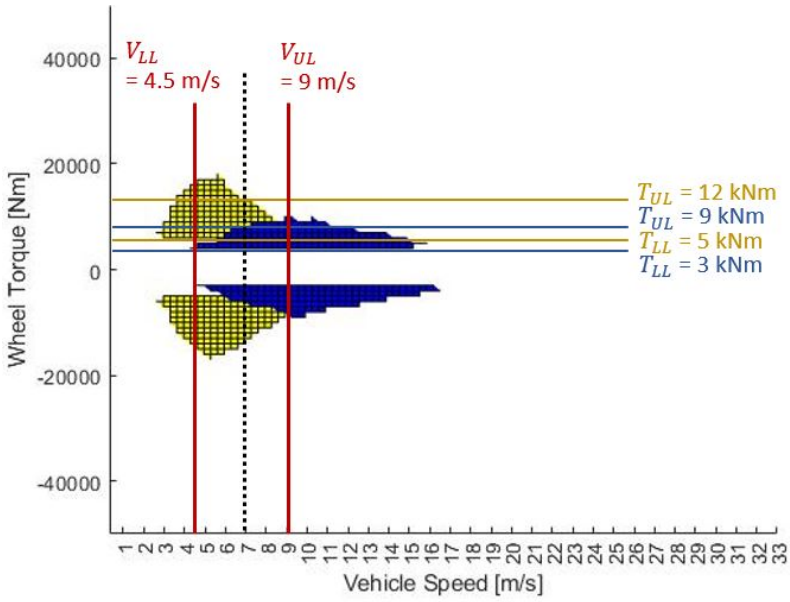

Figure 2.6: Torque contribution from EM1 and EM2 between the minimum and maximum speed in state 7.

The machines' torque contributions are summarized at each vehicle speed, resulting in the state operation island, $\mathbf{A}_{SOI}$, illustrated in Figure 2.7. The same method is applicable to all states, regardless of how many electric machines are activated.

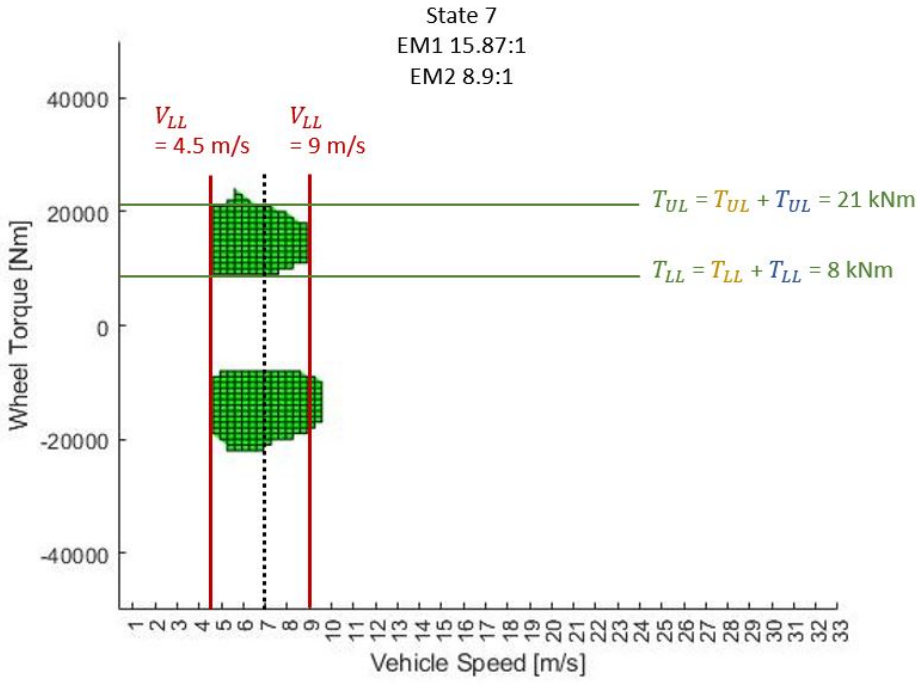

Figure 2.7: Illustration of the state operation island, $\mathbf{A}_{SOI}$, for state 7 with 97% efficiency.

2.2.4 State Selection Map

With the state operation islands defined for all states, the possible states at every operation point and efficiency thresholds are known. A MATLAB script starts an iterative process by computing the state operation islands at 0% efficiency threshold for all states and combines them in a cell matrix, where each element is a vector with the possible states. In the next iteration, the efficiency threshold is raised by a defined increment, and a new cell matrix with all possible states is constructed. Each element in the new cell matrix that is not empty overwrites the element in the cell matrix from the last iteration. By continuing this process until the efficiency threshold reaches 100%, the most optimal state is represented in each element of the final cell matrix, referred to as the *state selection map*. Figure 2.8 illustrates the iterative development of a state selection map.

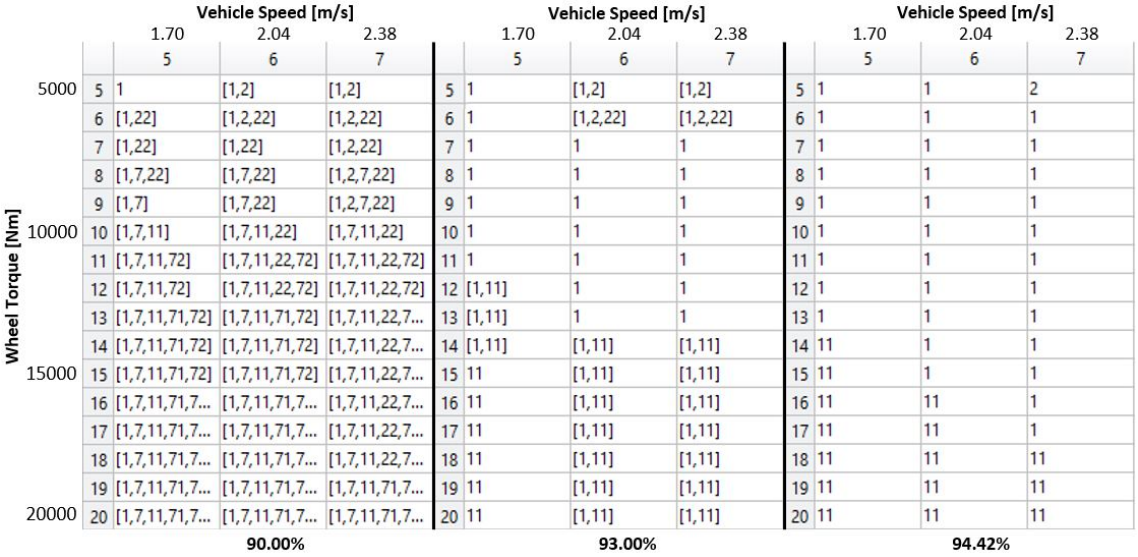

Figure 2.8: Three iterations of the state selection map.

The resulting state selection map is a 100x100 matrix where each element represents the optimal state choice at that specific wheel torque demand and vehicle speed, defined by the rows and columns. Since the aim of this thesis work is to compare an independent to a parallel control strategy, two state selection maps are constructed. See Figure 2.9 and 2.10, which illustrate examples of an independent and a parallel state selection map, where each state is marked in color. These state selection maps represent the optimal state choices at all vehicle speeds and wheel torque demands. As seen in the figures, the state selection map for the independent control strategy contains independent states, while the state selection map for the parallel control strategy only contains parallel states.

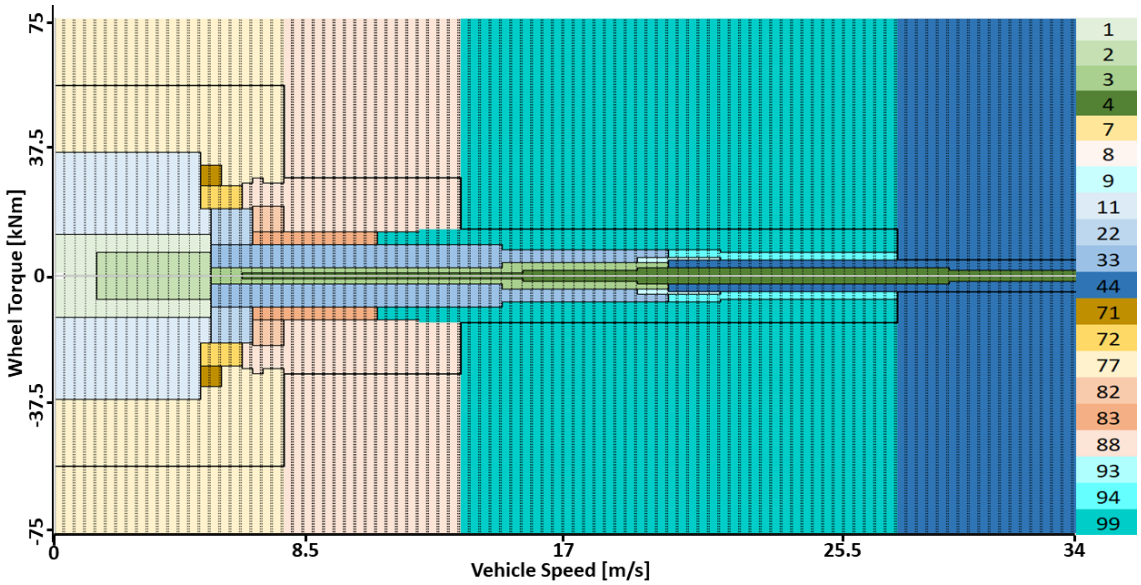

Figure 2.9: Illustration of a state selection map for an independent control strategy, with states marked in color.

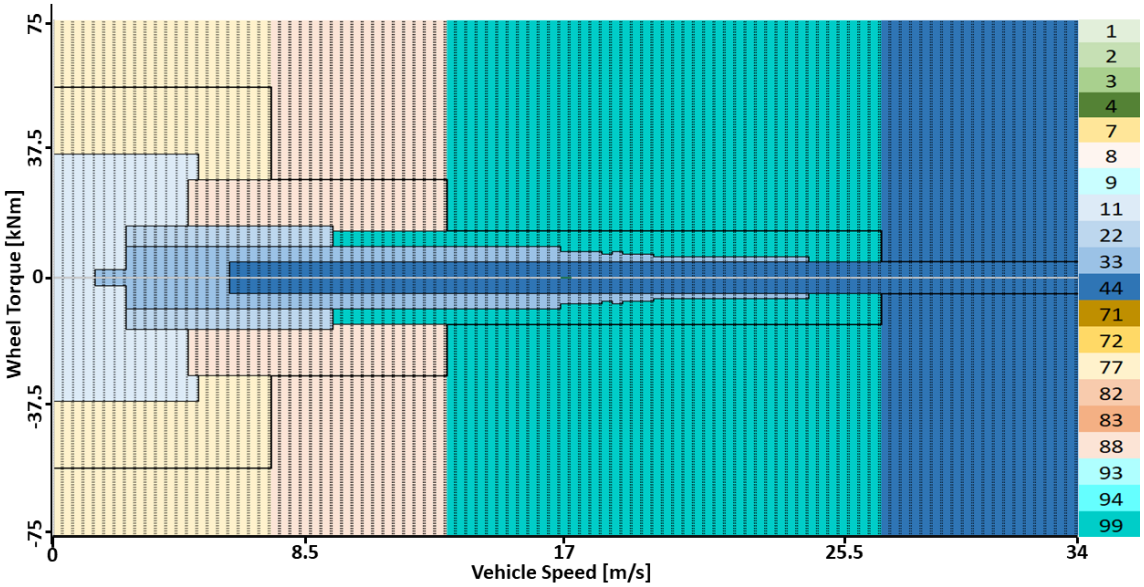

Figure 2.10: Illustration of a state selection map for a parallel control strategy, with states marked in color.

2.3 Gear Shifting Strategy

The state selection map defines which state is optimal in terms of efficiency for any wheel torque demand and vehicle speed, which is to be used as a gear-shifting strategy in Simulink. The state selection map is implemented into the Simulink environment by using a '2D-Lookup Table', see Figure 2.11. The state selection map is divided into two halves, one for positive and one for negative wheel torque

demand. Based on the sign of the wheel torque, a switch controls which of the two maps is used.

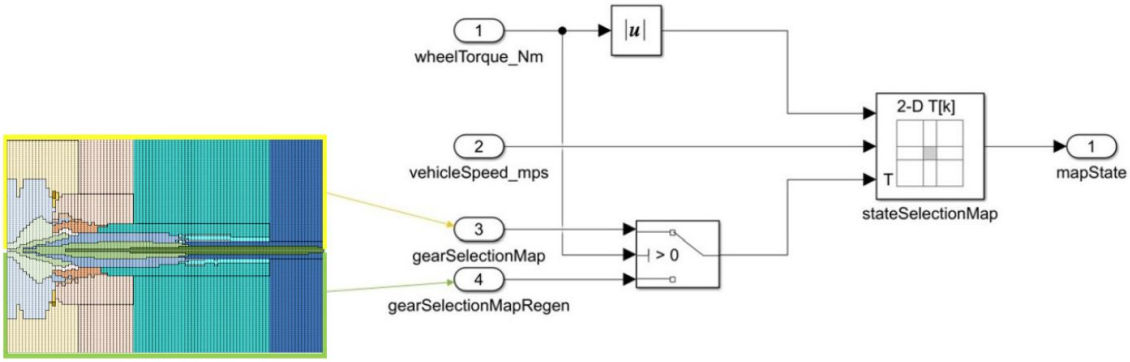

Figure 2.11: Simulink model for selecting states based on wheel torque and vehicle speed using the state selection map.

Using only the state selection map as a gear selection strategy results in the vehicle speed and wheel torque demand shown in Figure 2.12. As seen in the figure, the target speed increases rapidly from 30 km/h to 46 km/h at 73 s and is then gradually decreased at the rate of -1.75 km/h per second at 81 s. The wheel torque demand increases from 2 to about 29 kNm with the target speed increase. When the actual speed is approaching the target speed, the torque is reduced and then fluctuates until the target speed reduces gradually.

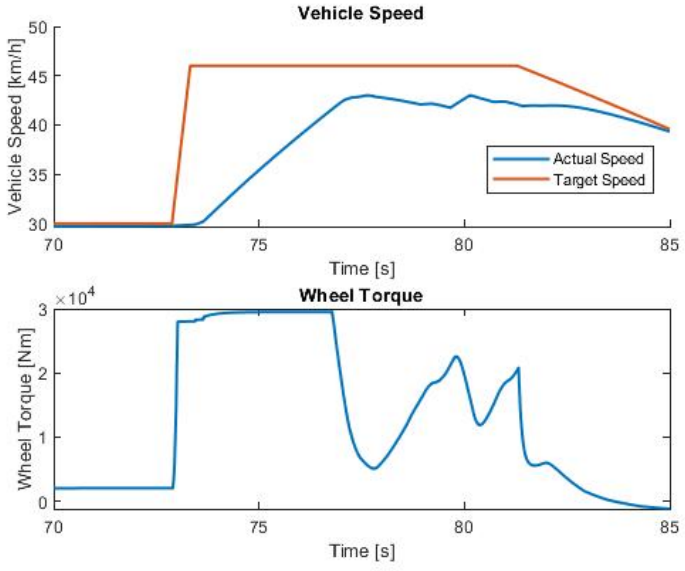

Figure 2.12: Vehicle speed and wheel torque demand.

As seen in Figure 2.12, the maximum target speed of $46km/h$ is not reached. Instead, the actual speed fluctuates between 41 and $43km/h$, indicating that there are problems with the gear selection. The traced state selection on the state selection map is shown in Figure 2.13.

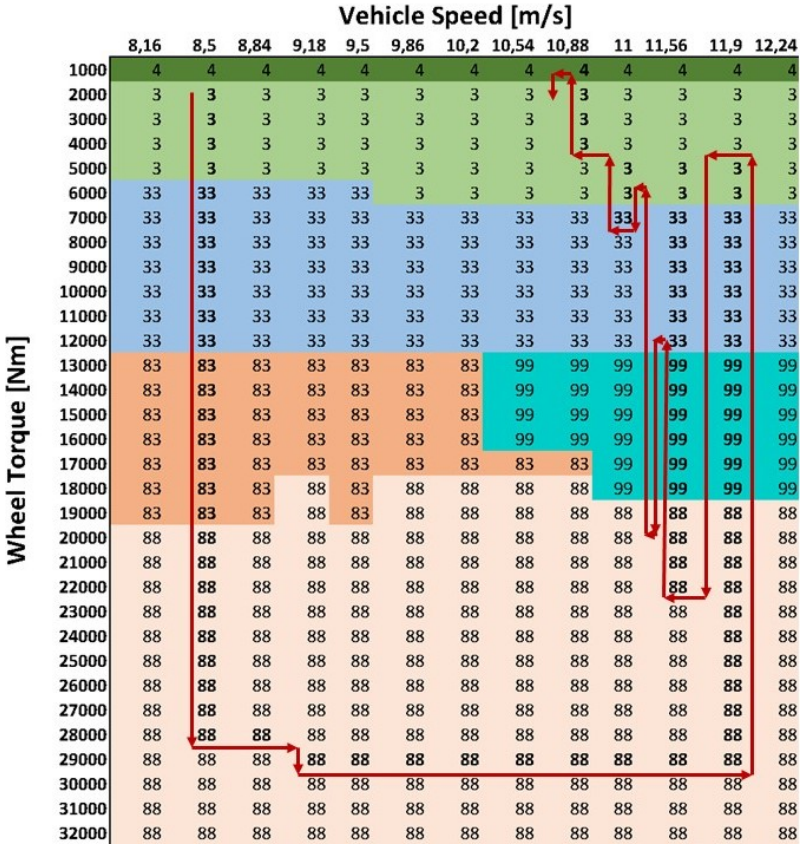

Figure 2.13: State selection tracing in the state selection map.

During the rapid increase of the target speed, the selected state goes from 3 to 88 via 33 and 83. During the acceleration, state 88 remains until the torque demand drops when approaching the target speed. Then, the selection goes through state 99 and 33 until finally reaching state 3. When state 3 is engaged, the torque starts rising again, leading to that state 88 being chosen again after going through states 33 and 99. The torque keeps fluctuating the gear selection until the target speed reduces which lets the state selection settle at state 3 and 4. This rapid change in state selection greatly affects the state selection to each axle, see Figure 2.14.

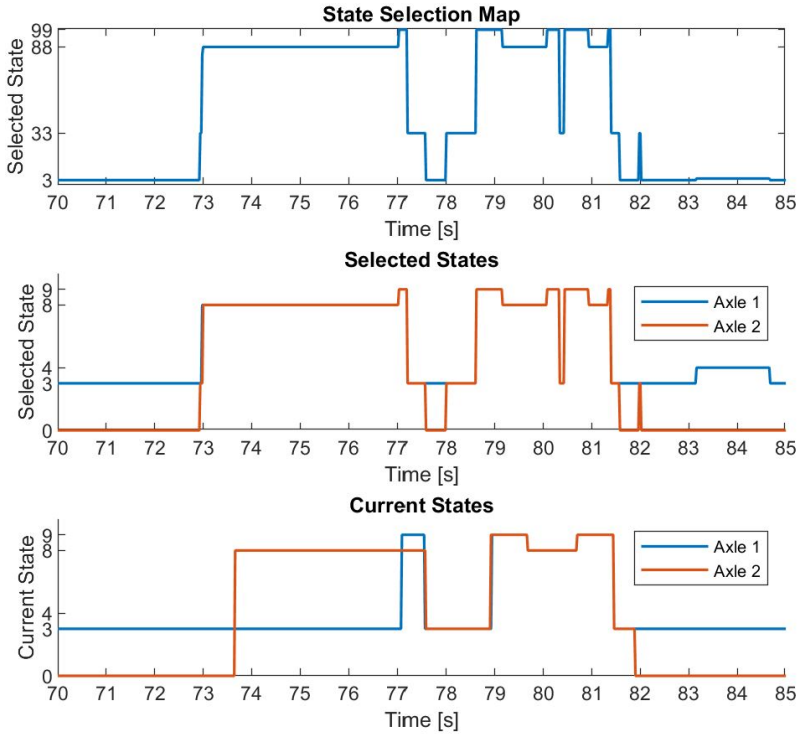

Figure 2.14: Selected and current states from the state selection map.

Since the state selection depends solely on the state selection map, the selected states for each axle are identical to the state map (except that the signal is divided into two signals, one for each axle). The current states differ from the selected states because the gearbox must complete the gear engagement process from the previous state selection before a selected state can become the current state. The fork actuation must be finished, and the electric machines must synchronize to the input shaft speed, which leads to a delay from when a newly selected gear has been sent to when it becomes a current gear. Therefore, rapid state selections might be missed and even disturb the engagement of the states. This happens to axle 1 at $73s$ where state 8 is chosen but state 3 remains engaged. This *failed shift* contributes to that the target speed of 46 km/h in Figure 2.12 is not reached.

2.3.1 Engagement Check

As previously shown, it is important to ensure that a selected state is allowed to engage before selecting a new state to avoid failed shifts. To confirm the engagement of a selected state before selecting a new state, a function referred to as "Engagement Check" is developed, which compares the current state to the selected one. If the current and selected states are equal, a new state from the state selection map is transmitted via a switch. During the interval in which a gear shift request is being processed and the gear engagement is underway, any incoming gear shift requests are not passed through the switch. This ensures that the gear shift process is not interrupted or compromised by new requests. It emphasizes the importance of allowing each gear shift to fully complete before considering additional changes, ensuring a reliable transition between gears. Each signal that gets passed through

the switch is stored in a memory, ensuring a steady selected state signal, see Figure 2.15.

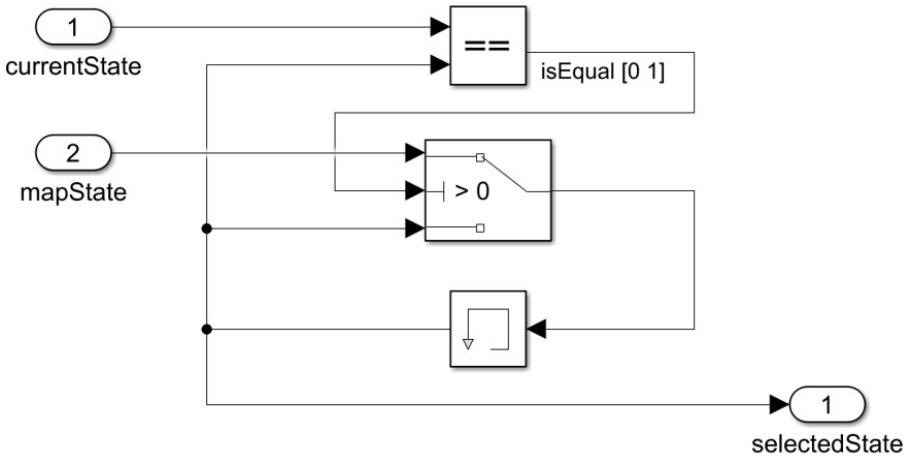

Figure 2.15: Simulink model for the Engagement Check.

Using this function, all selected states become current states, meaning that there are no incomplete shifts impeding the vehicle from reaching the target speed, see Figure 2.16.

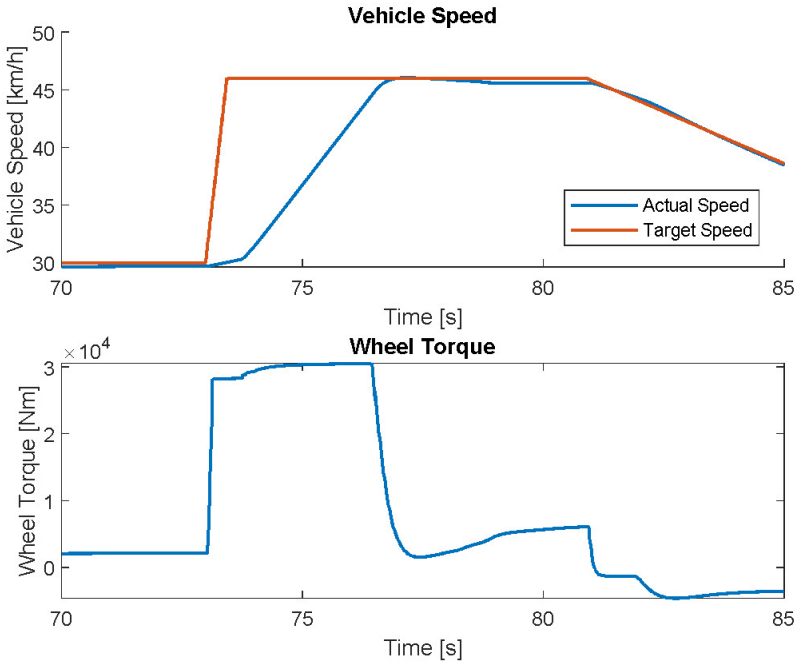

Figure 2.16: Graphs showing the vehicle speed and wheel torque demand.

Figure 2.17 shows the states sent from the state selection map, the selected and current states as well as the switch position for the engagement check. The switch position is 1 when the selected and current states are the same, and 0 when they are not. When the selected gear has changed during the gear shift process, the switch

position goes from 0 to 1 when the process is done and then immediately back to 0 again since a new selected state starts a gear shift process.

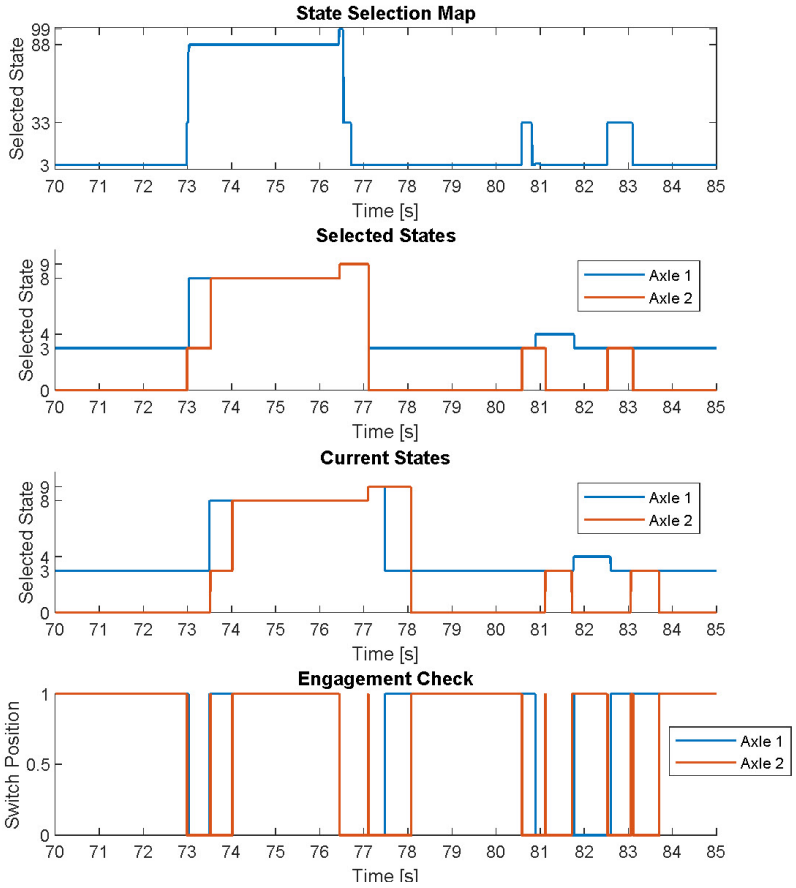

Figure 2.17: Selected and current states using Engagement Check.

As seen in the figure, there are multiple sub-one second shifts, which are not desirable for torque delivery, referred to as *mis-shifts*. During highly transient torque demands, large portions of the state selection map are swept through before the torque demand has settled. These sweeps through the state selection map generate a flow of state requests that are being sent to the Engagement Check. Selections from the flow of state requests will be sent, depending on the Engagement Check switch position.

2.3.2 Satellite Filter

To reduce the issue of rapid state changes due to sudden fluctuations in torque requirements, and consequently avoid rapid gear change requests that can result in failed shifts and poor torque delivery, a function termed "Satellite Filter" is introduced. This function involves the use of two additional points, referred to as *satellite points*, which are positioned ϵ_{sat} indices away from the desired operating point in the Y-direction. One satellite point lies ϵ_{sat} indices below the desired operating point and the other ϵ_{sat} above the operating point. When all three points are within the

same state island, a switch and memory are used similarly to the Engagement Check to transmit the state. See Figure 2.18.

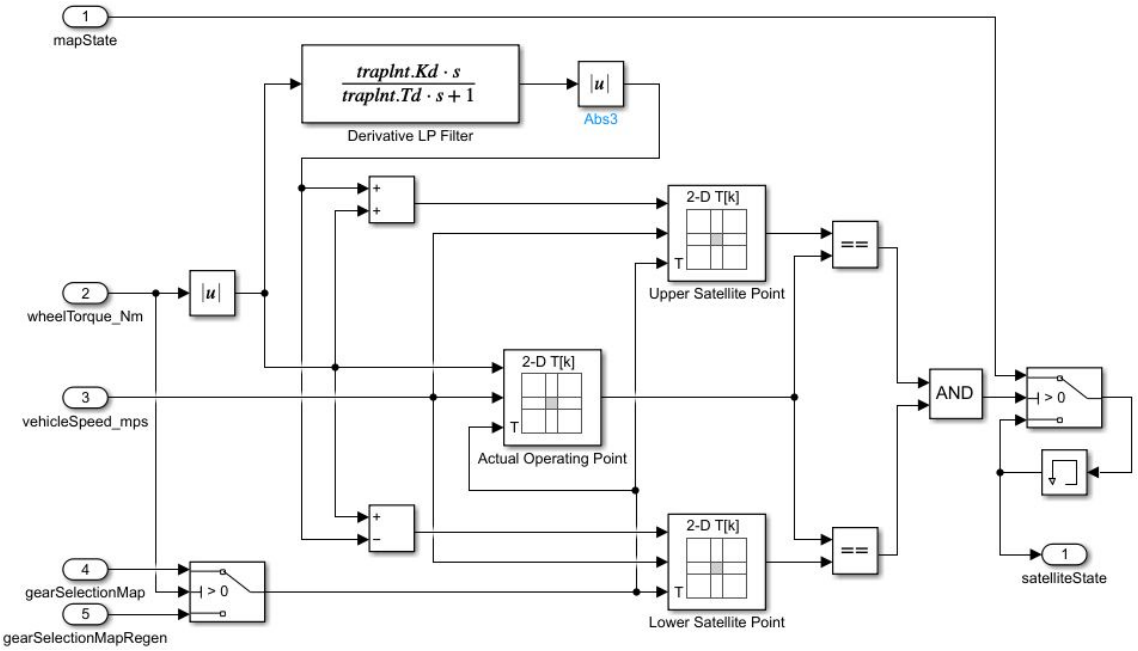

Figure 2.18: Implementation of the Satellite Filter in Simulink.

The amplitude ϵ_{sat} depends on the rate of change in wheel torque demand and is calculated by utilizing a derivative filter. The transfer function for this derivative filter, $G_{df}(s)$, effectively smooths out rapid fluctuations in torque demand. Using $G_{df}(s)$, the amplitude ϵ_{sat} is continuously calculated according to:

$$G_{df}(s) = \frac{k_d s}{1 + sT_d}[14] \tag{2.20}$$

$$\epsilon_{sat} = G_{df}(s) * T_{wheel,demand} \tag{2.21}$$

where k_d is the filter gain, and T_d is the filter's time constant. These parameters are to be tuned for the state selection map resolution and the propulsion system torque capabilities. For the state selection map size of 100x100 and the propulsion system at hand, it is found that $k_d = 0.00025$ and $T_d = 0.5$ results in good functionality. Figure 2.18 shows an illustration of how the Satellite Filter operates. Initially, when the torque demand and vehicle speed are in steady-state, the amplitude ϵ_{sat} is low, resulting in the satellite points being close to the operating point within the island of state 3. When the wheel torque requirement quickly rises, ϵ_{sat} becomes larger, resulting in the satellite points separating, which avoids the states 33 and 83. When the wheel torque requirement has settled between 28 and 30 kNm, the operating point and the satellite points are in the same state island, and state 88 is passed through the Satellite Filter.

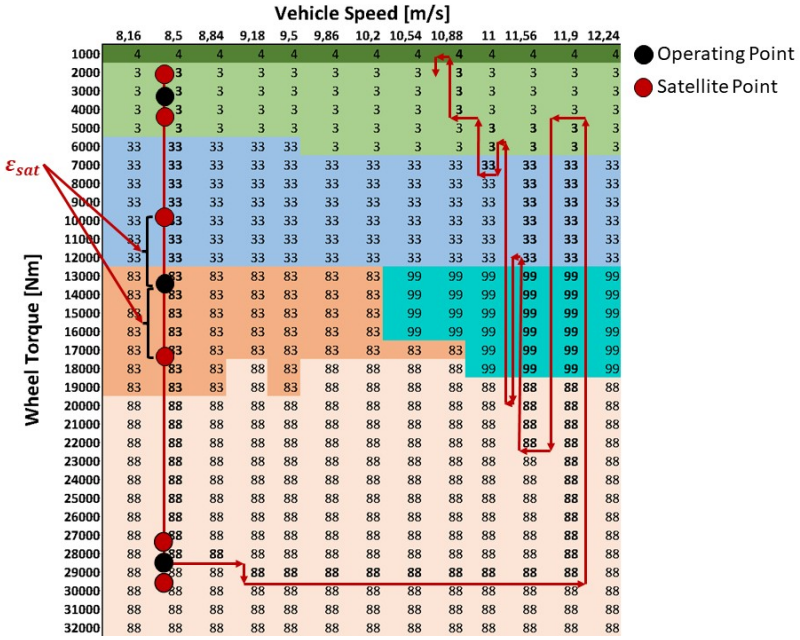

Figure 2.19: Function of the Satellite Filter.

Figure 2.20 shows how the Satellite Filter improves the state selection. As expected, state 33 and 83 are avoided, and state 88 is chosen instead at 73. Similarly, when the torque demand lowers, the states 99 and 33 are ignored. During this particular part of the driving cycle, the Satellite Filter reduces the number of selected states from 5 and 8 to 2 for both axles 1 and 2, respectively.

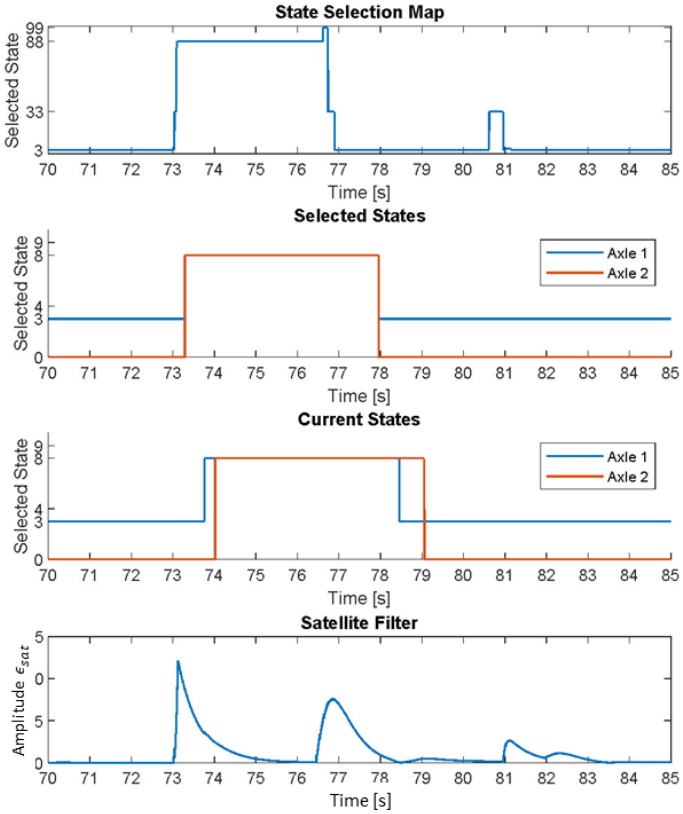

Figure 2.20: Selected and current states using the Satellite Filter.

Figure 2.20 shows that the Satellite Filter avoids mis-shifts at high torque change rate. Figure 2.21 shows a later part of the same drive cycle as the previous, where the selected state for axle 1 goes back and forth between state 3 and 4 from timestamp 95s to 118s. This type of shifting is undesired and referred to as *gear hunting*, where the wheel torque demand is at the border between two state islands. The Satellite Filter amplitude is not large enough to counteract the gear hunting between states when the change rate of the wheel torque demand is low.

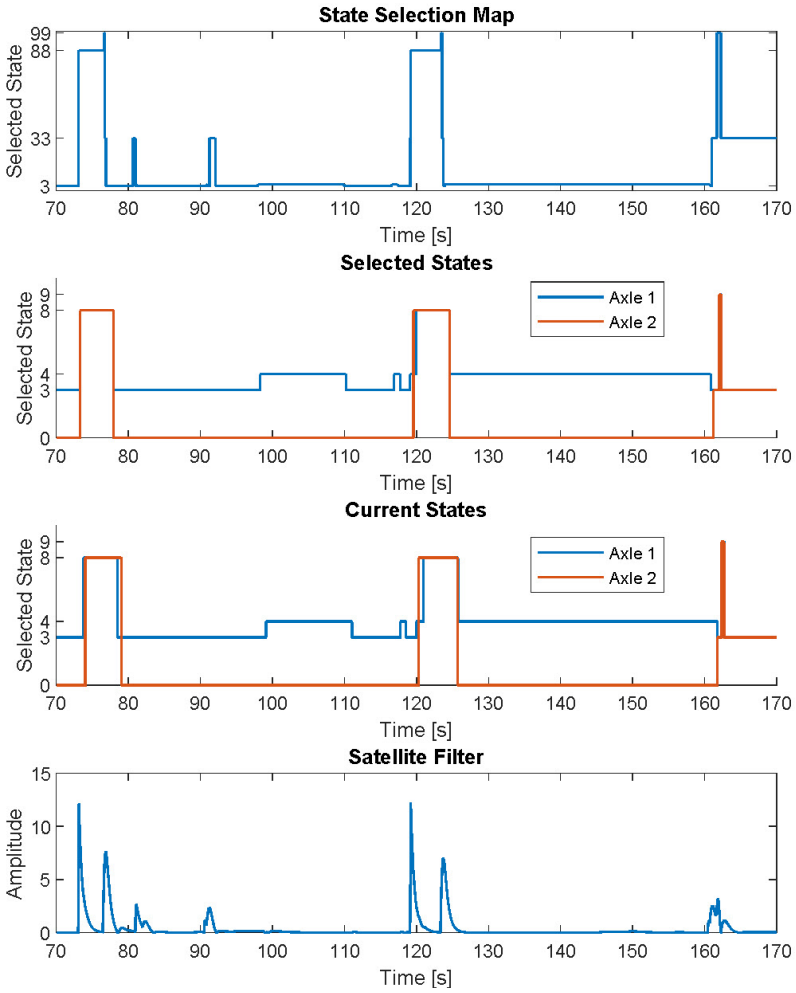

Figure 2.21: Gear hunting at low torque change rates.

2.3.3 Hysteresis

To avoid gear hunting at low torque change rates, a function referred to as Hysteresis is introduced. The Hysteresis function holds the current states as long as the wheel torque demand lies between a *high* and *low band*, which are defined as the wheel torque if the active motors produce 450 Nm and 50 Nm, respectively, through the engaged gears. The choice of 50 Nm for the low band is due to that the efficiency drops rapidly below this torque output, seen in Figure 2.2. While the electric machines have good performance even at the maximum torque of 500 Nm, 450 Nm is chosen for the high band to give the same margin as the low band. See the efficiency island in Figure **??** for reference. Additionally, a maximum speed of 7000 rpm is set to ensure that the motors are not stuck operating at a high speed. The Hysteresis function is implemented in Simulink according to Figure 2.22.

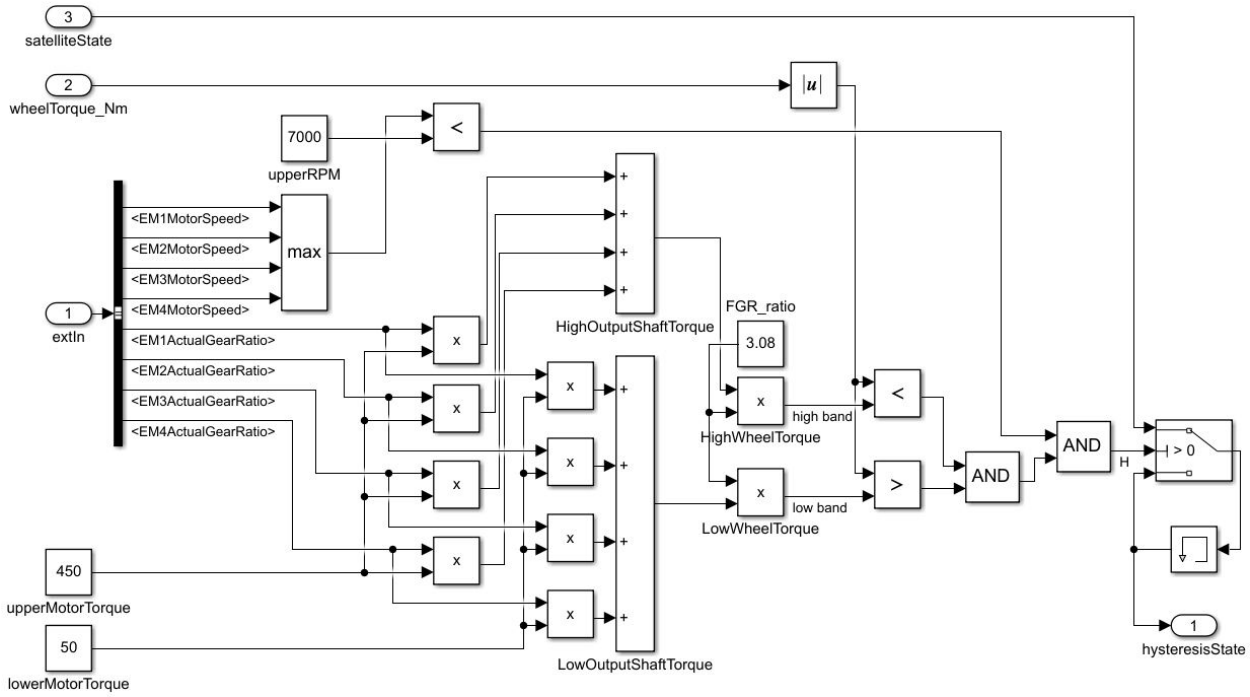

Figure 2.22: Illustration of the Hysteresis function implementation in Simulink.

The purpose of the Hysteresis function is to allow the current state to stay engaged even though the state selection map and Satellite Filter request a state change, as long as the active electric machines can operate with good (but not optimal) efficiency. This function sacrifices efficiency for better torque delivery and driveability. See Figures 2.23 and 2.24 for the Hysteresis function in operation on the same part of the drive cycle shown in Figure 2.21.

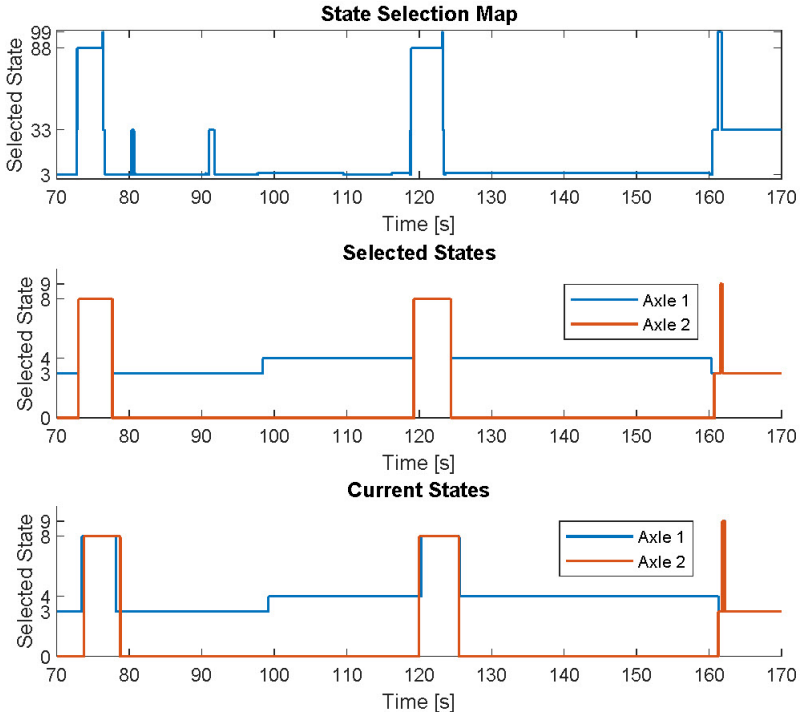

Figure 2.23: Hysteresis function operation during low torque change rate.

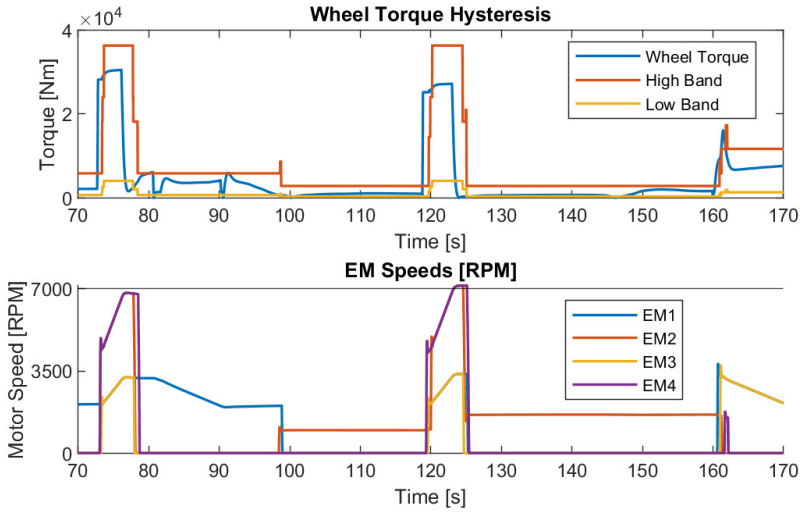

Figure 2.24: Wheel torque and electric machine speed using the Hysteresis function.

The gear hunting between states 3 and 4 are eliminated since the wheel torque does not fall below the low band of state 4. This is a significant improvement for the driveability of the truck since there will be fewer disruptions in the torque delivery. However, the Hysteresis function does not eliminate the risk of mis-shifts, which can be seen at 160*s* in Figure 2.23. This shows that the Hysteresis function works well for slow torque change rates, but does not ensure that the gears are held during rapid changes that are not eliminated by the Satellite Filter.

2.3.4 Hold

To avoid mis-shifts at low torque change rates, a function denoted as Hold is implemented. For each axle, once a gear shift request has been sent, no new gear shift request will be accepted for the next two seconds following the transmission of the previous signal. Consequently, any gear shift initiated will be in effect for at least two seconds. This is implemented using a combination of delay block, memory block, relational operator, and switch block within the control system, see Figure 2.25. The delay block introduces a fixed time delay after a gear shift request is sent, ensuring that a subsequent request can only be considered after the two-second interval. The memory block retains the state of the last gear shift request to facilitate comparison with new requests. The relational operator is used to cross-check the two-second hold of the gear state used. the switch block controls the flow of gear shift signals based on the evaluation from the relational operator, effectively preventing any new requests from being processed too soon after the last shift.

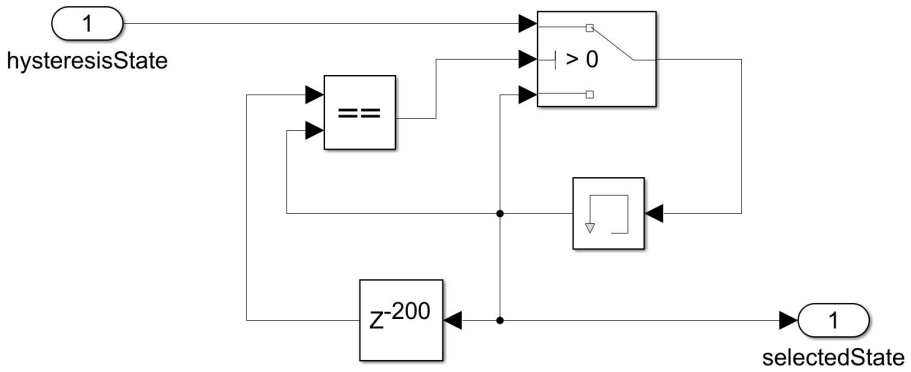

Figure 2.25: Implementation of the Hold function in Simulink.

As seen in Figure 2.26, the mis-shift at the timestamp 162 is ignored due to that state 33 being held during the time that the state selection map outputs 99.

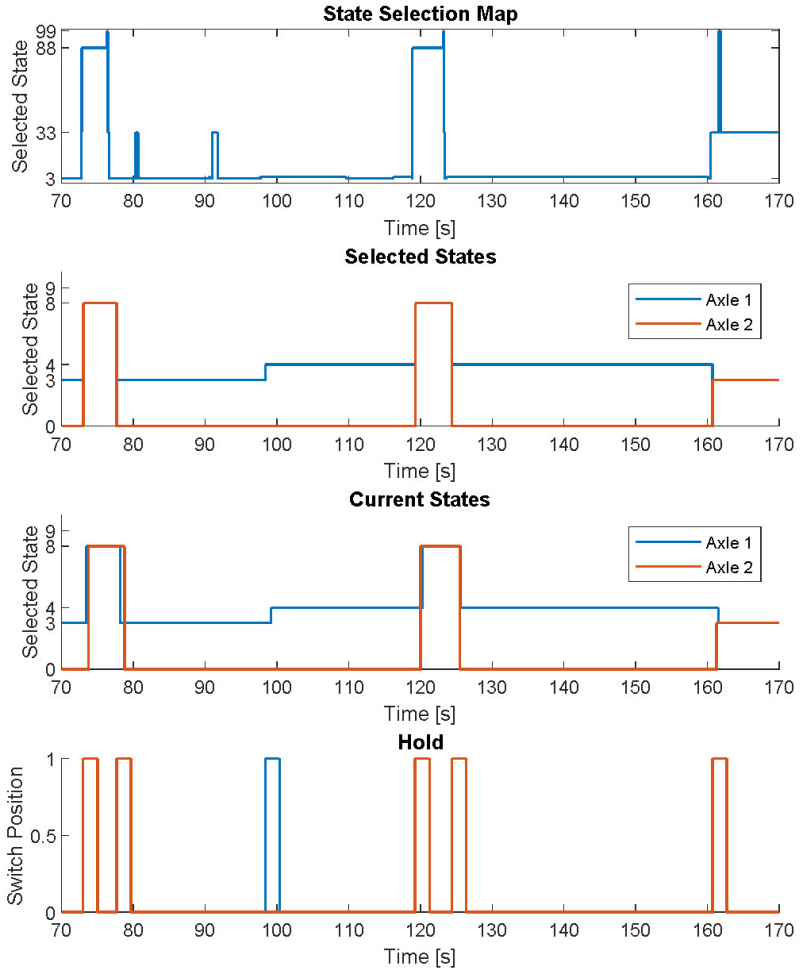

Figure 2.26: Hold function operation during a drive cycle simulation.

With the addition of the Hold function, the gear selection strategy operates as desired without failed shifts, gear hunting, or mis-shifts, ensuring good driveability and torque delivery while operating in states with high efficiency.

2.3.5 Simulink Model

As demonstrated in the previous subsections, implementing the gear selection strategy requires four key functions: Engagement Check, Satellite Filter, Hysteresis, and Hold. Figure 2.27 provides an overview of how these functions are implemented in Simulink, along with the necessary input and output parameters.

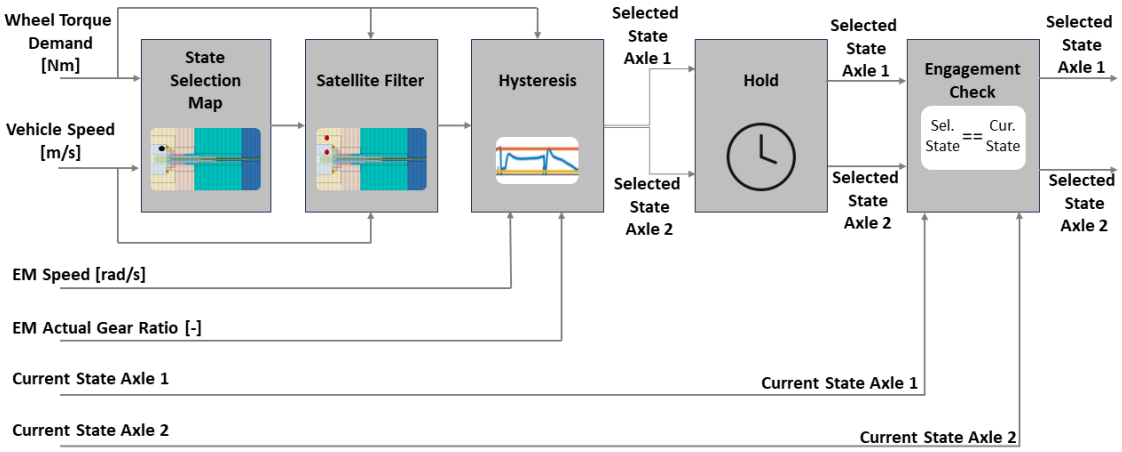

Figure 2.27: Flow of signals from input to output for the complete gear shifting strategy.

3

Results

The following chapter presents the results of this study. It presents the EM and gearbox efficiency maps, followed by the resulting state selection maps constructed from these for both independent and parallel control strategies. Next, the chapter delves into the results obtained from each implemented method in Simulink. Finally, it presents the results from all drive cycles and truck masses, as well as the simplified state selection map based on these results.

3.1 Efficiency Maps

This section describes the resulting efficiency maps for the electric machine and the mechanical efficiency of the gearbox. These efficiency maps are the foundation of the state selection maps, which are compared later in Section A.2.

3.1.1 Electric Machine

The given 42-by-21 matrix of the electric machine efficiency presented in the Methods chapter, see Figure 2.2, is re-scaled to 50-by-50, and all points outside the field weakening region defined by the maximum positive and negative torque are set to zero. The electric machine has a maximum speed of 10000 rpm and a maximum torque of 500 Nm, with the field weakening region starting at approximately 5600 rpm.

This results in the efficiency map in Figure 3.1, which has identical efficiency islands as the given efficiency map, which is expected. The efficiency map has a relatively large efficiency island with above 97% efficiency. Most of the efficiency map is above 95% efficiency, with exceptions for torque levels below 70 Nm and high torque levels below 2500 rpm. The electric machine performs similarly but with slightly less efficiency at negative torque in generator mode.

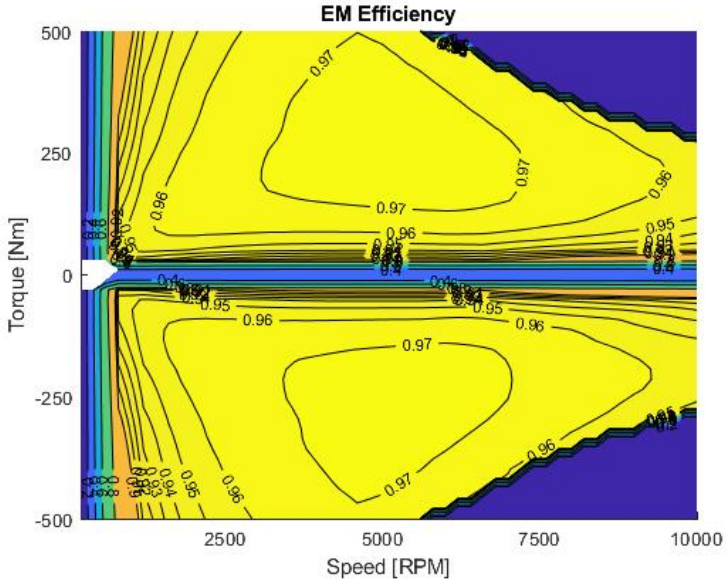

Figure 3.1: Interpolated 50x50 efficiency map of the electric machine

Because of the large area covered by above 95% efficiency, the shape of the efficiency map is rather flat. It does, however, have distinct peaks at approximately 5600 rpm and ±260 Nm where the efficiency is 97.4%.

3.1.2 Mechanical Efficiency

The gearbox efficiency matrix $\boldsymbol{\eta}_{gb}$ is calculated according to (2.7) for each gear, see Figure 3.2 for the $\boldsymbol{\eta}_{gb}$ of gear 1.

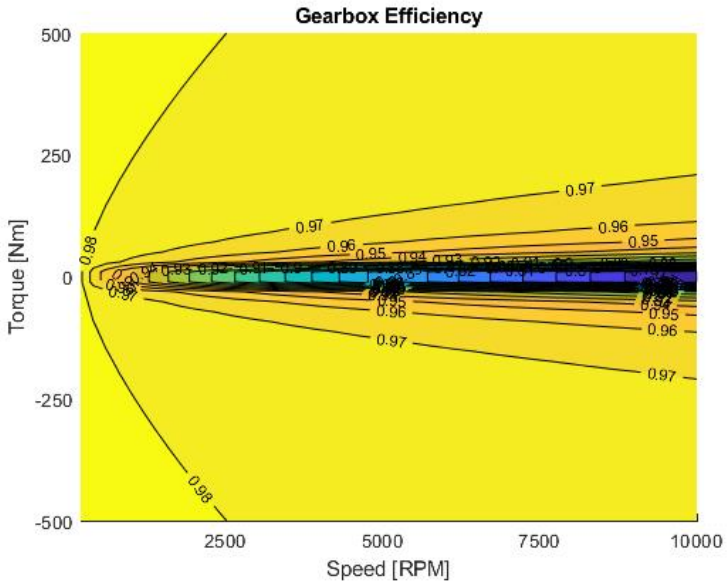

Figure 3.2: Gearbox efficiency for all operating points of the electric machine for gear 1

As seen in the figure, the efficiency decreases with speed due to friction losses from the bearings, etc. The gearbox efficiency is also higher at higher torques, which is due to that the frictional losses from the gear teeth are lower relative to the throughput power at high torque than at low torque. $\boldsymbol{\eta}_{gb}$ is then element-wise multiplied by the rest of the propulsion system efficiency. See Figure 3.3 for a comparison of the EM efficiency with and without the gearbox efficiency.

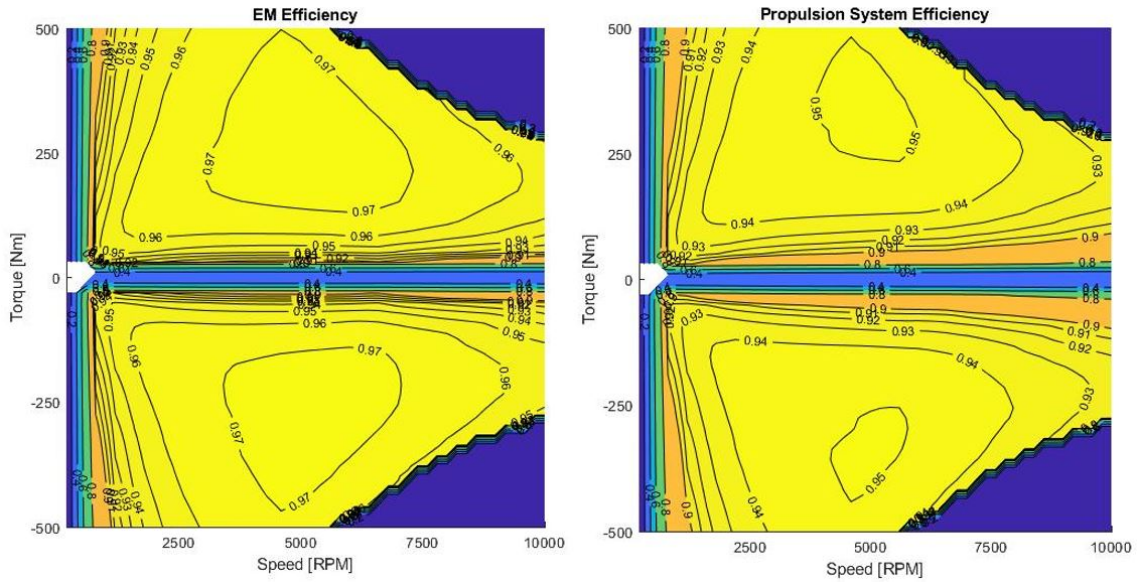

Figure 3.3: Comparison of electric motor efficiency without and with mechanical efficiency

As previously stated, the peak EM efficiency without the gearbox efficiency is 97.4% at 5600 rpm and 260 Nm. If the gearbox efficiency is included, the peak efficiency drops to 95.2%, and the operation point is shifted to 5000 rpm and 340 Nm. This shows that the gearbox efficiency influences the optimal operation point of the propulsion system.

3.2 State Selection Map

The state selection map is a crucial aspect of the control strategies examined in this study. It determines the optimal states in terms of efficiency for all operation points of the vehicle.

3.2.1 Independent State Selection Map

The independent control strategy state selection map is generated using all defined states in Table 1.2 on page 6, and is illustrated in Figure 3.5 where all states are marked in color. As seen, states 44, 77, 88, and 99 cover large portions of the surface, and these are the states with the highest torque capabilities at their respective vehicle speed. The black border indicates the maximum wheel torque that the active motors

can produce in these states. However, since the wheel torque demand may exceed this limit, the states are also defined beyond these borders.

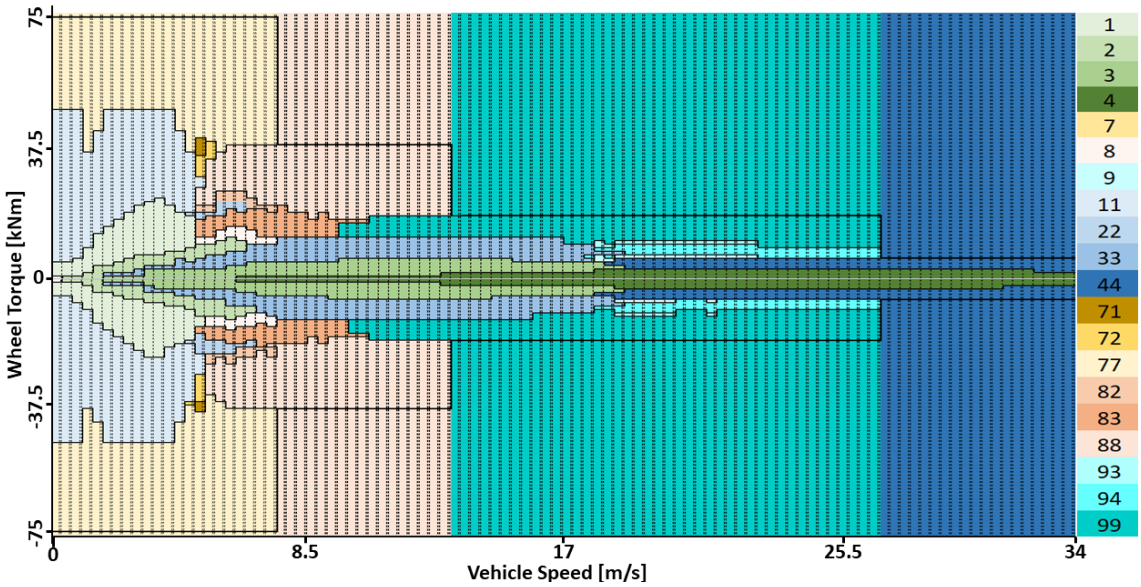

Figure 3.4: Illustration of complete state selection map for the independent control strategy, with states marked in color.

As can be seen in Figure 3.5, state 7 is missing. This state has been filtered out of the state selection map because, even at its highest efficiency island, state 11 achieves higher efficiency by utilizing two electric machines with the same gear ratio. The positive and negative torque sides of the map differ slightly due to the electric machine efficiency map being asymmetrical.

3.2.2 Parallel State Selection Map

The parallel control strategy state selection map is generated using the parallel states 11, 22, 33, 44, 77, 88, and 99, defined in Section 1.2.2 on page 6. Consequently, the resulting state selection map contains fewer and larger islands. Due to the asymmetrical electric machine efficiency map, the state selection map for the parallel control strategy differs for positive and negative torque.

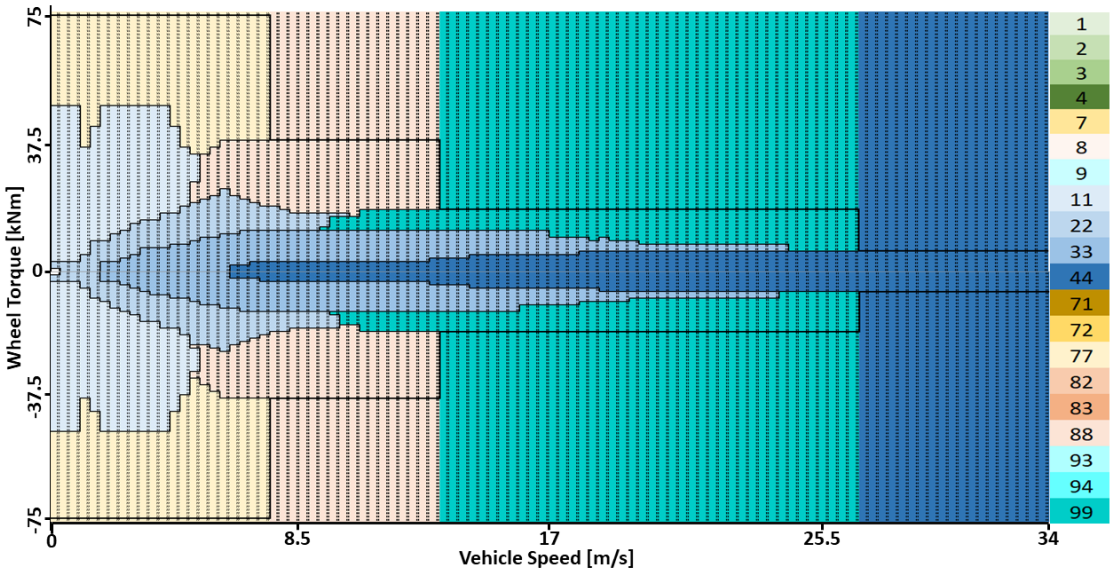

Figure 3.5: Illustration of complete state selection map for the parallel control strategy, with states marked in color.

3.3 Gear Selection Strategy

The most efficient state at every operation point is defined by the state selection map. However, a compromise between efficiency and the number of selected shifts must be made to ensure driveability and satisfactory torque delivery. This is accomplished by the functions defined earlier: the Satellite Filter, Hysteresis, Engagement Check, and Hold. This section evaluates each function's effect on average efficiency and the number of selected states. Additionally, the time duration of the shifts is studied to ensure that the gear selection strategy results in satisfactory torque delivery and driveability.

3.3.1 Average Efficiency and Number of Selected States

An optimized control strategy has a low number of selected states while retaining high efficiency. To evaluate the impact of each of the four functions implemented in Simulink on these properties, the EU Highway drive cycle was used with 35300kg of truck mass, using each function in the order described in Section 2.3. During this process, the average efficiency and the number of selected states for the axles were logged, see Figure 3.6. The baseline is when the state selection is determined solely by the state selection map, resulting in an average of 770 selected states, and an average efficiency of 82.5%. With the addition of the Engagement Check, the number of selected states drops to 682 on average, and the efficiency increases to 83.9%. As a result, all selected states become engaged. When the state selection during transient wheel torque demand is eliminated using the Satellite Filter, the average number of selected states further reduces to 536, and the average efficiency

remains at 83.9%. A large portion of quick shifts due to gear hunting at low torque change rates are eliminated with the Hysteresis, leading to the average number of selected states reducing further to 198. However, since the Hysteresis allows less optimal states to stay engaged to improve driveability, the average efficiency drops to 83.4%. With the addition of the Hold function, the average efficiency remains approximately the same, and the average number of selected states increases slightly to 203.

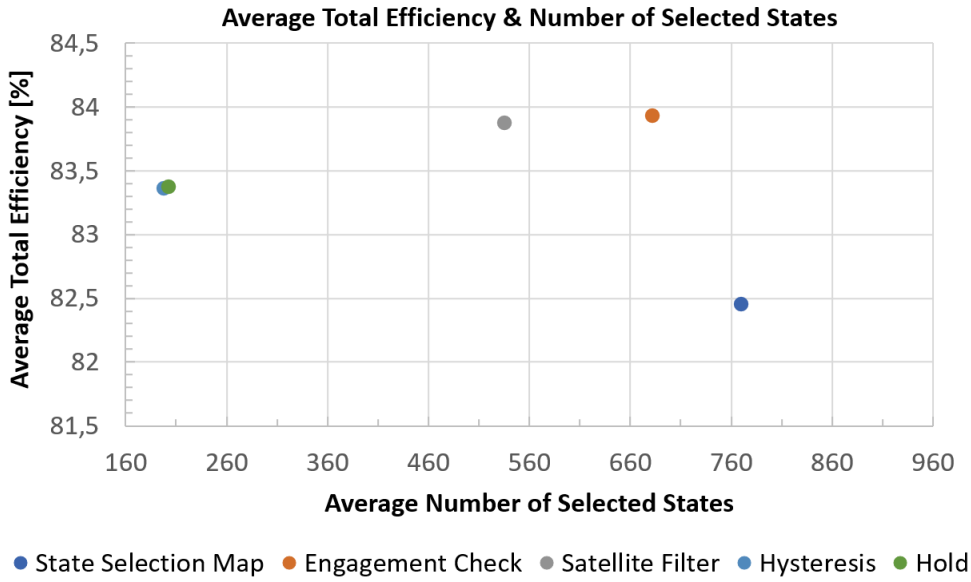

Figure 3.6: Scatter plot of the effect on average efficiency and number of selected states of each state selection method.

3.3.2 Shift Duration

From Figure 3.6, it is not clear that the Hysteresis and Hold functions have improved the state selection since the efficiency is reduced. However, the figure does not reflect the time duration during which the states are engaged, which is an important factor in ensuring good driveability. The time duration for each selected state is logged from the same drive cycle and truck mass, presented in Figure 3.7. The shifts are categorized into three categories. Mis-shifts are as previously defined, state selections that are engaged less than 1 second, which should be avoided to ensure satisfactory torque delivery. Shifts that are engaged between 1 and 2 seconds are referred to as *transient shifts*, which are typically necessary during acceleration and deceleration. Shifts that are engaged for 3 seconds or longer are categorized as *operating shifts*, which typically occur when the torque demand has settled.

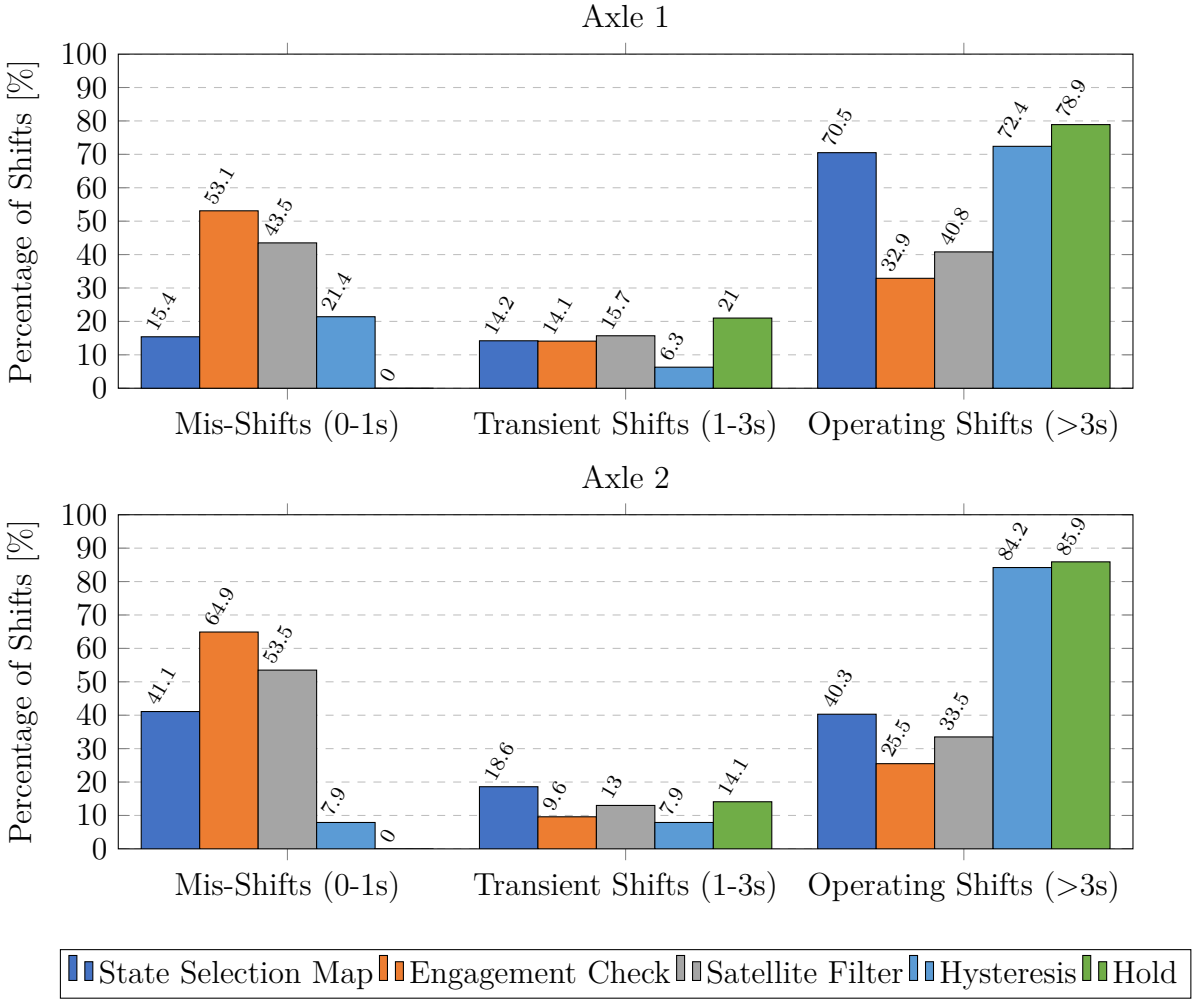

Figure 3.7: Percentage of mis-, transient, and operating shifts during the driving cycle for each state selection method.

When the state selection is made directly from the state selection map, axle 1 and axle 2 have 15.4% and 41.1% mis-shifts, respectively. The Engagement Check reduces the number of failed shifts, as explained in Section 2.3.1, which increases the number of mis-shifts to 53.1% and 64.9% for the axles respectively. The Satellite Filter eliminates the shifts during rapid changes in torque demand, reducing the number of mis-shifts to 43.5% and 53.5% respectively. With the addition of the Hysteresis, most mis-shifts during low transient torque demands are also eliminated, reducing the number of mis-shifts to 21.4% and 7.9%. Finally, the Hold function eliminates all mis-shifts by ensuring that each state selection gets 2 seconds to engage and operate. The results from Figure 3.6 and 3.7 show that in order to achieve satisfactory torque delivery without mis-shifts, the average axle efficiency is slightly reduced from 83.9% to 83.4%.

3.4 Independent and Parallel Control Strategy

In this section, the independent control strategy is compared against the parallel control strategy to evaluate the performance gains in terms of the number of selected states and average total efficiency.

3.4.1 EU Highway Drive Cycle

This section presents the vehicle performance results during the EU Drive Cycle, predominantly characterized by highway driving conditions. Figure 3.8 shows data points from the drive cycle using the independent control strategy for all three truck masses, differentiated by color. There are large clusters of data points at 50, 70, and 85 km/h which are typical speeds for EU highways, [15]. At 18000 kg, most of the clusters are covered by state 4 during coasting. When the torque demand increases at coasting speeds, states 3 and 44 are primarily applied. When the mass increases to 35300 kg, states 94 and 99 are utilized during coasting. The same is true at 64000 kg, with the addition that states 77 and 88 gain significance during acceleration. It is also noteworthy to mention that during 64000 kg, the power demand from the drive cycle is higher than the possible output power from the system, which is shown by the blue data points being outside of the maximum torque-boarder for states 88 and 99.

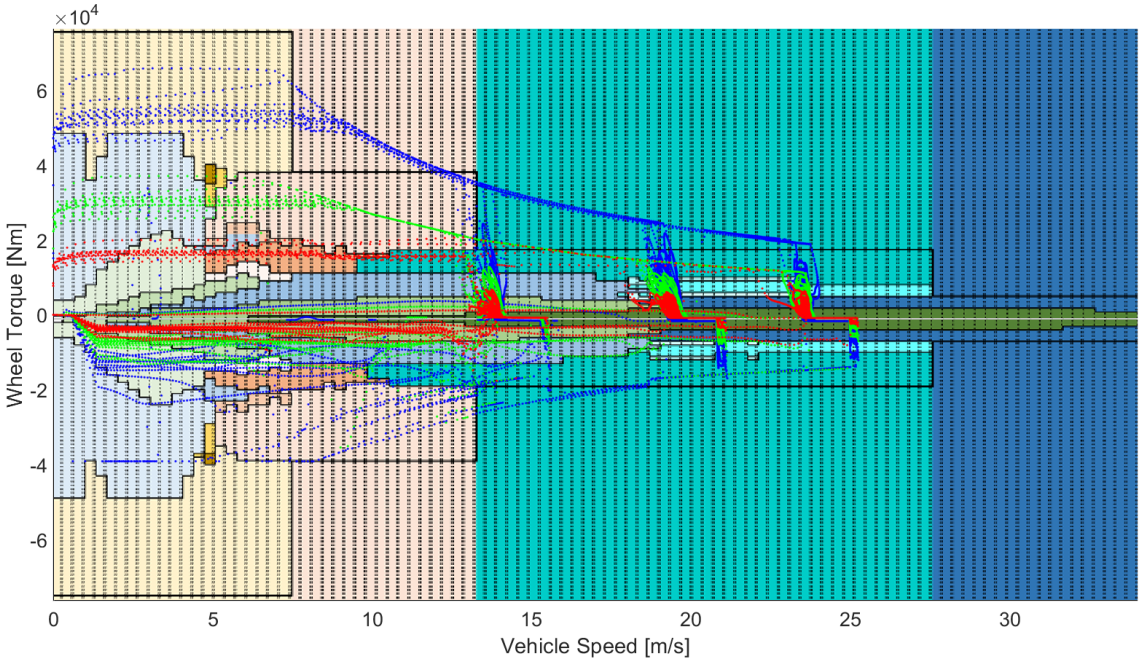

Figure 3.8: Operation points on the independent control strategy state selection map from the EU Highway drive cycle for 18000 kg (red), 35300 kg (green), and 64000 kg (blue) total truck mass.

Comparing the independent to the parallel control strategy operation map, state 4 is replaced by state 44 which covers all cluster points for 18000 kg. At 35300 kg, states 33 and 99 are needed to supply the demanded torque during coasting and

even state 88 during acceleration. At the maximum weight of 64000 kg, state 99 gains significance, similar to the independent control strategy.

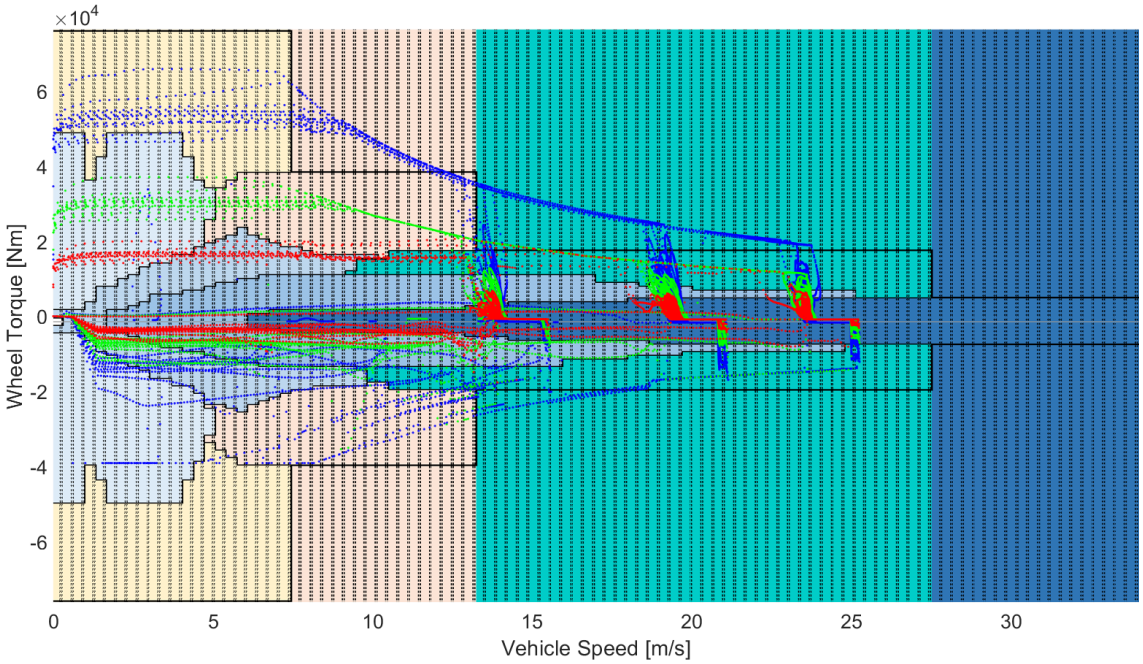

Figure 3.9: Operation points on the parallel control strategy state selection map from the EU Highway drive cycle for 18000kg (red), 35300kg (green) and 64000kg (blue) total truck mass.

Figure 3.10 illustrates the different map states usage for the independent and the parallel control strategy for a truck with a total mass of 18000 kg. As expected, states 4 and 44 are frequently utilized in the independent control strategy, accounting for 41.7% and 19.2% of the drive cycle, respectively. This indicates that the torque demand is low enough that EM2 alone can propel the truck with satisfactory efficiency at high speeds and low total mass. The parallel control strategy utilizes state 44 for 64.9% of the driving cycle, propelling the truck with EM2 and EM4 even during low torque demands.

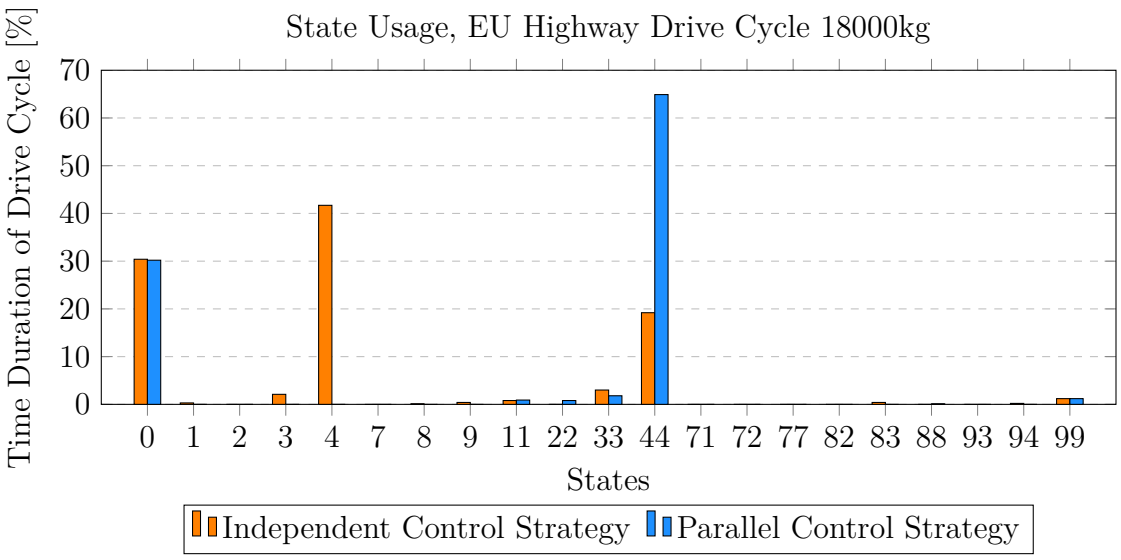

Figure 3.10: State usages for independent and parallel control strategies during EU Highway drive cycle with 18000 kg total mass.

Table 3.1 presents the number of shifts for both control strategies as well as the energy efficiencies during the drive cycle. The independent control strategy demands about $20-25\%$ more shifts than the parallel control strategy while retaining 0.98% better average total efficiency. During 45.5% of the drive cycle, the independent control strategy utilized an independent state, such as state 4, rather than a parallel state. This indicates that the state selection varies significantly between the strategies and is mostly due to the fact that the independent control strategy often engages state 4 during coasting.

Table 3.1: Results for independent and parallel control strategies during EU Highway drive cycle with 18000 kg total mass.

	Sel. States [n]		MDS Avg. Eff [%]				GB Avg. Eff [%]		Axle Avg. Eff [%]
	EA1	EA2	MDS1	MDS2	MDS3	MDS4	GB1	GB2	
Parallel Control	101	101	93.47	94.10	93.47	94.1	94.55	94.55	83.34
Independent Control	118	137	93.29	94.22	89.79	95.36	95.18	96.01	84.32

Figure 3.10 shows the state usage for both control strategies when the total mass is raised to 35300 kg for the same EU Highway drive cycle. With the higher mass, the variation in state usage has increased. As previously noted in Figure 3.9, the parallel control strategy utilizes states 33 and 99 in segments where state 44 was used at the lower mass. The independent control strategy has also chosen independent states with higher torque capabilities, such as states 94 and 9 instead of state 4. The utilization of independent states is 46.9%, which is similar to the results for the lower total mass.

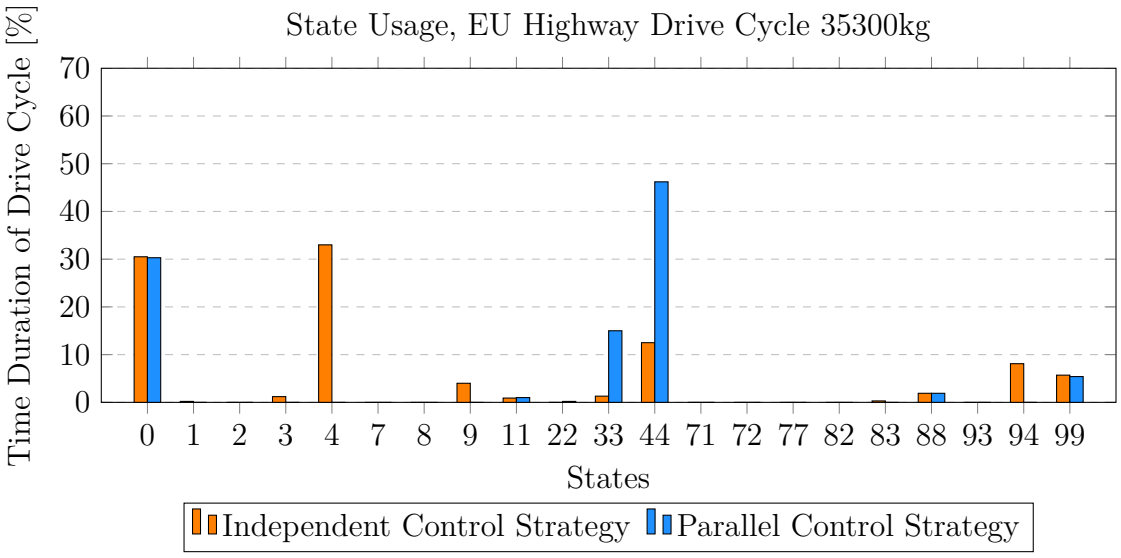

Figure 3.11: State usages for independent and parallel control strategies during EU Highway drive cycle with 35300 kg total mass.

Table 3.2 presents the resulting efficiencies and the number of selected states. Overall, the number of selected states has increased by about 80% with the higher total mass. However, the difference in the number of selected states between the strategies has decreased, and the average axle efficiencies are very similar, with the independent control strategy achieving only 0.06% higher efficiency.

Table 3.2: Results for independent and parallel control strategies during EU Highway drive cycle with 35300 kg total mass

	Sel. States [n]		MDS Avg. Eff [%]				GB Avg. Eff [%]		Axle Avg. Eff [%]
	EA1	EA2	MDS1	MDS2	MDS3	MDS4	GB1	GB2	
Parallel Control	181	181	95.62	89.25	95.62	89.25	94.50	94.40	83.59
Independent Control	183	201	95.26	92.22	93.43	92.13	94.79	94.68	83.65

Finally, Figure 3.12 presents the state usage when the total mass is raised to 64000 kg. As expected, the utilization of states with high torque capabilities increases further with the increased mass. Now, state 99 is commonly used for both strategies, while the utilization of states 4 and 44 has reduced. Although state 94 has become more frequently used, the overall usage of independent states for the independent control strategy has decreased to 38.7%. While this is a reduction, it still indicates that there are distinct differences in state selection between the individual and parallel control strategies, even for high total masses when driving on EU highways.

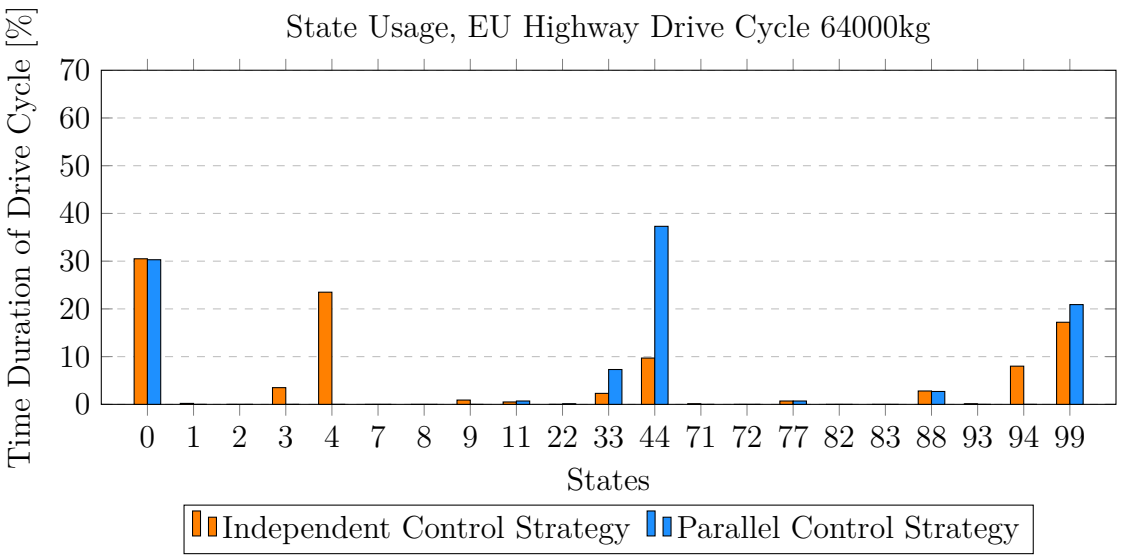

Figure 3.12: State usages for independent and parallel control strategies during EU Highway drive cycle with 64,000 kg total mass.

Table 3.3 shows the resulting efficiencies and the number of selected states for both strategies. With the increased mass, the number of selected states has increased further by about 40% and are now very similar for both strategies. The average efficiencies between the axles are very similar, with the independent control achieving 0.22% better overall efficiency.

Table 3.3: Results for independent and parallel control strategies during EU Highway drive cycle with 64000 kg total mass.

	Sel. States [n]		MDS Avg. Eff [%]				GB Avg. Eff [%]		Axle Avg. Eff [%]
	EA1	EA2	MDS1	MDS2	MDS3	MDS4	GB1	GB2	
Parallel Control	242	242	94.20	89.39	94.20	89.39	93.88	93.88	82.57
Independent Control	242	279	93.80	88.07	94.4	91.71	93.32	95.10	82.79

Comparing the individual and parallel control strategies during the EU Highway drive cycle, it is concluded that states 4, 44, and 99 are most frequently used due to that the truck mostly operates at high speed. Of these states, only state 4 is unique to the independent control strategy, and with increased total truck mass, the independent strategy leans more and more towards states 44 and 99. However, between 38.7 and 45.5% of the drive cycle remains in state 4 or any other of the individual states depending on the mass. This shows that there are large differences in state selection between the independent and parallel control strategies during operation at EU highways. Despite this, the difference in total efficiency for the electrified axles is 0.98% when the truck is at curb weight and below 0.22% when the truck weighs 35300 kg or more.

To evaluate why lower mass truck has slightly better driveline efficiency even though the differences in utilization of individual states are similar is further studied here. It is found that when the truck weighs 18000 kg and operates at 80 km/h, which is the highest legal speed for heavy-duty trucks in the EU, the operation point of EM2

in state 4 is close to the highest efficiency island.[15] When state 44 is engaged at the same drive cycle segment, the wheel torque demand is divided equally between EM2 and EM4, resulting in the operating points being in a less optimal region of the electric machine efficiency map. This is shown in Figure 3.13, where the operation points from 50 seconds of highway operation at 80 km/h with varying road inclination are presented for state 4 and state 44.

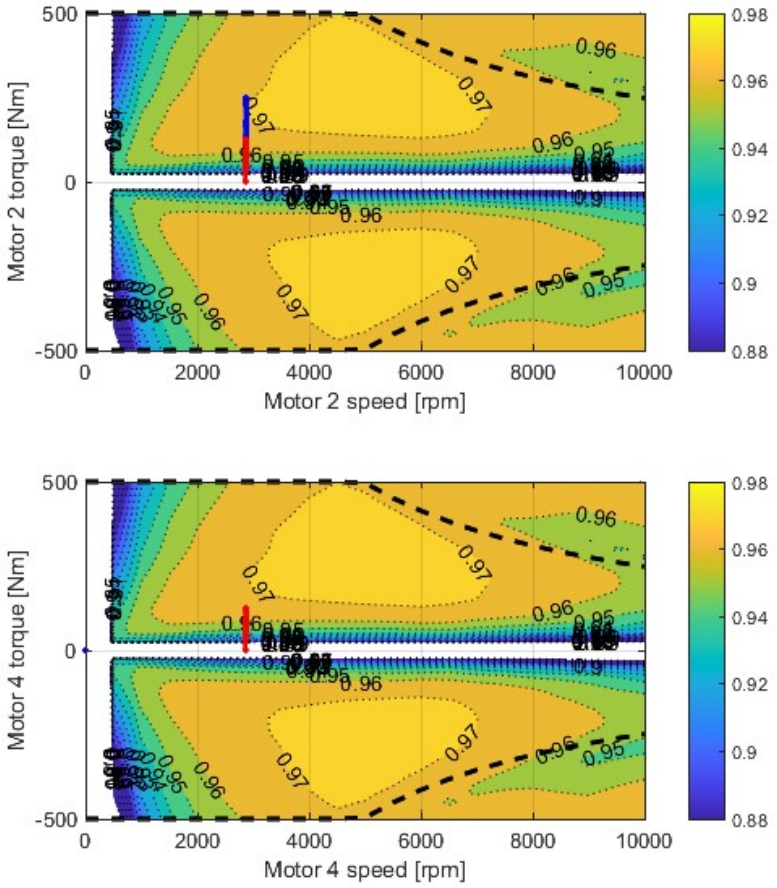

Figure 3.13: Operating points for EM2 and EM4 in state 4 (blue) and state 44 (red) at $80 km/h$ with varying road inclination.

With only a slight increase in motor torque demand, the operating points for state 44 would be on the same island as the operating points for state 4. Thus, when the truck is loaded with more mass, the torque demand rises, leading to similar performance between states 44 and 4. This explains the 0.98% efficiency difference when the truck weighs 18000 kg and why the difference is below 0.14% when the truck is loaded.

3.4.2 US Highway Drive Cycle

US highways are typically limited to 70 mph (or 113 km/h), which is significantly higher than the EU highway speed limit, [16]. Figure 3.14 shows the resulting operating points for the three total masses during the US highway drive cycle, using the independent control strategy. This drive cycle has a higher number of data

clusters compared to the EU drive cycle, with vehicle speeds ranging from 25 mph to 70 mph. Even at higher speeds, state 4 covers most of the cluster points for 18000 kg, while state 44 is required when the weight is increased to 35300 kg. At 64000 kg, state 99 is needed at cruising speeds below the rotational speed limit of EM1 and EM3. In addition to the data points outside of the torque limit for states 88 and 99 during acceleration, it is worth noting that state 44 is unable to produce the required torque during coasting at high speeds occasionally.

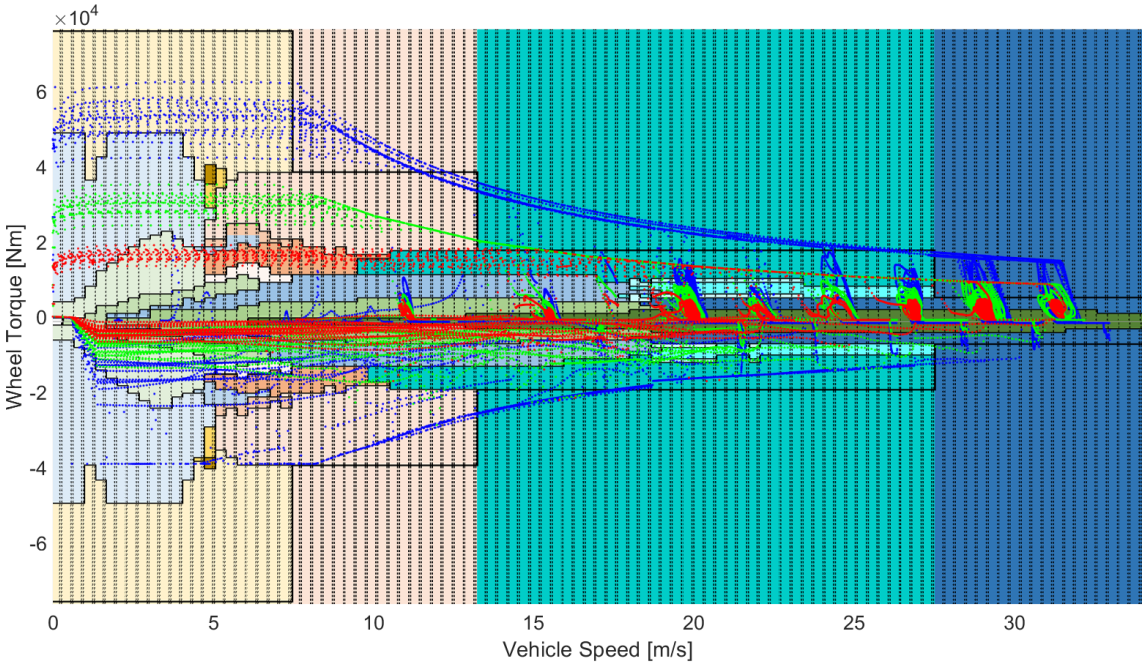

Figure 3.14: Operation points on the independent control strategy state selection map from the US Highway drive cycle for 18000 kg (red), 35300 kg (green), and 64000 kg (blue) total truck mass.

The differences in state selections between the independent and parallel control strategies mirror the variations observed during the EU drive cycle. At higher speeds, the influence of state 4 increases as its operational range expands, further enhancing its significance. See Figure 3.15.

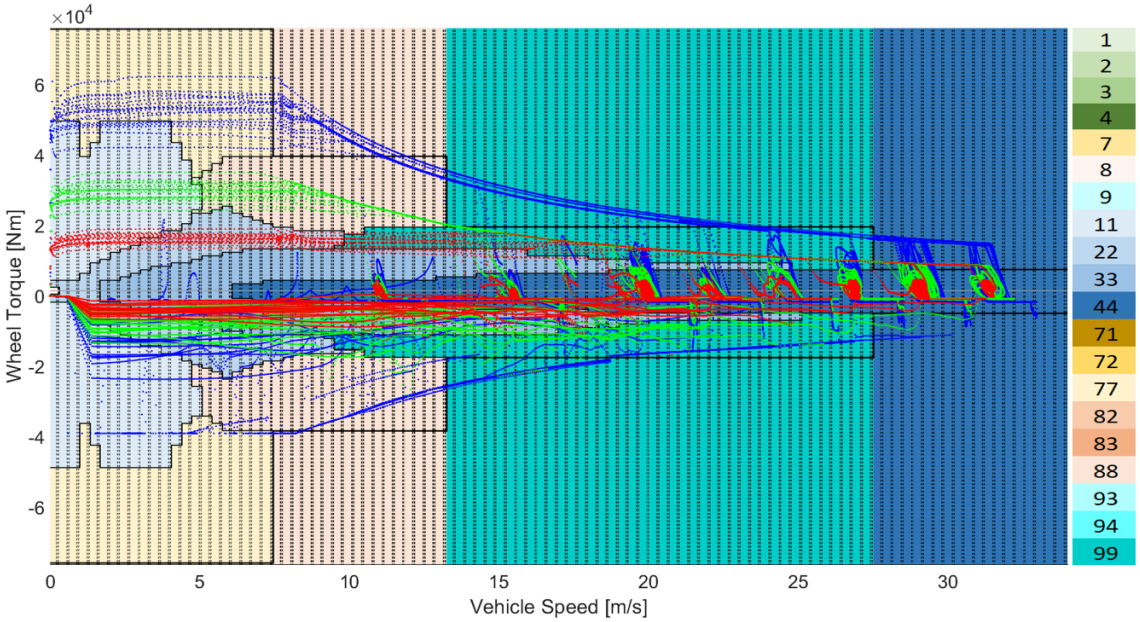

Figure 3.15: Operation points on the parallel control strategy state selection map from the US Highway drive cycle for 18000 kg (red), 35300 kg (green), and 64000 kg (blue) total truck mass.

The state usage for a truck with 18000 kg total mass is shown in Figure 3.16. The results are similar to the state usage for a truck with the same mass driving on EU highways, previously shown in Figure 3.10. As seen, states 4 and 44 are the most frequently used states, with the independent control strategy using independent states for 48.2% of the drive cycle.

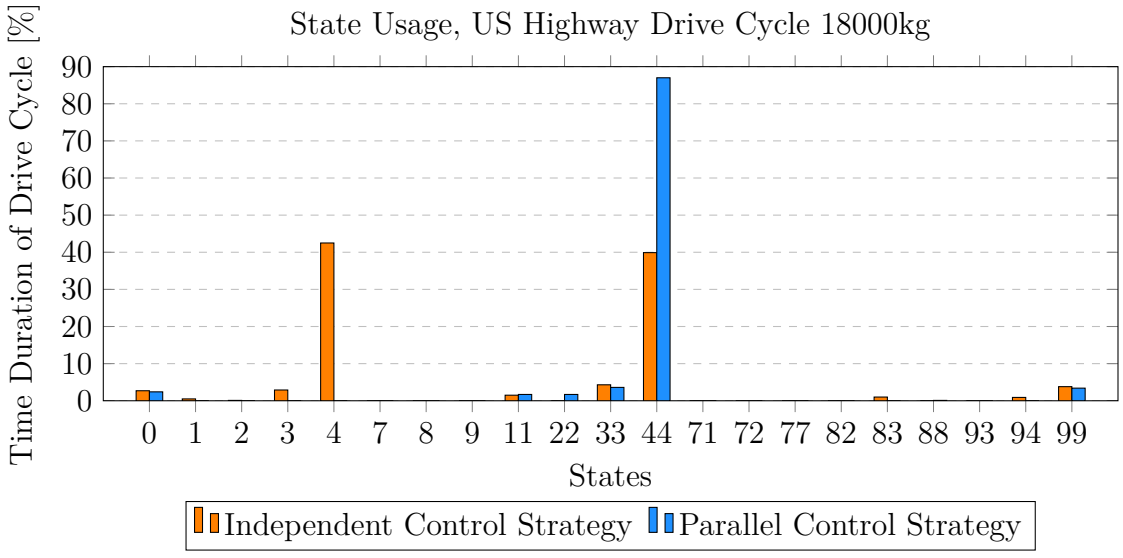

Figure 3.16: State usages for independent and parallel control strategies during US Highway drive cycle with 18000 kg total mass.

Table 3.4 shows the number of selected states and efficiencies for the complete US highway drive cycle for a truck with a mass of 18000 kg. Compared to the EU high-

way drive cycle, the parallel and independent control strategies have more similar results for the average axle efficiency, with only a 0.63% difference. This indicates that during higher speeds, state 4 and state 44 are operating at similar efficiencies.

Table 3.4: Results for independent and parallel control strategies during US highway drive cycle with 18000 kg total mass.

	Sel. States [n]		MDS Avg. Eff [%]				GB Avg. Eff [%]		Axle Avg. Eff [%]
	EA1	EA2	MDS1	MDS2	MDS3	MDS4	GB1	GB2	
Parallel Control	144	144	87.73	95.24	87.73	95.24	94.96	94.96	85.39
Independent Control	154	213	86.04	95.37	90.49	95.80	95.42	95.79	86.02

When increasing the mass to 35300 kg, both strategies exchange state 4 and state 44 to state 99 to handle the higher torque demand in some instances, see Figure 3.17. Additionally, the independent control strategy uses state 94 for 5.6% of the drive cycle, which keeps the independent state usage at 47.9% for the independent control strategy. This correlates well with the state selection for the EU highway drive cycle at the same weight, although the vehicle speeds differ.

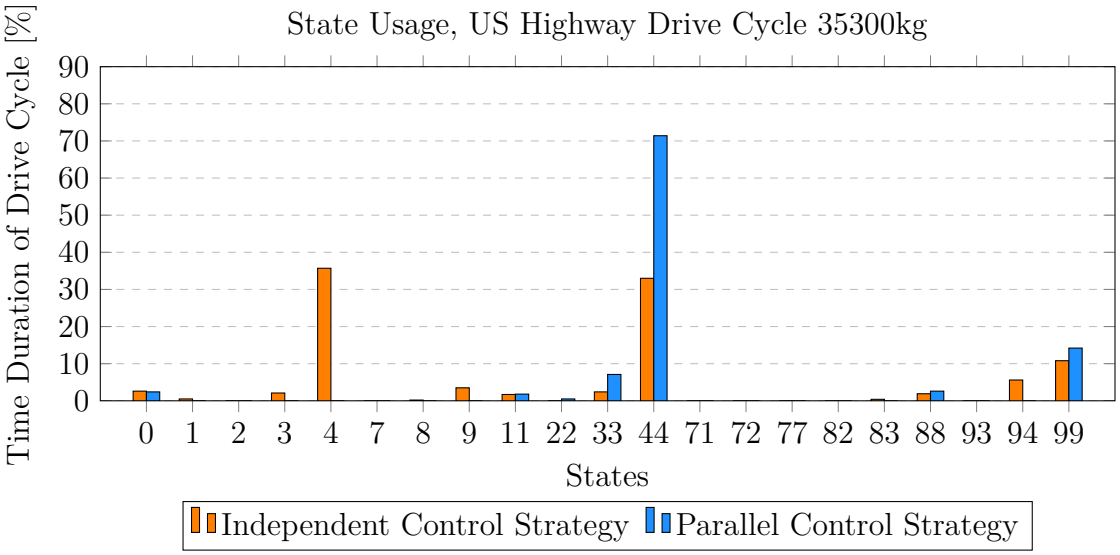

Figure 3.17: State usages for independent and parallel control strategies during US Highway drive cycle with 35300 kg total mass.

Table 3.5 shows the number of selected states and efficiencies for the complete US highway drive cycle for a truck with a mass of 35300 kg. Interestingly, the number of selected states for axle 1 are the similar for both strategies, but for axle 2 the independent control strategy does about 50% more selections than the parallel control strategy. This is likely due to the fact that state 44 is engaged and disengaged, resulting in the independent control strategy achieving 0.59% higher efficiency than the parallel control strategy.

Table 3.5: Results for independent and parallel control strategies during US highway drive cycle with 35300 kg total mass.

	Sel. States [n]		MDS Avg. Eff [%]				GB Avg. Eff [%]		Axle Avg. Eff [%]
	EA1	EA2	MDS1	MDS2	MDS3	MDS4	GB1	GB2	
Parallel Control	209	209	92.43	94.09	92.43	94.09	94.69	94.69	84.61
Independent Control	208	306	93.02	93.64	87.96	94.94	94.70	94.83	85.20

Figure 3.18 presents the state usages for 64000 kg total mass for the US highway drive cycle. Once again the results are similar to the EU highway drive cycle, with states 99 and 88 being more frequently used for both strategies and state 94 being used more by the independent control strategy. Even at this high total vehicle mass, the usage of independent states such as state 4 and state 94 is 44.6%.

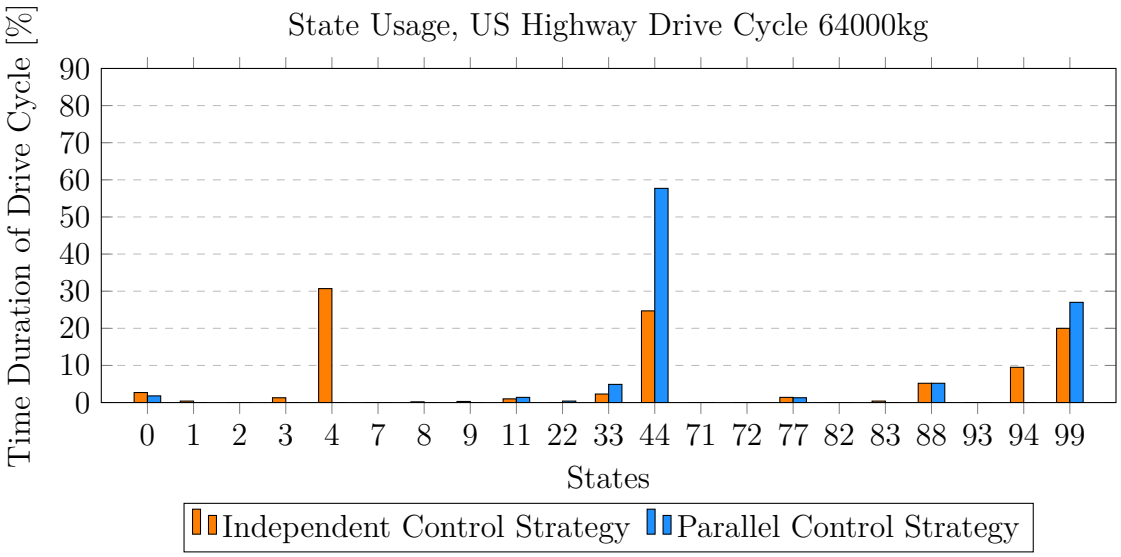

Figure 3.18: State usages for independent and parallel control strategies during US Highway drive cycle with 64000 kg total mass.

Table 3.6 presents the resulting number of state selections and efficiencies for the US highway driving cycle for a truck with 64000 kg total mass. Similar to the EU highway drive cycle, the number of selected states has once again increased with the increased vehicle mass. Additionally, the trend found at 35300 kg of engagement and disengagement of state 44 using the independent control strategy is present even at 64000 kg. The result is that the independent control strategy achieves 0.41% better average efficiency.

Table 3.6: Results for independent and parallel control strategies during US highway drive cycle with 64000 kg total mass.

	Sel. States [n]		MDS Avg. Eff [%]				GB Avg. Eff [%]		Axle Avg. Eff [%]
	EA1	EA2	MDS1	MDS2	MDS3	MDS4	GB1	GB2	
Parallel Control	349	349	92.93	92.12	92.93	92.12	94.23	94.23	83.51
Independent Control	335	434	92.89	90.68	91.84	93.88	93.63	95.59	83.92

The results from the US highway drive cycle reveal that the state selections closely resemble those of the EU highway drive cycle despite the higher speeds. However, the

US highway drive cycle engages and disengages state 44 more frequently compared to the EU highway drive cycle. It is also found that the independent control strategy makes use of independent states between 48.2 and 44.6% of the drive cycle depending on the weight. This indicates that even for the US highway drive cycle, the state selection differs significantly between the strategies. However, there is less difference in efficiency at lower vehicle weights for the two strategies, which indicates that the operating points for states 4 and 44 are in more optimal regions during high speeds. To confirm this, the operation points for when state 4 is chosen by the individual control strategy and state 44 is chosen by the parallel control strategy are studied. Figure 3.19 shows that during higher speeds, the demanded torque is higher, resulting in the operating points being closer to the most optimal efficiency islands.

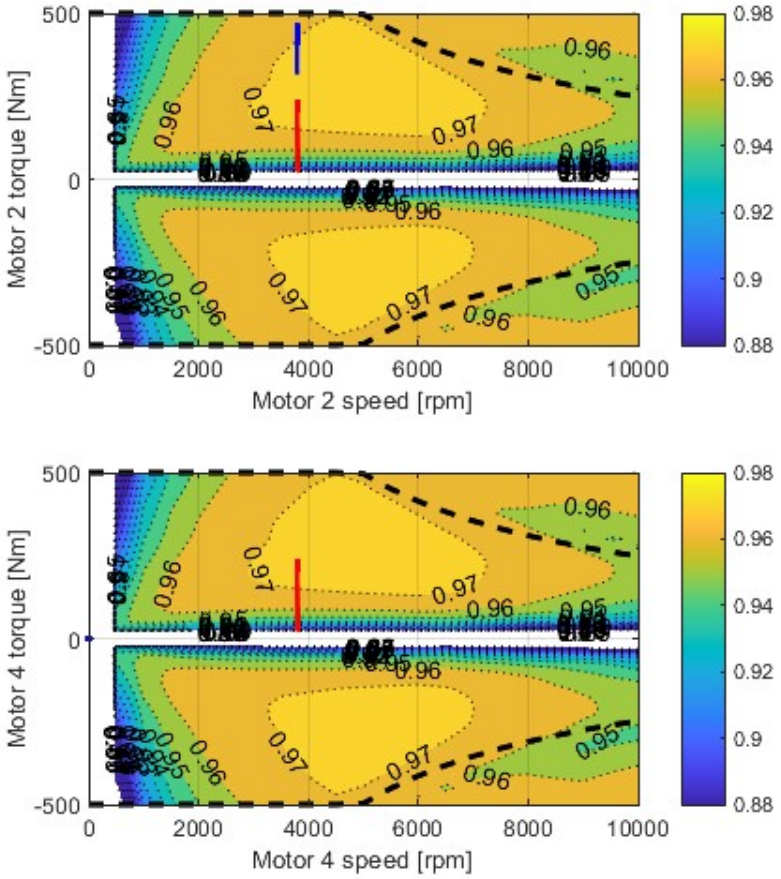

Figure 3.19: Operating points for EM2 and EM4 in state 4 (blue) and state 44 (red) at 70 mph with varying road inclination.

3.4.3 City Drive Cycle

In this section, the independent and parallel control strategies are evaluated in city driving scenarios. Figure 3.20 shows the operation points on the independent control strategy state map, which are centered around the lower speed region. In this part of the map, there are numerous smaller islands to select from. This mainly concerns the selection for lower truck masses, which sweep through many islands, while the

selection for heavier trucks operates above the cluster of smaller state islands. States 3 and 4 cover many data points in the low torque region, while states 77, 88, and 99 are required for the higher torque regions.

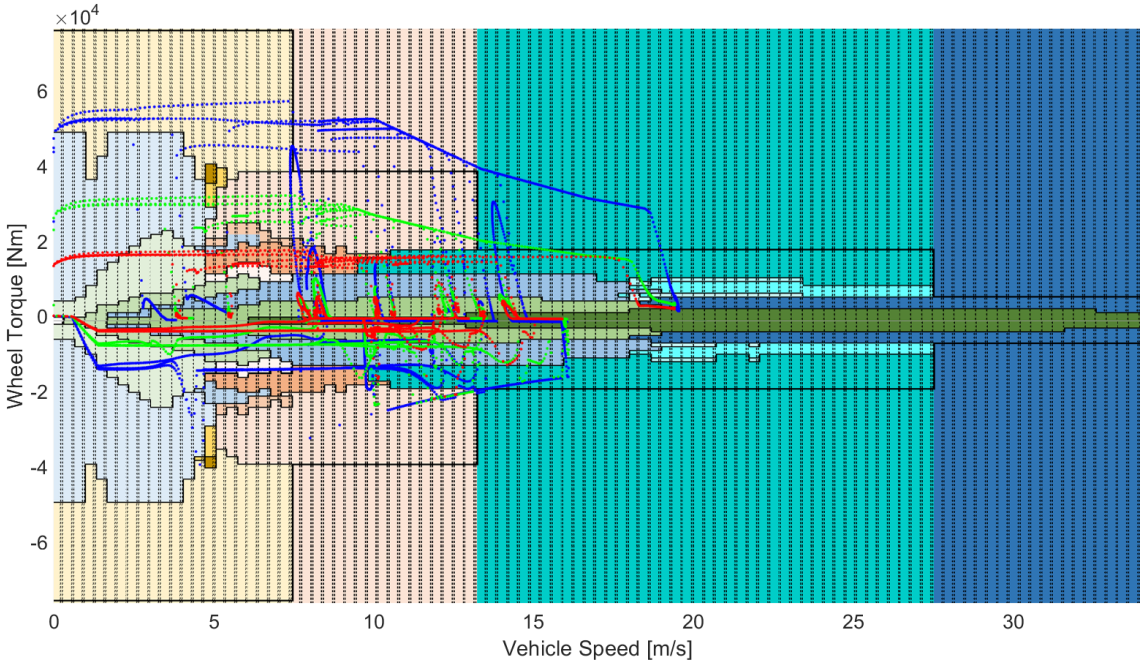

Figure 3.20: Operation points on the independent control strategy state selection map from the City drive cycle for 18000 kg (red), 35300 kg (green) and 64000 kg (blue) total truck mass.

The parallel control strategy has a significantly less crowded selection map in the lower speed region. States 11, 22, 33, and 44 cover almost all operating points for the 18000 kg truck mass, while states 77, 88, and 99 gain significance with increasing truck mass.

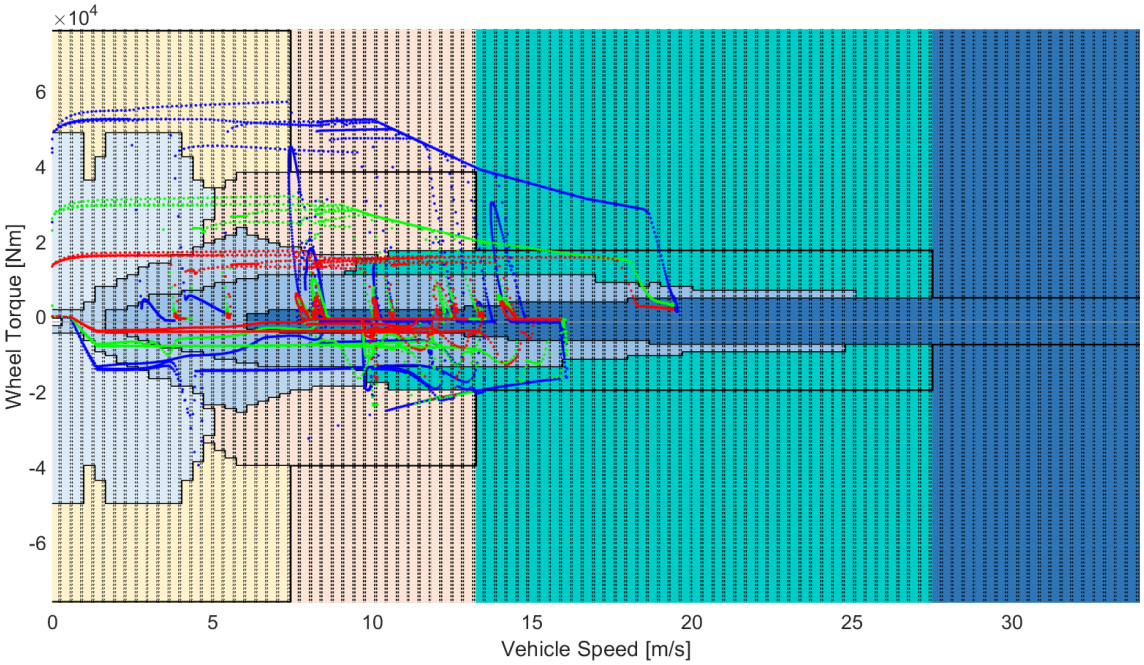

Figure 3.21: Operation points on the parallel control strategy state selection map from the City drive cycle for 18000 kg (red), 35300 kg (green) and 64000 kg (blue) total truck mass.

The state map usage shown in Figure 3.22 reflects the conclusions drawn from Figures 3.20 and 3.21. While state 44 covers more than half the operation points in the parallel control strategy state selection map, the state is never engaged using the independent control strategy. The difference in state selections between the strategies is significantly greater during city driving compared to highway driving when the total mass is 18000 kg, with an individual state usage of 61.1% for the individual control strategy. Of these states 3 and 4 are primarily used for the individual control strategy, whereas the parallel control strategy predominantly chooses states 33 and 44. Considering the city traffic speed and the light load, these low torque state choices are expected operating points.

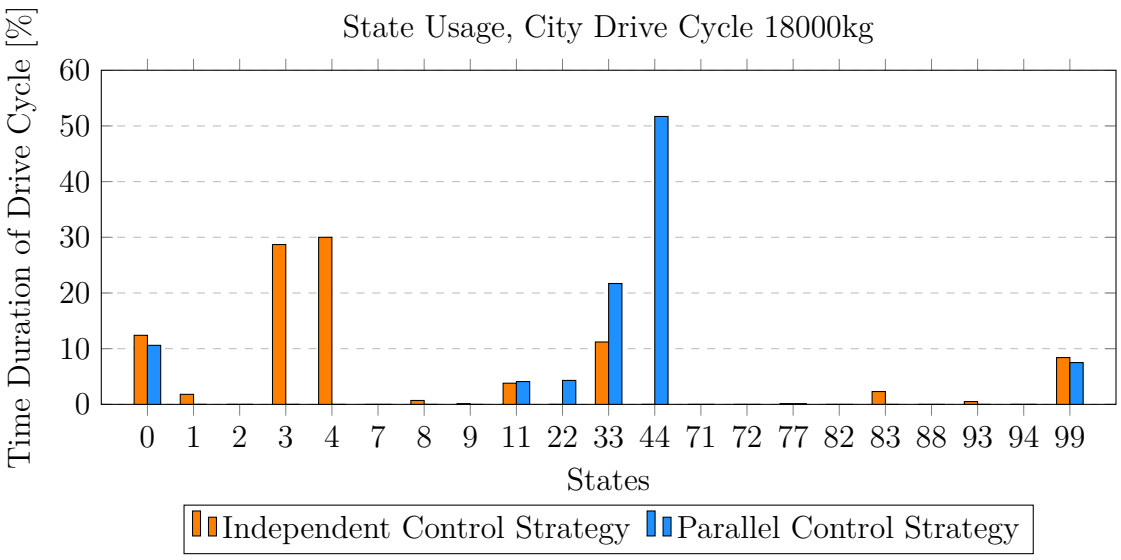

Figure 3.22: States usages for independent and parallel control strategies during city drive cycle with 18000 kg total mass.

Table 3.7 shows that the two strategies have a similar amount of selected states, but that the independent control strategy achieves 1.79% higher efficiency. At light loads and city speeds, the operation point on the parallel control strategy state map is at states 33 and 44, both of which activates two electric machines in pair and divides the torque demand equally. The independent control strategy, on the other hand, utilizes the single electric machine states 3 and 4, resulting in higher electric machine torque demand, which generally results in higher MDS efficiency. However, the data in Table 3.7 suggests that the higher overall efficiency can be attributed to the increased gearbox efficiency rather than the MDS efficiency. This is consistent with the gearbox efficiency depicted in Figure 3.2 on page 40, where higher torque throughput results in higher efficiencies.

Table 3.7: Results for independent and parallel control strategies during city drive cycle with 18000 kg total mass.

	Sel. States [n]		MDS Avg. Eff [%]				GB Avg. Eff [%]		Axle Avg. Eff [%]
	EA1	EA2	MDS1	MDS2	MDS3	MDS4	GB1	GB2	
Parallel Control	51	51	88.39	85.14	88.39	85.14	92.41	92.41	77.58
Independent Control	61	44	84.73	89.68	88.76	91.22	92.92	94.08	79.37

When the truck mass increases to 35300 kg, the usage of states 3 and 4 decreases by 8% and 6.1%, respectively, while the usage of state 88 rises from 0% to 12.6% for the independent control strategy. The same trend is found for the parallel control strategy, where the usage of state 44 decreases by 15.5% while states 88 and 99 increase by 12.1% and 12.2%, respectively. The state usages between the two strategies remain distinct, with the independent control strategy utilizing independent states 51.6% of the time.

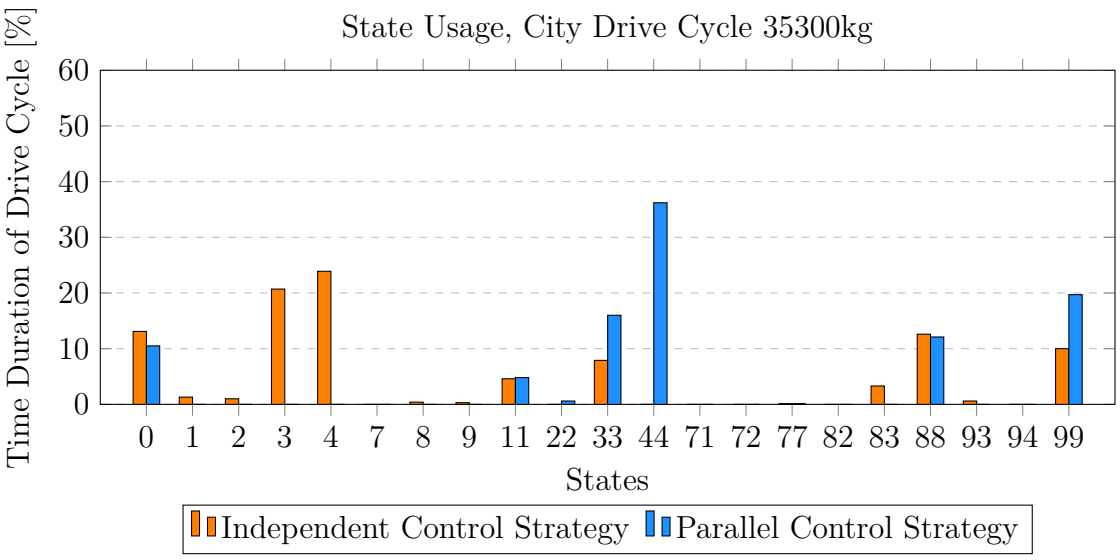

Figure 3.23: States usages for independent and parallel control strategies during city drive cycle with 35300kg total mass.

A similar number of states are used for the strategies, as seen in Table 3.8. Interestingly, the independent state selection achieves 1.12% higher efficiency than the parallel state selection, which is higher than the 0.91% difference observed at 18000 kg. To evaluate this difference, the operating points in Figure 3.20 and 3.21 are examined. During acceleration, the positive torque demand is of such magnitude that both strategies seem to utilize the same parallel states 11, 88, and 99. However, the negative torque demand is lower, resulting in the independent control strategy using states 1 and 2 frequently below 6 m/s, while the parallel control strategy uses states 33, 22, and 11. Due to the low torque demand, the single motor states 1 and 2 results in higher efficiency.

Table 3.8: Results for independent and parallel control strategies during City drive cycle with 35300 kg total mass.

	Sel. States [n]		MDS Avg. Eff [%]				GB Avg. Eff [%]		Axle Avg. Eff [%]
	EA1	EA2	MDS1	MDS2	MDS3	MDS4	GB1	GB2	
Parallel Control	59	59	89.66	81.64	89.66	86.64	92.66	92.66	78.46
Independent Control	61	51	86.24	82.90	86.77	92.61	91.50	94.39	79.58

The results for the highest total mass of 64000 kg differ significantly from the city drive cycle with the lower vehicle masses. The usage of states 77 and 88 increases drastically for both strategies, which is expected since these are the two states with the highest torque capabilities. The parallel control strategy reduces the usage of states 44 and 99 in the change of these states, while the independent control strategy reduces the usage of states 3 and 4. See Figure 3.24 for the state usages.

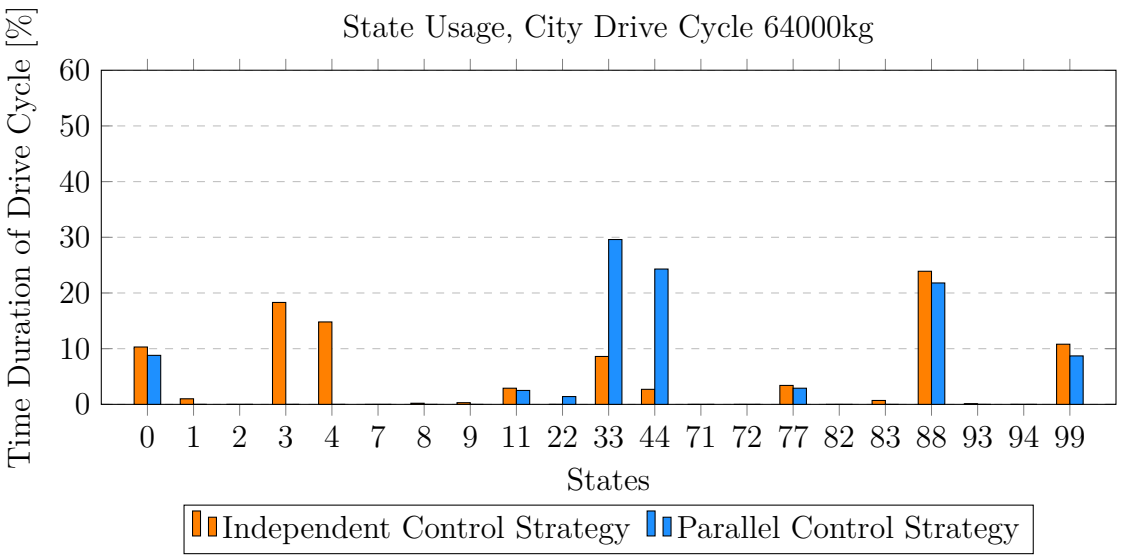

Figure 3.24: State usages for independent and parallel control strategies during City drive cycle with 64000 kg total mass.

The efficiencies for the 64000 kg configuration also differ compared to the lighter truck masses, as seen in Table 3.9. The average efficiency for the parallel control strategy increases to 80.0%, but the efficiency for the independent control strategy drops to 79.0%. As a result, the parallel control strategy achieves a 1.00% higher efficiency compared to the independent control strategy. This is particularly noteworthy because, in all other drive cycles, the independent control strategy has been the most efficient.

Table 3.9: Results for independent and parallel control strategies during city drive cycle with 64000 kg total mass.

	Sel. States [n]		MDS Avg. Eff [%]				GB Avg. Eff [%]		Axle Avg. Eff [%]
	EA1	EA2	MDS1	MDS2	MDS3	MDS4	GB1	GB2	
Parallel Control	72	72	85.79	89.77	85.79	89.77	93.36	93.36	80.04
Independent Control	68	66	85.37	86.47	85.69	91.12	92.11	93.94	78.95

The reason for the independent control's lower efficiency is further studied. It is found that due to the relatively frequent shifting caused by the transient torque demands in city traffic, 2.30% of the independent control strategy operation time is spent transitioning between states. This occurs because, when a new state is requested, one axle may shift to the new state faster than the other, causing the propulsion system to temporarily operate in an undefined state combination. During the transitioning states, the operating points of the MDS are unknown and are likely to have low efficiency, resulting in an overall low performance. Since the parallel control system sends the same signals to both axles simultaneously, this issue does not arise with the parallel control strategy.

3.5 Simplification of the State Selection Map

From the results referred to in the plots and tables in Section 3.4, it is observed that there are map states that are either unused or very little used across any of the considered truck masses or driving conditions. This observation led to the decision to delete certain states from the independent control state selection map to determine how this would lead to the change of distribution in state islands. The states removed from the original independent state selection map are 2, 8, 22, 71, 72, 82, and 93.

The simplified state selection map is generated by using the same methodology described in Section 2.2 and suppressing these states. Figure 3.25 shows this transition of the state selection map and how surrounding states displace the removed islands.

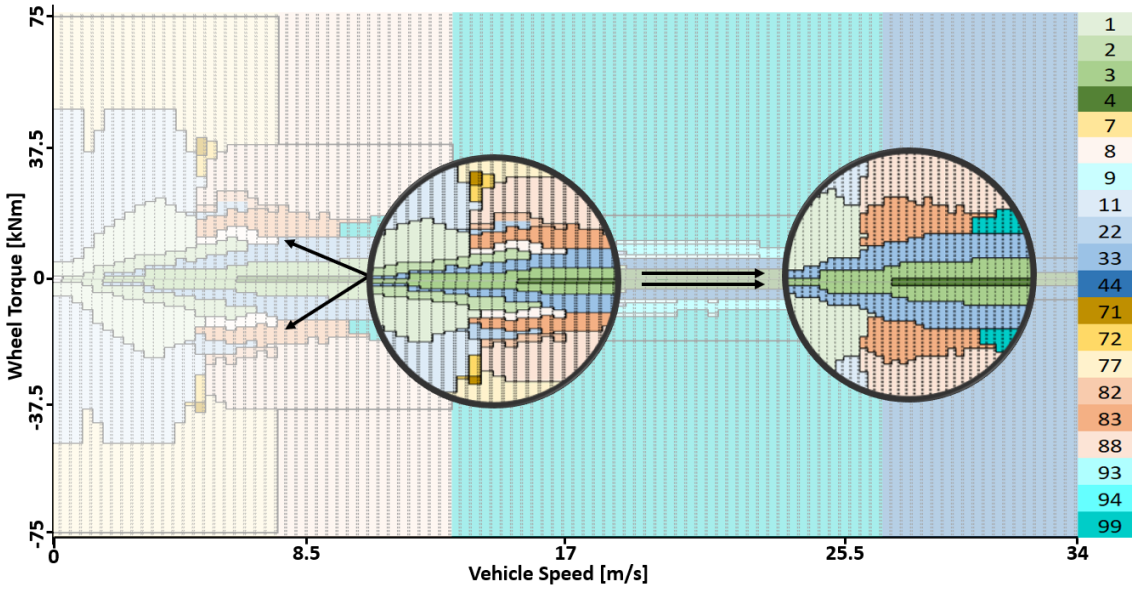

Figure 3.25: Simplification of the state selection map.

As seen in the figure, the previously busy area containing multiple small islands is now replaced by states 3, 33, 83, and 88. When this area is further studied, it is found that these states lay in such order that if the torque demand rises, the electric machines will be engaged in sequence. If state 3 is engaged initially and the torque demand rises, the neighboring state 33 will be selected which engages gear 3 on the second axle. If the torque demand further increase, the state 83 followed by state 88 will be selected, engaging gear 2 on the first axle and then on the second axle. An illustration of this sequential engagement of electric machines is shown in Table 3.10.

		Axle1		Axle2	
		EM1	EM2	EM3	EM4
States	3	3	0	0	0
	33	3	0	3	0
	83	3	2	3	0
	88	3	2	3	2

Table 3.10: Engagement of electric machines in sequence, from state 3 to 88.

A similar approach can be utilized to further simplify the map, as shown in Figure 3.26. As seen in the figure, there are small islands of state 9 at vehicle speeds between 17-23 m/s in the lower wheel torque demand region which has not been eliminated in the previous simplification.

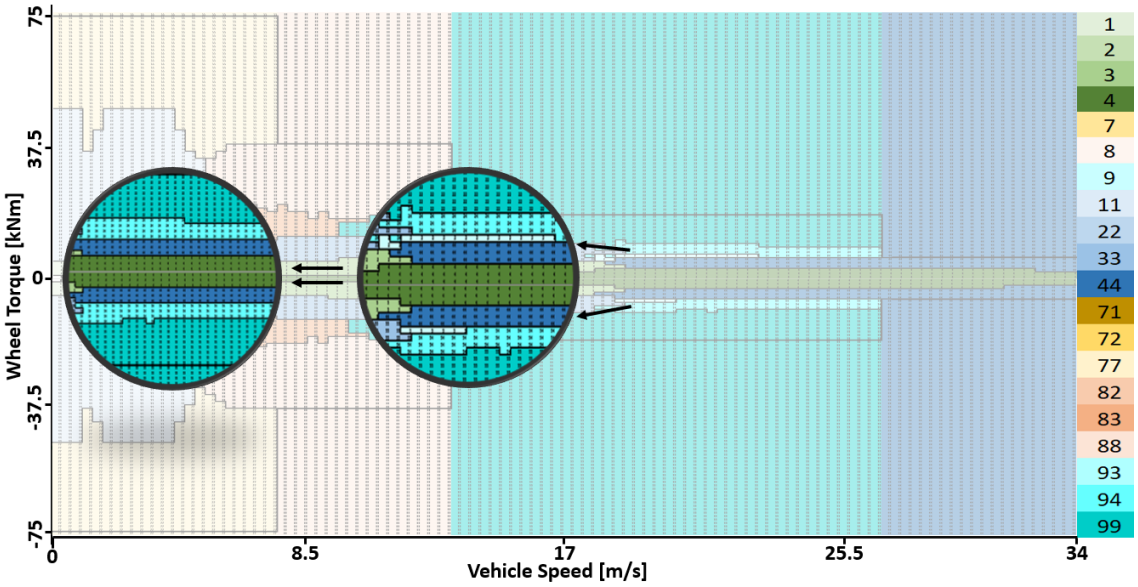

Figure 3.26: Elimination of state 9 in the simplified state selection map.

Although this state is used both during the EU and US Highway drive cycle when the truck mass is 35300kg, as seen in Figure 3.17 and 3.11, it results in an inconvenient engagement and disengagement of electric machines if the wheel torque demand rises. If state 4 is engaged initially and the wheel torque demand rises, state 44 will be selected which engages gear 4 on the second axle. When the wheel torque demand further increases, state 9 will be selected which disengages gear 4 on the second axle and engages gear 3 on the first axle. If the wheel torque demand continues to rise, state 94 will be selected, consequently re-engaging gear 4 on the second axle, followed by state 99 which engages gear 3 on the second axle. See Table 3.11 for an illustration of the engagement of electric machines.

Table 3.11: Undesired engagement and disengagement of gear 4 on the second axle due to state 9.

		Axle1		Axle2	
		EM1	**EM2**	**EM3**	**EM4**
States	**4**	0	**0**	**0**	**4**
	44	0	**4**	**0**	**4**
	9	**3**	**4**	**0**	**0**
	94	**3**	**4**	**0**	**4**
	99	**3**	**4**	3	4

By eliminating state 9, the electric machines are engaged in sequence. This modification to the state selection map aims to streamline the transitioning between states at higher vehicle speeds. While this elimination may affect the efficiency since state 9 is determined by the state selection map to be the most efficient state in these specific operating points, it is deemed necessary to ensure smooth gear shifting. See Table 3.12 for an illustration of the engagement of electric machines in sequence.

Table 3.12: Engagement of electric machines in sequence, from state 4 to 99.

		Axle1		Axle2	
		EM1	**EM2**	**EM3**	**EM4**
States	**4**	**0**	**0**	**0**	**4**
	44	**0**	**4**	**0**	**4**
	94	**3**	**4**	**0**	**4**
	99	**3**	**4**	**3**	**4**

The result of the simplification of the state selection map is shown in Figure 3.27. The state selection map consists of the parallel states 0, 11, 33, 44, 77, 88, 99 and the independent states 1, 3, 4, 83 and 94. Thus, 7 of the 8 parallel states remain, while only 5 of the 13 independent states are left after simplification.

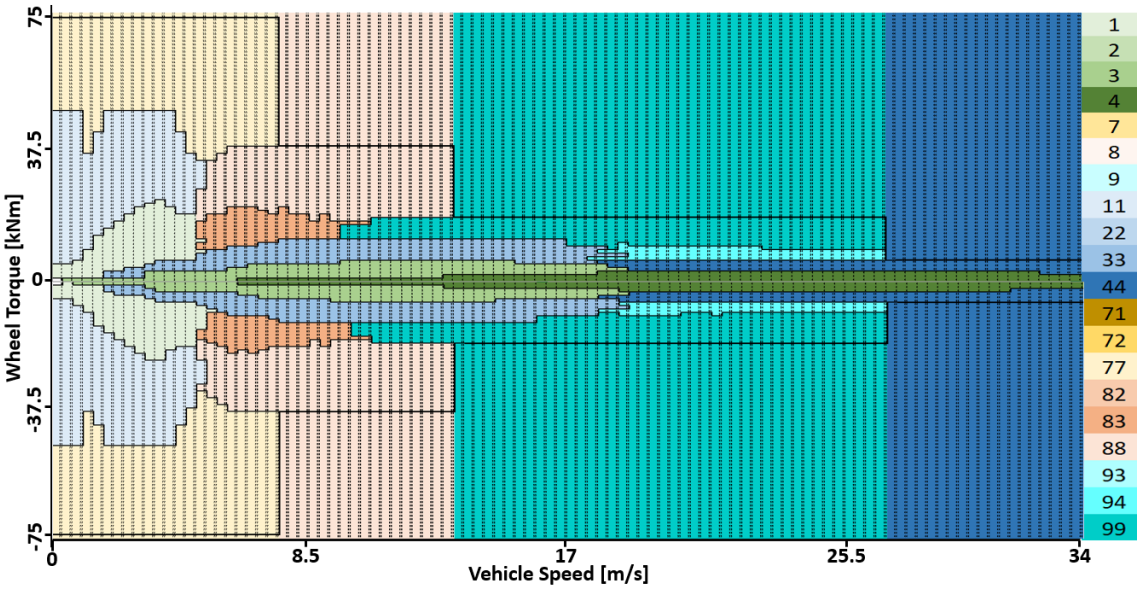

Figure 3.27: Simplified State Selection Map

The three driving cycles with the three truck masses are simulated with this state selection map to evaluate the effect of the simplification on efficiency. Table 3.13 shows the results after simplification, and Table 3.14 shows the previous results for the independent state selection map before simplification from Section 3.4 as a reference.

Table 3.13: Results after simplification of the state selection map.

		EU Highway Drivecycle Driveline Efficiency [%]	US Highway Drivecycle Driveline Efficiency [%]	City Drivecycle Driveline Efficiency [%]
Truck Mass	18000 kg	84.16	85.91	80.30
	35300 kg	83.32	84.89	80.95
	64000 kg	82.86	83.94	78.94

Table 3.14: Results before simplification of the state selection map.

		EU Highway Drivecycle Driveline Efficiency [%]	US Highway Drivecycle Driveline Efficiency [%]	City Drivecycle Driveline Efficiency [%]
Truck Mass	18000 kg	84.32	86.02	79.37
	35300 kg	83.65	85.20	79.58
	64000 kg	82.79	83.92	78.95

Comparing these results, it is apparent that even though states 2, 8, 9, 22, 71, 72, 82, and 93 are eliminated, the efficiency only differs slightly. Thus, the simplified state selection map is equally efficient while ensuring further improved torque delivery.

4
Discussion

This chapter presents outline of the results obtained from the research conducted for this thesis. It includes discussion of the findings, followed by a section of potential future directions for advancing the project.

4.1 Results

This section examines the results derived from the efficiency maps, which were instrumental in constructing the state selection maps. It then addresses the resolution of the state selection maps and explores the potential for optimizing the gear selection strategy. Additionally, the discussion includes an evaluation of the drive cycles utilized to test the gear selection control strategies, and how the results led to a simplification of the state selection map.

4.1.1 Efficiency Map

The total efficiency map used in this thesis work is constructed by element-wise multiplication of the electric machine efficiency map and the gearbox efficiency map for each gear. Ideally, the complete MDS efficiency, including the inverter losses, should also be considered when constructing the total efficiency map, as described in Section 2.1.
A study on how the MDS efficiency map could be obtained from the Simulink model was conducted during this thesis work, but the results were deemed too uncertain due to that the model was dependent on the environment and coolant temperature. This method can be read about in Appendix A.1.1, as well as a resulting state selection map of which performance is compared to the state selection map used in this project. As seen in the appendix, the MDS efficiency map achieved a 0.21% higher efficiency during the EU Highway drive cycle compared to the map based on the EM without the inverter. Therefore, if the MDS efficiency map was as robust as the EM efficiency map, the MDS efficiency map would have been a better choice. However, the EM efficiency map is more suitable to use for the total efficiency map for this project, due to the fact that the EM efficiency map can be directly obtained from the model. The decision is based on the fact that repeatability and convenience outweigh the slight improvement in total efficiency, which is questionable if the model is to be used to develop a specific gear selection strategy for a production electrified axle. However, the scope of this project is rather to investigate the behavior of a Simulink model with simplified components which may be changed in the future. In

such scenarios, it is beneficial to have a model that is quickly adaptable, which is the reasoning behind the use of the EM-based efficiency map for this project.

A further attempt to construct an efficiency map including the ESS was also done in this thesis work, which can be read about in Appendix A.3. However, as explained in Section 2.1, the ESS efficiency is not relevant to the gear selection strategy.

4.1.2 State Selection Maps

The state selection map is a central component of this project since it decides which state is most efficient at each operating point. As explained in Section 2.2, the state selection map is constructed by combining the total efficiency map from the electric machines and gearboxes with the gear ratios of all states in an iterative process.

A related key assumption is the resolution of the state selection map, which in this project is a 100x100 matrix for the positive and negative torque each. If the resolution is increased, it is possible that the state islands change shapes and that the borders between states might become less abrupt. This might lead to variation in state selections, which could potentially increase or decrease efficiency. On the other hand, a reduction in resolution would result in faster iteration of the state selection map while possibly sacrificing optimal state selections. If a map-based state selection strategy is to be implemented, the resolution of the state selection map should be evaluated based on computational efforts and efficiency gains. Further investigations need to be done with regard to this, where the resolution limits for such maps are known.

4.1.3 Gear Selection Strategy

The aim of the thesis is to optimize the gear selection strategy with regard to efficiency and number of shifts while ensuring satisfactory torque delivery. The optimization of the system is a compromise between efficiency and number of shifts. If a large number of shifts are being made, the state selection map is traced more accurately, resulting in the most efficient states being chosen. However, the torque delivery is disrupted with each shift, necessitating that some shifts must be disregarded to maintain good drivability. Every disregarded shift means the system operates in a less optimal state.

Since the number of selected gears depends on the speed and torque demand from the drive cycle, the system's optimization cannot be determined solely by the number of shifts. To evaluate if the system is optimized, the results illustrated in Figures 3.6 and 3.7 in Section 3.3 are studied and combined into Figure 4.1.

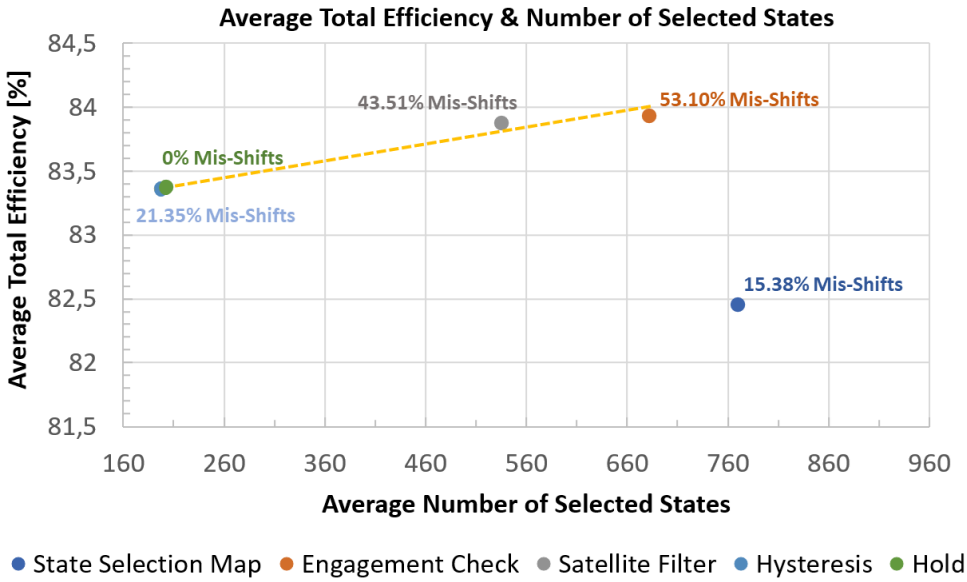

Figure 4.1: Average total efficiency and number of selected states with trend line illustrating that the average total efficiency reduces proportionally with the average number of selected states.

A trend line between the points illustrates the relationship between efficiency and the number of shifts if the state selection from the state selection map, which resulted in numerous failed shifts, is disregarded. As observed, the number of mis-shifts decreases along this trend line until it reaches 0%, indicating that the system is close to the highest achievable efficiency with zero mis-shifts. This suggests that the system is converging towards optimized efficiency and number of shifts.

However, the parameters k_d and T_d for the Satellite Filter function, the upper and lower torque bands for the Hysteresis, and the 2 second delay of the Hold function could potentially be refined, leaving room for further improvements to the average efficiency and number of shifts.

4.1.4 Independent and Parallel Control Strategy

Ideally, the gear selection strategies would be evaluated against all possible driving scenarios. However, Due to the time limit of this thesis work, the performance of the independent and parallel control strategy is only evaluated using three weights: 18,000 kg, 35,300 kg, and 64,000 kg, and the EU Highway, US Highway, and City drive cycles. These drive cycles simulate both lower speeds during city traffic as well as highway speeds, and since the weight is varied, the drive cycles also simulate a large variety of torque demands. The tested operating points are shown in Figures 3.8, 3.14 and 3.20 in the Results chapter.
The tested driving scenarios cover both high and low torque demands and almost all vehicle speeds. However, some areas of the state selection map are left empty. For example, there are few points at torque demands around 10kNm and 40kNm during speeds between 0 and 7 m/s. This indicates that the results would have been

more accurate if more than three vehicle masses were used. However, the coverage of the state selection map is considered sufficient to establish the obtained results.

4.1.5 Simplification of State Selection Map

For the simplification of the state selection map, in the first step based on map state usage considered, the Independent State Selection map was modified by removing the unused and less frequently used states. In the next step, to ensure better sequence in the engagement of multiple electric machines, the state selection map was modified by removing state 9 to arrive at the final state selection map, which is very close to the parallel state selection map with few significant independent map states. Here, 5 of the 13 independent states 1, 3, 4, 83, 94 are retained, while 6 of 7 parallel map states 11, 33, 44, 77, 88, 99 are retained.

4.2 Future Work

This section discusses potential further work related to the project, which was either out of scope or was not possible to evaluate due to the project's time limitation.

4.2.1 Inverter Efficiency

As previously discussed in Section 4.1.1, the inverter efficiency has not been considered when constructing the gear selection strategy in this project. Since the inverter losses may affect the efficiency islands, the complete MDS efficiency map should be used for generating the state selection map in further development.

4.2.2 Gear Selection Strategy Parameters

The Simulink model used for the state selection described in Section 2.3 consists of four functions: Satellite Filter, Hysteresis, Engagement Check, and Hold. The amplitude between the satellite points in the Satellite Filter is dependent on the parameters of the derivative filter, k_d and T_d, which represent the gain and the time constant. In this project, these are set to $k_d = 0.00025$ and $T_d = 0.5$. For improved function, these parameters could be further tuned, but since satisfactory results were obtained with these constants, no further tuning was done after the development of the method.

The same could be argued to be true for the torque and speed limits for the Hysteresis, which were based on the EM efficiency map. Additionally, the time constant for the Hold method should be further evaluated to ensure that 2 seconds is sufficient for all driving scenarios.

4.2.3 Torque Distribution

The torque distribution between the electric machines affects the operation points, which subsequently impacts the efficiency. As described in the limitations in Section

1.5.3, an existing model for the torque distribution is used. This model divides the combined wheel torque demand equally between the electric machines, which results in that each electric machine outputs the same power. This is a simple torque distribution method that could be optimized by altering more torque to the active electric machines, which would benefit from operating at higher torque levels. This is an area which could be further investigated to optimize total efficiency, however for the purpose of this paper, equal power-based torque distribution is considered sufficient to evaluate the gear selection.

4.2.4 State Distribution Between Axles

The developed gear selection strategy primarily engages the first electrified axle, with the second axle serving as a secondary support that is never engaged independently of the first axle, as shown in Section 1.2. From a simulation standpoint, the results would be the same if, for example, state 7 would engage only the gears on the second axle while leaving the first axle in neutral. However, from a vehicle dynamics standpoint, this could potentially affect traction or road behavior. Additionally, for equal utilization of the electric machines to ensure robustness, it is necessary to distribute the states between the two axles. If this gear selection strategy is to be implemented, a recommendation is to consider these factors.

5
Conclusion

The thesis work resulted in the development of a successful gear selection strategy for a truck with dual electrified axles, which is optimized with regard to efficiency and number of shifts, ensuring satisfactory torque delivery. An independent control strategy is evaluated against a parallel control strategy with respect to average propulsion system efficiency and number of shifts, concluding that independent control is more efficient during certain operating points. However, these benefits are most significant at lower total vehicle masses. Furthermore, several states are seldom used, which indicates that certain gears in the electric axle are unnecessary.

Bibliography

[1] IEA, Global CO2 emissions from trucks and buses in the Net Zero Scenario, 2000-2030, IEA, Paris, https://www.iea.org/data-and-statistics/charts/global-co2-emissions-from-trucks-and-buses-in-the-net-zero-scenario-2000-2030 (2024-01-18)

[2] IEA, Global CO2 emissions from transport by sub-sector in the Net Zero Scenario, 2000-2030, IEA, Paris https://www.iea.org/data-and-statistics/charts/global-co2-emissions-from-transport-by-sub-sector-in-the-net-zero-scenario-2000-2030-2 (accessed: 2024-01-18)

[3] IEA (2023), Global EV Outlook 2023, IEA, Paris https://www.iea.org/reports/global-ev-outlook-2023 (accesed: 2024-01-18)

[4] Volvo Trucks, "Switch to Electric," volvotrucks.com, Dec. 22, 2022. https://www.volvotrucks.com/en-en/trucks/electric/why-electric-trucks-.html, (accessed: 2024-01-18)

[5] Dana, "Electrification Capabilities Commercial Vehicle Market," dana.com, Feb. 2, 2021. https://www.dana.com/globalassets/resource-library/commercial-vehicle/brochures/cv-electrification-brochure.pdf (accessed: 2024-01-18)

[6] Zhang, Lipeng & Li, Liang & Qi, Bingnan & Song, Jian. (2015). Configuration Analysis and Performance Comparison of Drive Systems for Pure Electric Vehicle. SAE Technical Papers. 2015

[7] G. Wartgow, "How fleets can benefit from electric axles," Fleet Maintenance, Jun. 05, 2019. https://www.fleetmaintenance.com/equipment/battery-and-electrical/article/21081923/how-fleets-can-benefit-from-electric-axles (accessed 2024-01-19).

[8] M. Vehviläinen et al., "Simulation-Based Comparative Assessment of a Multi-Speed Transmission for an E-Retrofitted Heavy-Duty Truck," Energies, vol. 15, no. 7, p. 2407, Jan. 2022, doi: https://doi.org/10.3390/en15072407., (accessed: 2024-01-22)

[9] A. Morozov, K. Humphries, T. Zou, T. Rahman, and J. Angeles, "Design, Analysis, and Optimization of a Multi-Speed Powertrain for Class-7 Electric Trucks," SAE International Journal of Alternative Powertrains, vol. 7, no. 1, pp. 27–42, 2018, https://www.jstor.org/stable/26559566?saml_data=eyJzYW1sVG9rZW4iOiIwMmExYmU4Yy00MDMzLTRmZjUtYjJkMS1kOTkwNTk5NGNhY2YiLCJpbnN0aXR1dGlvbklkcyI6WyJjYzY1MWYzNC1iYzhjLTQxODQtYjc3ZS05NDQ4Mzg3Y2ZjZWIiXX0&seq=2 (accessed: 2024-01-22)

[10] Hughes A, Drury B. "Electric Motors and Drives: Fundamentals, Types and Applications 4th ed". Elsevier Science & Technology; 2013

https://search.ebscohost.com/login.aspx?direct=true&db=cat07472a&AN=clec.EBC1157393&site=eds-live&scope=site, (accessed 2024-01-23)

[11] P. Bergstrand, “How to determine the right axle configuration for your truck,” volvotrucks.com, Nov. 14, 2019. https://www.volvotrucks.com/en-en/news-stories/insights/articles/2019/nov/how-to-determine-the-right-axle-configuration-for-your-truck.html (accessed Jan. 25, 2024)

[12] U.S. Department of Transportation. "Compilation of Existing State Truck Size and Weight Limit Laws". (accessed: 2024-05-30) https://ops.fhwa.dot.gov/freight/policy/rpt_congress/truck_sw_laws/app_a.htm

[13] Žnidarič A. "Heavy-Duty Vehicle Weight Restrictions in the EU". European Automobile Manufacturers Association. (accessed: 2024-05-30) https://www.acea.auto/files/SAG_23_Heavy-Duty_Vehicle_Weight_Restrictions_in_the_EU.pdf

[14] K. J. Åström and R. Murray, Feedback Systems: An Introduction for Scientists and Engineers, Second Edition. Princeton University Press, 2021. https://books.google.se/books/about/Feedback_Systems.html?id=l5ODEAAAQBAJ&redir_esc=y, (accessed 2024-04-02)

[15] European Commission, "Current speed limit policies", 2020. https://road-safety.transport.ec.europa.eu/eu-road-safety-policy/priorities/safe-road-use/safe-speed/archive/current-speed-limit-policies_en, (accessed: 2024-04-02)

[16] U.S. Department of Transportation, Federal Highway Administration, "Maximum Posted Speed Limits on Rural Interstates", 2011. https://ops.fhwa.dot.gov/freight/freight_analysis/nat_freight_stats/docs/11factsfigures/table3_11.htm, (accessed: 2024-04-02)

[17] J. Cederbladh and J. Suryadevara, "Light-Weight MBSE Approach for Construction Equipment Domain - An Experience Report," 2023 30th Asia-Pacific Software Engineering Conference (APSEC), Seoul, Korea, Republic of, 2023, pp. 51-60

A

Appendix 1

A.1 EM and MDS Map SoC Comparison

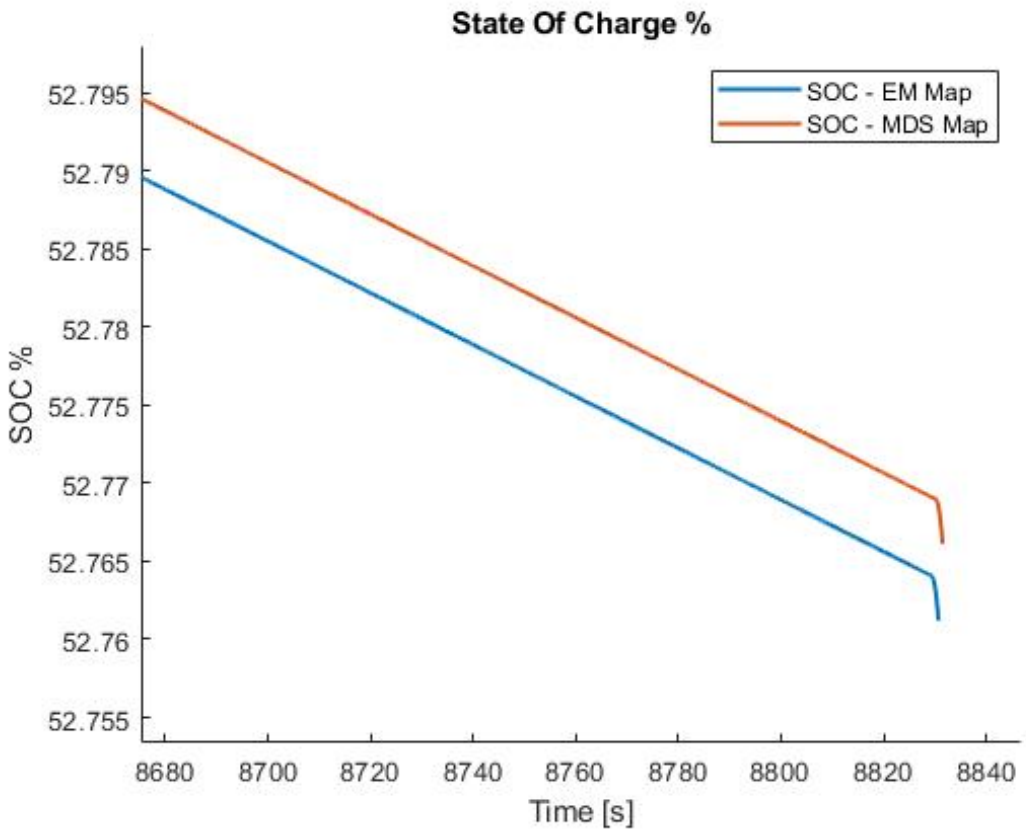

Figure A.1: SoC difference between EM and MDS based gear selection

A.1.1 Motor Drive System

The losses from the inverter are dependent on the gear selection because the switching frequency in the inverter depends on the rotational speed of the electric machine, and the current throughput is dependent on the torque. Therefore, the rotational speed and torque affect the switching losses and resistive losses in the inverter. The modeled losses in the Motor Drive System (MDS) are the conduction and switching losses from the transistors and diodes. To obtain efficiency values in a corresponding

50x50 matrix to the electric machine efficiencies, a "standalone" simulation model is built using the complete MDS model, see Figure A.3.

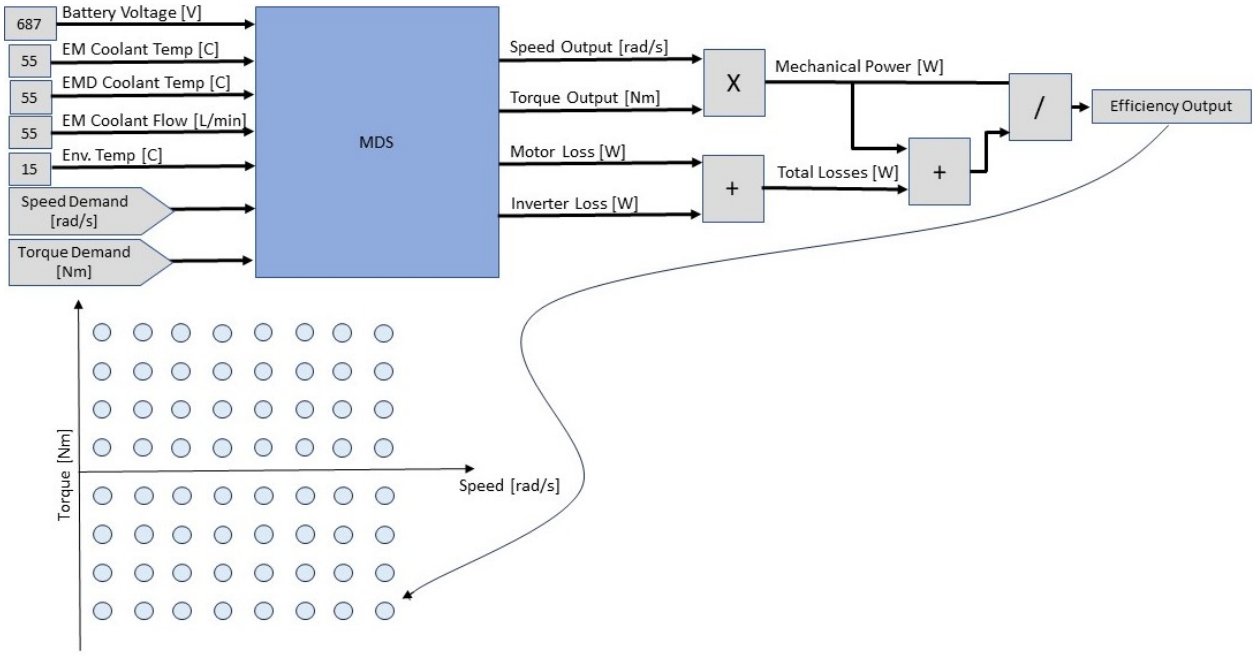

Figure A.2: Standalone model of electric machine in MATLAB Simulink

The input data to the model from the ESS is replaced with constant values. As seen in the figure, the required data to run the MDS model aside from the speed and torque demand is the battery voltage, the coolant temperature, and flow to the electric machine and inverter, as well as the environment temperature. This data is logged from a reference model using the same MDS model. The model outputs the actual motor speed and torque as well as the motor and inverter losses. The efficiency is calculated according to:

$$\eta_{MDS} = \frac{P_{Mech}}{P_{Mech} + P_{EMLoss} + P_{InvLoss}} = \frac{w_{EM} * T_{EM}}{w_{EM} * T_{EM} + P_{EMLoss} + P_{InvLoss}} \quad \text{(A.1)}$$

The speed demand is an already existing input to the model, but the torque demand comes from an external control system which needs slight modification to be manipulated. The speed and torque demand inputs are then connected to a workspace variable. The efficiency for all operating points are simulated and logged in a Matlab script with a nestled for-loop where the speed is varied from zero to the maximum speed, and the torque is varied from the maximum negative torque to the maximum positive torque in 50 increments. Because the MDS model has a limiter that limits the output power during the field weakening region, it outputs an efficiency even when the requested operating point lies above the maximum torque in the field weakening region. Therefore, an if-statement is used in the nestled for-loop that checks if the requested operating point is above the maximum power. For those operating points, the efficiency is set to 0. The resulting MDS efficiency map $\mathbf{A}_{\eta_{MDS}}$ is:

$$\mathbf{A}_{\eta_{MDS}} = \begin{vmatrix} \eta_{MDS_{1,1}} & \eta_{MDS_{1,2}} & \cdot & \cdot & \eta_{MDS_{1,50}} \\ \eta_{MDS_{2,1}} & \cdot & & & \\ \cdot & & \cdot & & \\ \cdot & & & \cdot & \\ \eta_{MDS_{50,1}} & & & & \eta_{MDS_{50,50}} \end{vmatrix} \tag{A.2}$$

The standalone model of the MDS logs the efficiency of the motor and inverter in a 50-by-50 efficiency map, see Figure A.3.

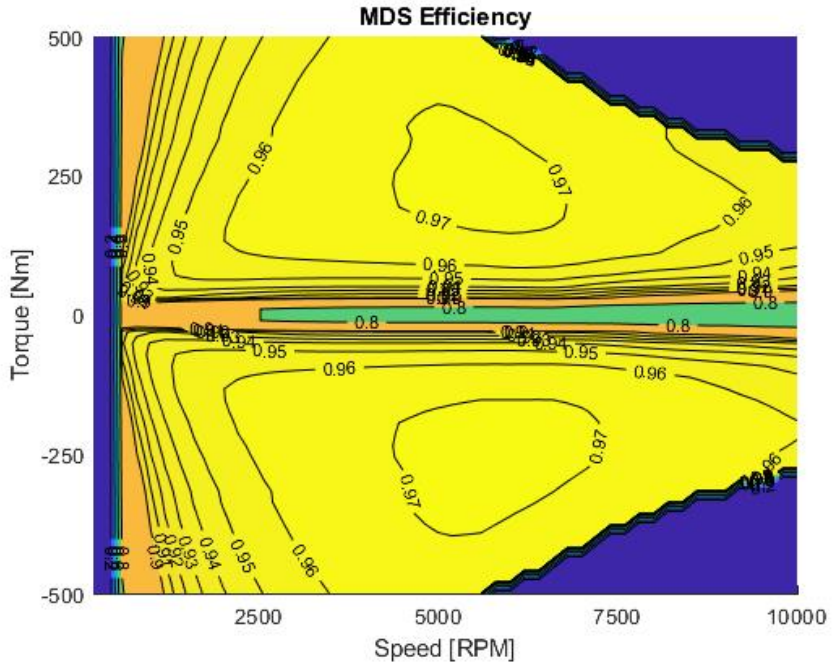

Figure A.3: 50x50 efficiency map of the motor drive system

Because the MDS efficiency is based on the same 42-by-21 matrix that represents the electric machine efficiency with the addition of the inverter losses, the MDS efficiency map looks similar to the EM efficiency map but with lower efficiency. Similarly to the electric machine efficiency, the peak efficiency is at approximately 5,600 rpm and ±260 Nm with a slightly lower value of 97.26% efficiency. Interestingly, while the EM efficiency map indicates the highest efficiency while producing positive torque, the MDS efficiency has a slightly larger efficiency island above 97% in the negative torque range.

A.2 EM & MDS Efficiency Map Comparison

This section explains how the EM state selection map and MDS state selection map, described in Sections 2.1.1 and **??**, affect the performance of the electric driveline in terms of the number of shifts, map states used, MDS efficiencies, and gearbox efficiencies.

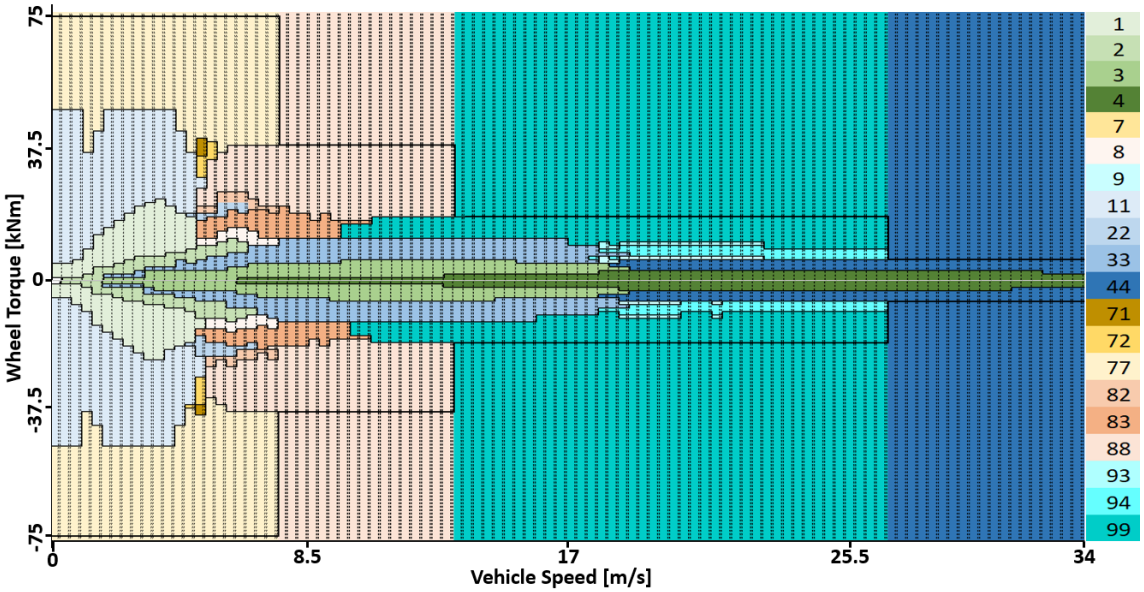

Figure A.4: Electric Machine State Map

Figure A.4 and A.5 illustrate state selection maps based on EM and MDS respectively.

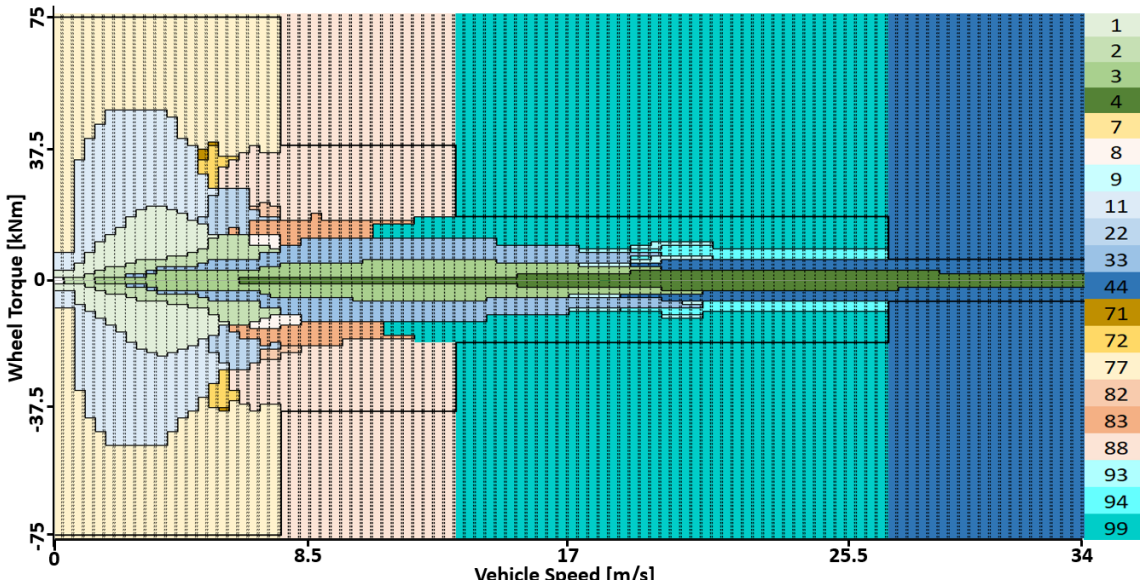

Figure A.5: Motor Drive System State Map

Table A.1: Comparison between EM Map and MDS Map

	Sel. States [n]		MDS Avg. Eff [%]				GB Avg. Eff [%]		Axle Avg. Eff [%]
	EA1	EA2	MDS1	MDS2	MDS3	MDS4	GB1	GB2	
EM Map	183	201	95.26	92.22	93.43	92.13	94.79	94.68	83.65
MDS Map	207	182	95.57	91.48	94.08	92.30	94.76	94.82	83.86

The data presented in Table A.1 is based on the truck driven on an EU highway

with a truck mass of 35,300 kg. It can be concluded that there is no significant difference in the efficiencies between the motors of the two axles, nor is there a large difference in the number of shifts between the maps used. It is observed that the final driveline efficiency is about 0.21% higher when using the MDS state selection map.

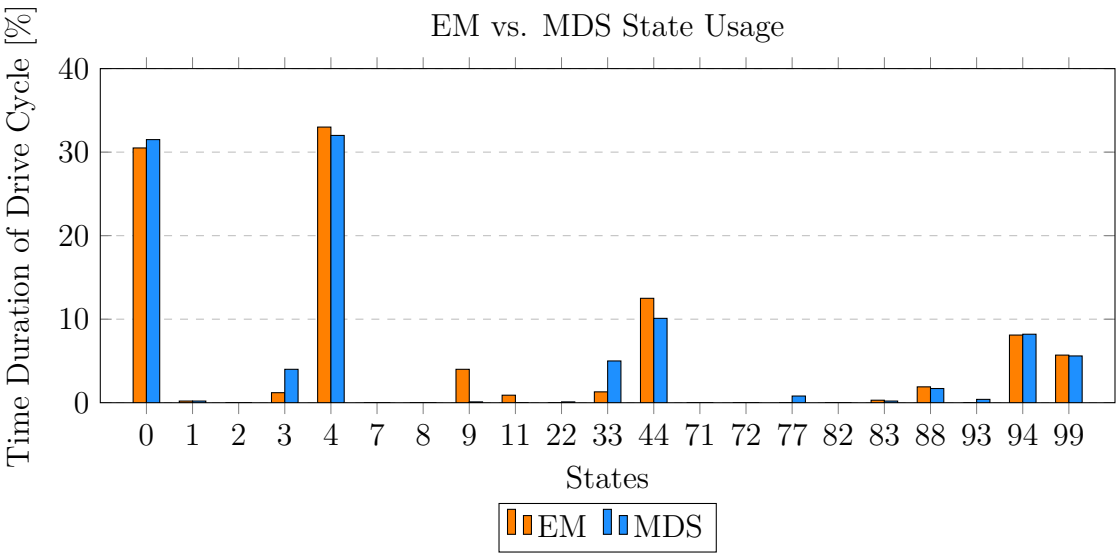

Figure A.6: State usage for state selection map based on EM and MDS efficiency maps.

The plot in Figure A.6 illustrates the usage of different map states in both the cases of EM and MDS-based state selection maps, respectively. The difference in state usage can be observed, the map state 44 being used 12.5% and 10.1% in the above cases respectively. In the case of an MDS-based map, state 3 is used 2.8% more than that of the based state selection map. The state 33 is used more by 3.1% when the MDS map is used for gear selection. This difference is due to the difference in the size of the state islands in both maps.

In addition to the consideration of driveline performance, a significant advantage of considering the EM state map is that it eliminates the need to build an additional standalone model, as explained in Section **??**. With the quicker generation of the EM state selection map compared to the MDS state selection map, there is the possibility to replace and test different motors in the driveline in a shorter timeline. When considering the difference in driveline efficiency in relation to the state of charge levels at the end of the drive cycle between the two maps, the difference is negligible, equating to 0.005% as referred to Figure A.1. Therefore, it can be concluded that using EM state selection maps is a preferable option in terms of the speed at which the EM state selection maps are generated compared to simulating the standalone model to generate the MDS state selection map.
Therefore it is concluded that EM based State Selection Map is a better choice to adapt to hardware changes to make a quick transition.

A.3 Electric Drive System

The EDS standalone model includes the Electrical Storage System (ESS), and unlike the MDS standalone model, the EDS model efficiency output is not immediately steady-state due to that the battery voltage takes time to settle. Therefore, the EDS efficiency must converge before being logged, see Figure A.7 for the efficiency output at $3000rpm$ and $150Nm$. The plot shows that the model converges after about $340s$ or when $\Delta\eta/dt < 0.01\%/200s$. The latter is used as the convergence condition which stops the simulation when fulfilled.

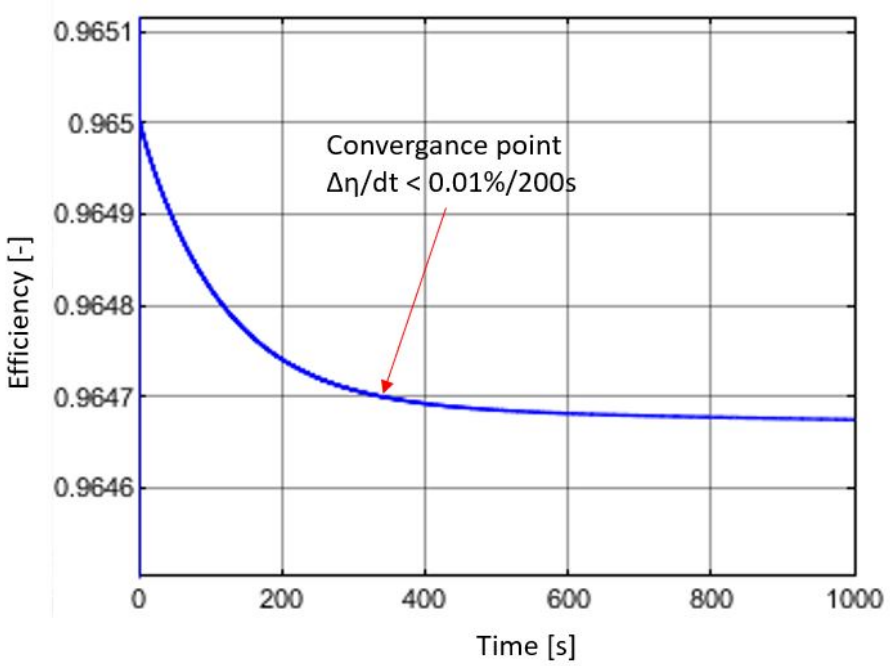

Figure A.7: Plot showing the convergence of EDS efficiency at $3000rpm$ and $150Nm$

When starting the simulation it is apparent that it runs slow compared to the MDS standalone model. To increase the simulation speed, the Simulink tools 'Fast Restart' and 'Accelerator'-mode is used, which increases the iteration time to $21.7s$. At this iteration rate, the 50-by-50 matrix would be generated in 14.5 hours. In addition, the time the model takes to converge in steady state is concerning. From a practical point of view, it is deemed unrealistic to log the efficiency value after minutes of steady state operation of the electric machine. In real operation conditions, both the torque and rotational speed of the electric machines will be transient which will result in fluctuations in the battery voltage and thereby varying total efficiencies of the EDS. With these factors in mind, the decision is made that because of the complex standalone model, slow simulation time and unreliable efficiency output, the EDS efficiency map is not suitable to use for this project.

DEPARTMENT OF SOME SUBJECT OR TECHNOLOGY
CHALMERS UNIVERSITY OF TECHNOLOGY
Gothenburg, Sweden
www.chalmers.se

CHALMERS
UNIVERSITY OF TECHNOLOGY